



**THERMODYNAMIC PROPERTIES OF 1-ETHYL-3-METHYLIMIDAZOLIUM ETHYL
SULPHATE WITH NITROGEN AND SULPHUR COMPOUNDS AT $T = (298.15 - 318.15)$
K AND $P = 1$ BAR**

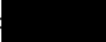
SIYANDA BRIAN CHULE

Submitted in fulfilment of the academic requirements for the
Masters of Applied Science (Chemistry)
Durban University of Technology, Chemistry Department, Durban, South Africa


2015

PREFACE

The work described in this thesis was performed by the author under the supervision of Professor N. Deenadayalu at Durban University of Technology, Durban, South Africa, 2014-2015. The study present original work by the author and has not been submitted in any form to any other university. It has been clearly stated in the text where use is made of the work of others.

Signed: 
Siyanda Brian Chule

Date: 29/3/2016

Signed: 
Prof. N. Deenadayalu (Supervisor)

Date: 29/3/2016

ACKNOWLEDGEMENT

The authors acknowledge the Department of Science and Technology for the purchase of an Anton Paar DSA 5000 M and an Anton Paar RXA 156 equipment and the National Research Foundation and the Durban University of Technology for funding of the project.

ABSTRACT

In this work, the thermodynamic properties for the binary mixtures containing the ionic liquid (IL): 1-ethyl-3-methylimidazolium ethyl sulphate ([EMIM] [EtSO₄]) were calculated. The binary systems studied were {pyridine (Py) or ethyl acetoacetate (EAA) or thiophene (TS) + [EMIM] [EtSO₄]}. The results were interpreted in terms of the intermolecular interactions between the (pyridine + IL), (ethyl acetoacetate + IL), and (thiophene + IL) molecules.

The physical properties: density, speed of sound, and refractive index were measured for the binary mixtures over the complete mole fraction range using an Anton Paar DSA 5000 M vibrating U-tube densimeter and an Anton Paar RXA 156 refractometer, respectively. The measurements were done at $T = (298.15, 303.15, 308.15, 313.15, \text{ and } 318.15)$ K and at $p = 0.1$ MPa. The experimental data was used to calculate the derived properties for the binary mixtures namely:- excess molar volume (V_m^E), isentropic compressibility (k_s), molar refractions (R) and deviation in refractive index (Δn).

For the binary mixtures, (Py or EAA or TS + IL), V_m^E was negative throughout the whole composition range which indicates the existence of attractive intermolecular interaction between (pyridine + IL) and (ethyl acetoacetate + IL) for (thiophene + IL), V_m^E was negative at low mole fraction of thiophene and became positive at high mole fraction of thiophene. For the binary mixtures (pyridine + IL), (ethyl acetoacetate + IL), k_s was positive indicating that the binary mixtures were more compressible than the ideal mixture. For the binary mixture (thiophene + IL) k_s was negative at low thiophene composition and positive at high composition indicating that the

binary mixture was less compressible than the ideal mixture at low thiophene composition and more compressible at high composition of thiophene. The molar refraction, R , is positive for the (Py or EAA or TS + IL) binary systems at $T = (298.15 - 318.15)$ K, molar refraction decreases as the organic solvent composition increases. For the binary mixture (pyridine + [EMIM] [EtSO₄]), Δn is negative at mole fractions < 0.75 of pyridine and positive at mole fractions > 0.75 at all temperatures and decreases with an increase in temperature. For the binary system (ethyl acetoacetate + [EMIM] [EtSO₄]), Δn values are positive over the entire composition range and at all temperatures and increases with an increase in temperature. Δn values for the (thiophene + IL) system are negative for mole fractions of thiophene < 0.62 and becomes positive for mole fractions of thiophene > 0.62 and Δn increases with an increase in temperature. The Redlich-Kister smoothing equation was used successfully for the correlation of V_m^E and Δn data. The Lorentz-Lorenz equation gave a poor prediction of V_m^E , but a good prediction of density or refractive index.

| CONTENTS | Page |
|---|-------------|
| PREFACE | i |
| ACKNOWLEDGEMENT | ii |
| ABSTRACT | iii-iiiv |
| CONTENTS | v-vii |
| LIST OF TABLES | xiii-x |
| LIST OF FIGURES | xi-xiv |
| LIST OF SYMBOLS | xv-xiv |
| Chapter 1 | 1 |
| INTRODUCTION | 1 |
| 1.1 Definition of ionic liquids | 1 |
| 1.2 History of ionic liquids | 1 |
| 1.3 Properties of ionic liquids | 2 |
| 1.4 Importance of ionic liquids | 3 |
| 1.5 Industrial uses of ionic liquids | 4 |
| 1.5.1 Cellulose processing..... | 5 |
| 1.5.2 Pharmaceuticals | 5 |
| 1.5.3 Solar thermal energy..... | 6 |
| 1.5.4 Batteries | 6 |
| 1.5.5 Biodiesel production..... | 7 |
| 1.6 Removal of industrial pollutants from wastewater | 8 |
| 1.7 Thermodynamic properties determined in this work | 10 |
| Chapter 2 | 13 |
| LITERATURE REVIEW | 13 |
| Chapter 3 | 30 |
| EXPERIMENTAL METHODS AND THEORETICAL FRAMEWORK | 30 |
| A. EXPERIMENTAL METHODS | 30 |

| | | |
|---|---|----|
| 3.1 | Excess molar volumes | 30 |
| 3.1.1 | Theory | 30 |
| 3.1.2 | Experimental methods for measurement of excess molar volumes | 32 |
| 3.1.2.1 | Dilatometer method | 32 |
| | (i) Batch method | 32 |
| | (ii) Continuous dilution method | 32 |
| 3.1.2.2 | Indirect method | 36 |
| 3.1.2.3 | Pycnometers | 36 |
| 3.2 | Speed of sound and isentropic compressibility | 37 |
| 3.2.1 | Theory | 37 |
| 3.2.2 | Mittal ultrasonic interferometer M-81G | 38 |
| 3.3 | Refractive indices and molar refraction | 40 |
| 3.3.1 | Theory | 40 |
| 3.3.2 | ATAGO RX 5000 refractometer | 41 |
| B. | THEORETICAL FRAMEWORK | 41 |
| 3.4 | Lorentz-Lorenz equation | 42 |
| 3.4.1 | Prediction of density by the Lorentz-Lorenz (L-L) approximation | 46 |
| 3.4.1.1 | Correlations and predictions | 46 |
| 3.4.1.2 | Prediction of density or refractive index | 46 |
| 3.5 | Redlich-Kister polynomial | 47 |
| Chapter 4 | | 49 |
| INSTRUMENTATION AND EXPERIMENTAL PROCEDURE | | 49 |
| A. | INTRUMENTATION FOR EXCESS MOLAR VOLUME, ISENTROPIC COMPRESSIBILITY, AND CHANGE IN REFRACTIVE INDEX | 49 |
| 4.1 | Apparatus and technique | 49 |
| 4.1.1 | Density and sound velocity meter (DSA 5000 M) | 49 |
| 4.1.2 | Definition of density | 49 |
| 4.1.3 | Oscillating U-tube method | 49 |
| 4.1.4 | Sound velocity analyser | 53 |
| 4.1.5 | Features of DSA 5000 M | 53 |
| 4.1.5.1 | Accuracy | 53 |
| 4.1.5.2 | Error detection | 54 |
| 4.1.5.3 | An overview of an Anton Paar refractive index analyser RXA 156 | 56 |
| 4.1.5.4 | Features of an Anton Paar refractive index analyser RXA 156 | 56 |
| 4.2 | Chemicals | 58 |
| 4.3 | Preparation of binary mixtures | 61 |
| B. | EXPERIMENTAL PROCEDURE | 61 |

| | | |
|-------------------------|---|-----|
| 4.4 | Density and speed of sound | 61 |
| 4.5 | Refractive indices | 62 |
| 4.6 | Systems studied in this work | 63 |
| Chapter 5 | | 64 |
| RESULTS | | 64 |
| 5.1 | Excess molar volume (V_m^E), isentropic compressibility (k_s), change in refractive indices (Δn), and molar refraction (R) | 64 |
| 5.2 | Prediction of density or refractive index | 89 |
| Chapter 6 | | 91 |
| DISCUSSION | | 91 |
| 6.1 | Density | 91 |
| | 6.1.1 Effect of temperature and composition on density | 91 |
| 6.2 | Excess molar volume | 91 |
| | 6.2.1 Effect of temperature and composition on the excess molar volume | 91 |
| 6.3 | Isentropic compressibility | 93 |
| | 6.3.1 Effect of temperature and composition on speed of sound | 93 |
| 6.4 | Change in refractive index | 93 |
| | 6.4.1 Effect of temperature and composition on refractive index | 93 |
| 6.5 | Prediction of density by the Lorentz-Lorenz (L-L) approximation | 97 |
| 6.6 | Correlation of excess molar volume by Lorentz-Lorenz (L-L) approximation | 102 |
| 6.7 | Prediction of refractive index by the Lorentz-Lorenz (L-L) approximation | 104 |
| Chapter 7 | | 109 |
| CONCLUSION | | 109 |
| REFERENCES | | 111 |
| Appendix | | 118 |

LIST OF TABLES

- Table 1.1 Properties of ionic liquid used in this work.
- Table 2.1 Qualitative V_m^E data for IL and organic solute with a common cation or anion or common organic solute obtained from the literature.
- Table 2.2 Δn data for (ILs + organic solvent) with a common cation or anion or common organic solute obtained from the literature.
- Table 2.3 k_s data for (ILs + organic solvent) with a common cation or anion or common organic solute obtained from the literature.
- Table 4.1 Specifications of the DSA 5000 M.
- Table 4.2 Specifications of the refractometer RXA 156.
- Table 4.3 Chemicals, suppliers, and mass % purity.
- Table 4.4 Comparison of experimental and literature density (ρ), speed of sound (u), and refractive index (n), of pure components at $T = (298.15, 303.15, 308.15, 313.15$ and $318.15)$ K.
- Table 5.1 Density (ρ), excess molar volume (V_m^E), speed of sound (u), and isentropic compressibility (k_s), for the binary mixture {pyridine (x_1) + [EMIM] [EtSO₄] (x_2)} at $T = (298.15, 303.15, 308.15, 313.15,$ and $318.15)$ K.
- Table 5.2 Density (ρ), excess molar volume (V_m^E), speed of sound (u), and isentropic compressibility (k_s), for the binary mixture {ethyl acetoacetate (x_1) + [EMIM] [EtSO₄] (x_2)} at $T = (298.15, 303.15, 308.15, 313.15,$ and $318.15)$ K.

- Table 5.3 Density (ρ), excess molar volume (V_m^E), speed of sound (u), and isentropic compressibility (k_s), for the binary mixture {thiophene (x_1) + [EMIM] [EtSO₄] (x_2)} at $T = (298.15, 303.15, 308.15, 313.15, \text{ and } 318.15)$ K.
- Table 5.4 Refractive index (n), molar refraction (R), and deviation in refractive index (Δn) for the binary mixture {pyridine (x_1) + [EMIM] [EtSO₄] (x_2)} at $T = (298.15, 303.15, 308.15, 313.15, \text{ and } 318.15)$ K.
- Table 5.5 Refractive index (n), molar refraction (R), and deviation in refractive index (Δn) for the binary mixture {ethyl acetoacetate (x_1) + [EMIM] [EtSO₄] (x_2)} at $T = (298.15, 303.15, 308.15, 313.15, \text{ and } 318.15)$ K.
- Table 5.6 Refractive index (n), molar refraction (R), and deviation in refractive index (Δn) for the binary mixture {thiophene (x_1) + [EMIM] [EtSO₄] (x_2)} at $T = (298.15, 303.15, 308.15, 313.15, \text{ and } 318.15)$ K.
- Table 5.7 Redlich-Kister fitting parameter and root-mean-square deviation (σ), for the binary mixtures at $T = (298.15, 303.15, 308.15, 313.15, \text{ and } 318.15)$ K.
- Table 5.8 Root mean square deviation (σ), obtained from the Lorentz-Lorenz equation for V_m^E , ρ and n of the binary mixtures at $T = (298.15, 303.15, 308.15, 313.15 \text{ and } 318.15)$ K.
- Table 6.1 Root mean square deviation (σ), between the experimental and predicted density for the binary mixtures at $T = (298.15, 303.15, 308.15, 313.15, \text{ and } 318.15)$ K.

Table 6.2 Root mean square deviation (σ), obtained from the Lorentz-Lorenz equation for V_m^E , of the binary mixtures at $T = (298.15, 303.15, 308.15, 313.15$ and $318.15)$ K.

Table 6.3 Root mean square deviation (σ), obtained from the Lorentz-Lorenz equation for n , of the binary mixtures at $T = (298.15, 303.15, 308.15, 313.15$ and $318.15)$ K.

LIST OF FIGURES

- Figure 1.1 Structure of: (a) IL, (b) pyridine, (c) thiophene, and (d) ethyl acetoacetate.
- Figure 3.1 Schematic representation of a batch dilatometer.
- Figure 3.2 Schematic representation of a continuous dilatometer.
- Figure 3.3 Schematic representation of pycnometer.
- Figure 3.4 Photograph of the Mittal ultrasonic interferometer M-81G instrument.
- Figure 3.5 Photograph of an ATAGO RX 5000 refractometer.
- Figure 4.1 Photograph of the density and sound velocity meter (DSA 5000 M).
- Figure 4.2 Photograph of the DSA 5000 M along with RXA 156 and Xsample 452.
- Figure 5.1 Plot of excess molar volume (V_m^E), for the binary system {pyridine (x_1) + [EMIM] [EtSO₄] (x_2)} against mole fraction of pyridine; at $T = (298.15, 303.15, 308.15, 313.15, \text{ and } 318.15)$ K. The solid lines represent corresponding Redlich-Kister correlation equation 5.21.
- Figure 5.2 Plot of excess molar volume (V_m^E), for the binary system {ethyl acetoacetate (x_1) + [EMIM] [EtSO₄] (x_2)} against mole fraction of ethyl acetoacetate; at $T = (298.15, 303.15, 308.15, 313.15, \text{ and } 318.15)$ K. The solid lines represent the corresponding Redlich-Kister correlation equation 5.21.
- Figure 5.3 Plot of excess molar volume (V_m^E), for the binary system {thiophene (x_1) + [EMIM] [EtSO₄] (x_2)} against mole fraction of thiophene; at $T = (298.15, 303.15, 308.15, 313.15, \text{ and } 318.15)$ K. The solid lines represent corresponding Redlich-Kister correlation equation 5.21.

- Figure 5.4 Plot of isentropic compressibility (k_s), for the binary system {pyridine (x_1) + [EMIM] [EtSO₄] (x_2)} against mole fraction of pyridine; at $T = (298.15, 303.15, 308.15, 313.15, \text{ and } 318.15)$ K. The solid lines represent corresponding Redlich-Kister correlation equation 5.21.
- Figure 5.5 Plot of isentropic compressibility (k_s), for the binary system {ethyl acetoacetate (x_1) + [EMIM] [EtSO₄] (x_2)} against mole fraction of ethyl acetoacetate; at $T = (298.15, 303.15, 308.15, 313.15, \text{ and } 318.15)$ K. The solid lines represent corresponding Redlich-Kister correlation equation 5.21.
- Figure 5.6 Plot of isentropic compressibility (k_s), for the binary system {thiophene (x_1) + [EMIM] [EtSO₄] (x_2)} against mole fraction of thiophene; at $T = (298.15, 303.15, 308.15, 313.15 \text{ and } 318.15)$ K. The solid lines represent corresponding Redlich-Kister correlation equation 5.21.
- Figure 5.7 Plot of change in refractive index (Δn), for the binary system {pyridine (x_1) + [EMIM] [EtSO₄] (x_2)} against mole fraction of pyridine; at $T = (298.15, 303.15, 308.15, 313.15, 318.15)$ K. The solid lines represent corresponding Redlich-Kister correlation equation 5.21.
- Figure 5.8 Plot of change in refractive index (Δn), for the binary system {ethyl acetoacetate (x_1) + [EMIM] [EtSO₄] (x_2)} against mole fraction of ethyl acetoacetate; at $T = (298.15, 303.15, 308.15, 313.15, \text{ and } 318.15)$ K. The solid lines represent corresponding Redlich-Kister correlation equation 5.21.
- Figure 5.9 Plot of change in refractive index (Δn), for the binary system {thiophene (x_1) + [EMIM] [EtSO₄] (x_2)} against mole fraction of thiophene; at $T = (298.15,$

303.15, 308.15, 313.15 and 318.15) K. The solid lines represents the Redlich-Kister correlation equation 5.21.

- Figure 6.1 Excess molar volume (V_m^E), of the binary mixture plotted against mole fraction x_1 of pyridine at $T = 298.15$ K {pyridine (x_1) + [EMIM] [MeSO₄] (x_2)}, \diamond , this work and \blacksquare , (Anantharaj and Banerjee 2013).
- Figure 6.2 Excess molar volume (V_m^E), of the binary mixture plotted against mole fraction x_1 of thiophene at $T = 298.15$ K {thiophene (x_1) + [EMIM] [MeSO₄] (x_2)}, \diamond , this work and \square , (Anantharaj and Banerjee 2013).
- Figure 6.3 Experimental density (ρ), of the binary mixture plotted against mole fraction x_1 of pyridine at $T = (298.15$ to $318.15)$ K. $T = 298.15$ K; \diamond , $T = 303.15$ K; \square , $T = 308.15$ K; Δ , $T = 313.15$ K; \times , and 318.15 ; \times . For the binary mixture {pyridine (x_1) + [EMIM] [EtSO₄] (x_2)}. The solid lines represent the corresponding prediction by the L-L approximation equation 3.4.8.
- Figure 6.4 Experimental density (ρ), of the binary mixture plotted against mole fraction x_1 of ethyl acetoacetate at $T = (298.15$ to $318.15)$ K. $T = 298.15$ K; \diamond , $T = 303.15$ K; \square , $T = 308.15$ K; Δ , $T = 313.15$ K; \times , and 318.15 ; \times . For the binary mixture {EAA (x_1) + [EMIM] [EtSO₄] (x_2)}. The solid lines represent the corresponding prediction by the L-L approximation equation 3.4.8.
- Figure 6.5 Experimental density (ρ), of the binary mixture plotted against mole fraction x_1 of thiophene at $T = (298.15$ to $318.15)$ K. $T = 298.15$ K; \diamond , $T = 303.15$ K; \square , $T = 308.15$ K; Δ , $T = 313.15$ K; \times , and 318.15 ; \times . For the binary mixture {TS (x_1) + [EMIM] [EtSO₄] (x_2)}. The solid lines represent the corresponding prediction by the L-L approximation equation 3.4.8.

Figure 6.6 Refractive index (n), of the binary mixture plotted against mole fraction x_1 of pyridine at $T = (289.15 \text{ K to } 318.15) \text{ K}$. \diamond , $T = 298.15 \text{ K}$; \square , $T = 303.15 \text{ K}$; Δ , $T = 308.15 \text{ K}$; \times , $T = 313.15 \text{ K}$; and \square , $T = 318.15 \text{ K}$. The solid lines represents the Lorentz – Lorenz (L-L) approximation equation 3.4.9.

Figure 6.7 Refractive index (n), of the binary mixture plotted against mole fraction x_1 of ethyl acetoacetate at $T = (289.15 \text{ K to } 318.15) \text{ K}$. \diamond , $T = 298.15 \text{ K}$; \square , $T = 303.15 \text{ K}$; Δ , $T = 308.15 \text{ K}$; \times , $T = 313.15 \text{ K}$; and \square , $T = 318.15 \text{ K}$. The solid lines represents the Lorentz – Lorenz (L-L) approximation equation 3.4.9.

Figure 6.8 Refractive index (n), of the binary mixture plotted against mole fraction x_1 of thiophene at $T = (289.15 \text{ K to } 318.15) \text{ K}$. \diamond , $T = 298.15 \text{ K}$; \square , $T = 303.15 \text{ K}$; Δ , $T = 308.15 \text{ K}$; \times , $T = 313.15 \text{ K}$; and \square , $T = 318.15 \text{ K}$. The solid lines represents the Lorentz – Lorenz (L-L) approximation equation 3.4.9.

LIST OF SYMBOLS

| | | |
|-------------|---|---|
| A_i | = | polynomial coefficient. |
| M_1 | = | molar mass of organic solvent ($\text{g}\cdot\text{mol}^{-1}$). |
| M_2 | = | molar mass of ionic liquid ($\text{g}\cdot\text{mol}^{-1}$). |
| σ | = | standard deviation. |
| x_1 | = | mole fraction of the 1 st component. |
| x_2 | = | mole fraction of the 2 nd component. |
| T | = | temperature. |
| $V_{m,1}^E$ | = | molar volume of the first component ($\text{cm}^3\cdot\text{mol}^{-1}$). |
| V_m | = | molar volume ($\text{cm}^3\cdot\text{mol}^{-1}$). |
| V_m^E | = | excess molar volume ($\text{cm}^3\cdot\text{mol}^{-1}$). |
| $V_{m,1}^*$ | = | molar volume of the pure IL ($\text{cm}^3\cdot\text{mol}^{-1}$). |
| $V_{m,2}^*$ | = | molar volume of the pure organic solvent ($\text{cm}^3\cdot\text{mol}^{-1}$). |
| ρ | = | density ($\text{g}\cdot\text{cm}^{-3}$). |
| k | = | polynomial degree. |
| n | = | number of experimental points. |
| u | = | speed of sound ($\text{m}\cdot\text{s}^{-1}$). |

k_s = isentropic compressibility ($T \cdot \text{Pa}^{-1}$).

Δn = refractive index deviation.

n^{id} = ideal refractive index.

R = molar refraction.

n = refractive index of the mixture.

n_1 = refractive index of 1st component.

n_2 = refractive index of 2nd component

INTRODUCTION

1.1 Definition of ionic liquids

Ionic liquids are a class of organic salts that are entirely made of ions; they have a boiling point below 373 K and have extremely low vapour pressure Gonzalez *et al.* (2006). The room temperature ionic liquids (RTIL), are organic salts composed of organic cations and anions which are held together by columbic forces. They can be optimized by modifying their physical properties by preparing their binary mixtures with organic solvents or water.

1.2 History of ionic liquids

The first ionic liquid: ethylammonium nitrate (m.p. 285.15 K) was reported in 1914 by Paul Walden, he examined the electrical conductivity of ethylammonium nitrate. This IL was produced by neutralising ethylamine with concentrated nitric acid (Walden 1914). In 1963 the scientists A. Lowell and J. King conducted a research for replacing LiCl/KCl molten salts electrolyte which was used in thermal batteries because it had high melting temperature (608.15 K) and this induced problems inside batteries (Binnemans 2005). The research team found that the mixture of chloroaluminates, alkali halides and aluminium chlorides (NaCl/AlCl₃) have low m.p. (380.15 K) than LiCl/KCl electrolyte. Hence chloroaluminate electrolyte was applied in thermal batteries. The modern era of ILs started in 1978, where, (Wasserscheid and Welton 2007) found that alkylpyridinium chloroaluminates was a possible new class of nonaqueous electrolytes. They found that the compounds were relatively easy to reduce electrochemically or chemically. The dialkylimidazolium cations were found to be more stable to reduction.

The chloroaluminates have low melting point and dialkylimidazolium cations are more stable to reduction, this scientific evidence made dialkylimidazolium chloroaluminates to be called the first generation of ionic liquids. The first water stable ionic liquids were discovered by Zaworokto in 1978, they were based on alkyylimidazolium and new developed anions such as tetraflouroborate, hexaflouroborate, nitrate, sulfate and acetate. In 1992 (Wilkes and Zaworotko 1992) developed 1-ethyl-3-methylimidazolium tetraflouroborate and 1-ethyl-3-methylimidazolium methyl carbonate because there were air stable, water stable and have relatively low m.p. than chloroaluminates anions. They stopped the use chloroaluminates anions. The first ILs based on imides and methides were reported in 1995 by (Fuller *et al.* 1994) as Li-ion battery electrolytes. The ILs based on pyrrolidinium cations were reported in 1999 by (MacFarlane *et al.* 1999).

1.3 Properties of ionic liquids

Ionic liquids (IL) are a class of organic salts that are made of ions; they have a boiling point below 373.15 K and have extremely low vapour pressure. They have tunable chemical and physical properties and hence are used as alternative solvents to the traditional organic compounds.i.e volatile organic compounds (VOCs). These changes leads into useful properties of ionic liquids such as the ability to exclude water, ability to recycle, non-flammable behaviour, wide electrode windows, high conductivity, high solubility of metal salts, and non-volatility. The organic solvents used in this study were chosen because they interact with the ionic liquid through hydrogen bonding, making it possible to understand their intermolecular interaction with the ionic liquid.

1.4 Importance of ionic liquids

The ionic liquids are entirely composed of anions, they have unique attractive chemical and physical properties. They are green solvents with minimal detrimental effect on the environment.

They are attractive because of their advantageous physico-chemical properties such as high thermal stability, negligible vapour pressure, non-toxic, electrochemical stability, high solvating power, high dissolving power, etc. The choice of a cation and anion making the ionic liquid can be chosen specifically to change the physical properties such as polarity, viscosity, density and conductivity (Khupse and Kumar 2010). The properties of ionic liquids can also be finely tuned by changing the temperature and pressure. Since the ionic liquids have negligible vapour pressure, they are a good alternative to the volatile organic compounds because they do not evaporate to the environment (Singh and Kumar 2008). The ionic liquids can be used as solvents in a wide range of inorganic and organic materials. Some ionic liquids are immiscible with organic solvents and can be used as alternative polar solvents in biphasic systems to separate and recover polar components in the reaction mixture.

Transport properties are an important factor in chemical reactions, electrochemistry, and liquid-liquid extraction. Ionic liquids are regarded as proper solvents in these different kinds of chemistries because it is possible to change their transport properties in order to favour certain experimental or chemical conditions. It is possible to change the hydrophobicity, viscosity, and density of ionic liquids, one typical example is when the alkyl chain length is increased from butyl to octyl of a series of 1-alkyl-3-methylimidazolium cations. This results in an increased hydrophobicity and viscosity of the IL, whilst densities decrease. The importance of ionic liquids in electrochemistry is high because it is possible to control ionic conductivity, viscosity, the width of the electrochemical potential window, and volatility of the electrolyte solution. RTILs have the ability to maintain high ionic conductivity, fast ion mobility during redox reactions, large electrochemical potential windows and low volatility (Faridbod *et al.* 2011).

1.5 Industrial uses of ionic liquids

Many papers have detailed the ILs' applications (Manuel *et al.* 2008) and (Gonzalez 2006). Nitrogen and sulphur are atmospheric pollutants which are largely emitted by coal industries, petroleum industries and other energy sectors. The desulphurization and denitrification process is an important process which is used to reduce the amount of nitrogen and sulphur released into the atmosphere. The process can be optimized by using ionic liquids, because ionic liquids are environmentally friendly. It is important to know the physiochemical properties of ILs with aromatic sulphur and nitrogen compounds (Anantharaj and Banerjee 2011). Ionic liquids have many important industrial uses; it can be used in stoichiometric organic synthesis. In organic reactions the ionic liquid is used as a solvent to increase the rate of formation of the product and to make a chemical reaction to be selective, one example observed is when the ionic liquid is used in the Diels-Alder reaction.

There are higher reaction rates and selectivities in the polar solvent compared to non-polar solvent. Ionic liquids can be used in catalysed reactions to dissolve transition metal complexes and support organic chemistry, i.e. A nickel complex is dissolved in chloroaluminate ionic liquid while the dimerization of alkenes occurs. It was also demonstrated that ethylene polymerisation was possible in the same solvent system (Dyson and Geldback 2007). Ionic liquids are also used in electrochemical sensors and biosensors to modify the response; a chemical sensor is a device which gives continuous information about some specific chemical properties of its environment while an electrochemical biosensor is a device which converts a biological response to a measurable electrical signal (Faridbod *et al.* 2011). The chloroaluminates (AlCl_3) ionic liquids are used as electrolytes in batteries, however they are very hygroscopic. Therefore they are used with strict precautions under a dry atmosphere.

ILs have many different kinds of industrial uses, few industrial uses are described below:

1.5.1 Cellulose processing

Cellulose are natural organic materials found abundantly on earth, they are very important in the manufacture of paper, body care products, packing materials, and textile fibers. Their importance is great because they are renewable raw material. Only 200 million tons of the 40 billion tons get renewed per year to be re-used as raw material. Cellulose are insoluble in water or in organic solvents because of the existing strong intermolecular hydrogen bonding, this prevents them to be used extensively. The dissolution of cellulose can be achieved either by physical dissolution in a suitable ionic liquid or chemical derivatization. ILs are used to dissolve cellulose because they are effective in breaking the intermolecular hydrogen bonds within the cellulose (Hermanutz *et al.* 2008).

1.5.2 Pharmaceuticals

The pharmaceutical industries are well recognised all over the world for producing medicines and drugs which are helpful to people. They have been facing a great challenge associated with the consumption of medicines and high waste discharged into the environment. Ionic liquids have been used in the pharmaceutical industries to recover active pharmaceutical ingredients (APIs), this reduces large volumes of pharmaceutical wastes. The approach was done by using aqueous biphasic system based on IL (IL-based ABS) in a single step and using IL aqueous solution to extract APIs using solid-liquid extraction process (IL-based SLE).

1.5.3 Solar thermal energy

Solar thermal energy is the most easily generated form of energy on earth, its main application is to generate electricity. The problem with solar energy is that its availability is controlled by many factors such as time, weather condition, and latitude. This challenge is controlled by storing solar radiation as thermal energy in storage fluid. There are a number of storage media which have been used, molten salt mixture made of sodium nitrate NaNO_3 , sodium nitrite NaNO_2 and potassium nitrate KNO_3 have been applied to store solar energy, however the mixture have relatively high melting point, i.e. 415.15 K. This makes the pipelines to freeze and causing high operation cost. Another media used is organic oil such as Santotherm 55. The problem with the organic oil is low heat capacity which can be improved by increasing the storage volume, limited temperate range below 573.15 K), and higher construction costs. Ionic liquids are appropriate solvents for storing solar energy because they have low melting point and therefore there is no freezing of pipes, there is wide temperature range for liquid and wide electrochemical window (Reddy *et al.* 2003).

1.5.4 Batteries

Ionic liquids are very important solvents in the battery manufacturing industries because they can be used as electrolyte solution. The arrangement of the cation and anion of the ionic liquid is an important aspect, ionic liquids generally have large cation, are asymmetrical, and the anion have a delocalised charge. These arrangements prevent the packing of ions and ordered crystal structure from forming in the ionic liquid. The chemical interaction occurring in ionic liquids are different than those in molecular solvents. The unique chemical interaction occurring in ionic liquids lead into dramatic changes in the physiochemical properties of ionic liquids, which makes IL good electrolytes in batteries (Armand *et al.* 2009).

These changes leads into useful properties of ionic liquids such as ability to exclude water, non-flammable behaviour, wide potential windows, high conductivity, and high solubility of metal salts, non-volatility (Plechkova and Seddon 2008), (Rogers and Seddon 2003), (Freemantle 1998), and (Abbott and Ryder 2013). Ionic liquids are used as an electrolyte solution in lithium batteries, their use in lithium batteries enable one to overcome challenges often incurred with the use of these Li-battery such as increasing energy demand, environmental effects and supply limit (Sadoway 2012). The common used electrolyte solution in lithium battery is ethylene carbonate-dimethyl carbonate (EMC-DMC). This electrolyte solution is not recommended because it does not conduct ions well and as a result there is a narrow potential window. There is no safety when this electrolyte is used, accidental overcharging in the EMC-DMC lithium battery can cause uncontrollable oxidation which leads to the device failure. These side reactions can cause explosion or fire, ionic liquids on the contrary when used as electrolytes media in lithium battery there is safety because ionic liquids are more stable, non-volatile, and non-flammable (Jung *et al.* 2012).

1.5.5 Biodiesel Production

Ionic liquids are considered efficient and effective catalyst; they are used as catalysts to speed up the conversion of vegetable oils and animal fats to produce biodiesel, they are environmental friendly, because waste is minimised when using ionic liquids as catalysts. They are recyclable; hence waste discharged into the environment is minimised. The waste that is generated during biodiesel production is converted into useful products (Andreani *et.al.* 2012).

1.6 Removal of industrial pollutants from wastewater

There are many methods that have been applied to remove hazardous materials from wastewater in the past time but they were not effective, these processes include: biological treatment, adsorption, chemical oxidation, membrane filtration, coagulation, and photochemical degradation. Adsorbent materials such as nanoporous silica, zeolite, hematite, and mesoporous TiO₂ have demonstrated good separation and purification of wastewater when polymerised with ionic liquids. Ionic liquids with asymmetric cation and anion can be fine-tuned to favour specific physicochemical properties, hence when the ionic liquid is polymerised with one of the above mentioned adsorbent a poly (ionic liquid) (PILs) is formed. The use of PILs is good since they can be fine-tuned as hydrophobic solvents, which makes it possible to adsorb the heavy metal ions or organic pollutants from water. When the heterogeneous phase is formed the separation of heavy metal ions or organic pollutants becomes convenient (Kong and Jiang 2013).

Table 1.1 below lists the properties of the ionic liquid used in this work.

Table 1.1 Properties of ionic liquid used in this work.

| PROPERTY | PROPERTY VALUE |
|---------------------------|---|
| Polarity | 47-49 |
| Freezing point | < 373.15 K |
| Liquidus range | 298.15 - 473.15 K |
| Viscosity | < 100 Cp |
| Dielectric constant | ≤ 30 (F · m ⁻¹) |
| Vapour pressure | Usually negligible |
| Specific conductivity | < 10 mS · cm ⁻¹ |
| Electrochemical windows | 2V - 4.5V |
| Molar conductivity | < 10 Scm ² · mol ⁻¹ |
| Solvent and / or catalyst | Excellent for many organic reactions |

1.7 Thermodynamic properties determined in this work

In this work, the IL used was: 1-ethyl-3-methylimidazolium ethyl sulfate and the three solvents used were: pyridine, ethyl acetoacetate, and thiophene. The binary mixtures were: (Py + EAA + TS or [EMIM] [EtSO₄]). Pyridine is an organic solvent produced mostly through the reaction of acetaldehyde and formaldehyde with ammonia. It is used as a solvent in organic chemistry and in industrial processes; it is a versatile solvent and is easily produced in large amounts. It is volatile and need to be stored in a closed container (Santodonato *et al.* 1985). Ethyl acetoacetate is used as an intermediate compound to produce a wide variety of compounds, such as amino acids, analgesics, antibiotics, vitamin B and dyes, inks, and perfumes (European commission 2002). It is also used as a solvent in pharmaceutical, paint industries, and as plasticizers in plastic industries. Thiophene is an aromatic compound and a colourless liquid with a mildly pleasant odour. It is used as a building block in agrochemicals and pharmaceuticals (Chaudhary 2012). The structures of the chemicals used in this work are presented in Figure 1.1

Excess molar volume (V_m^E), isentropic compressibility (k_s), deviation in refractive index (Δn), and molar refraction (R) values for {pyridine or ethyl acetoacetate or thiophene + [EMIM] [EtSO₄]} binary systems have been calculated from experimental data at $T = (298.15 \text{ to } 318.15) \text{ K}$ over the whole mole fraction range. The Redlich-Kister polynomial was used to fit V_m^E and Δn data. The Lorentz-Lorenz equation was used to correlate V_m^E and predict density or refractive index for the binary systems.

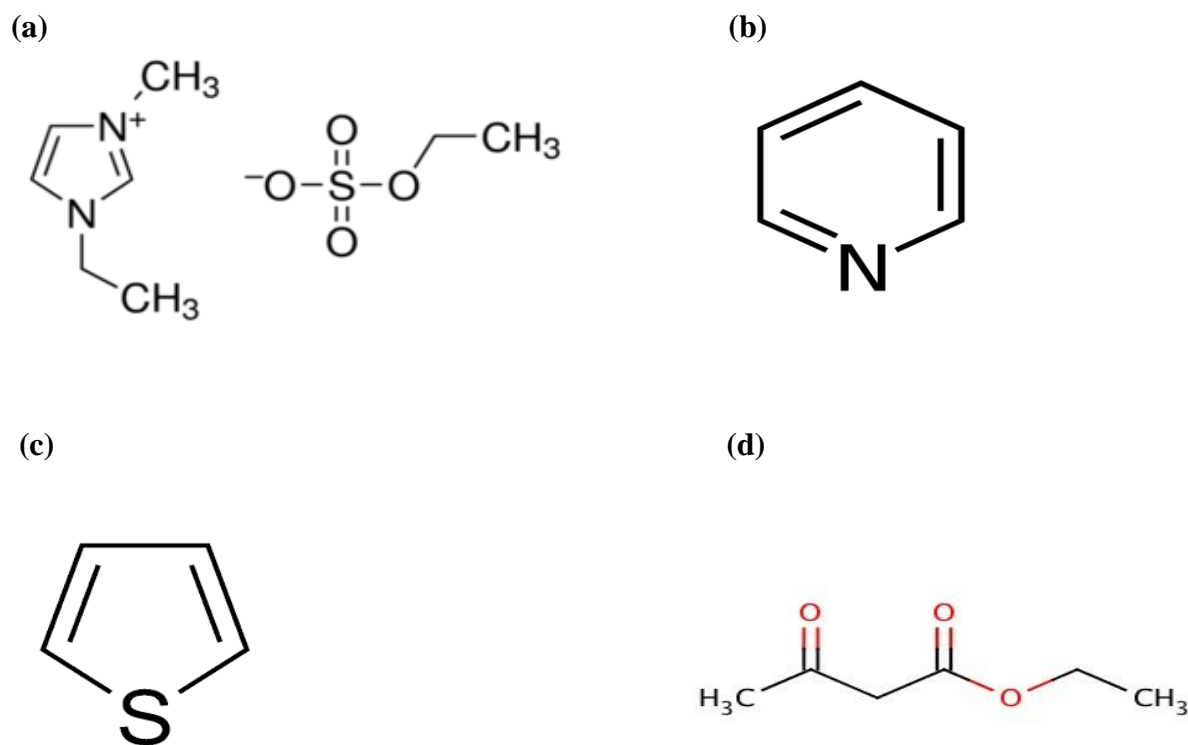


Figure 1.1 Structure of: (a) IL, (b) pyridine, (c) thiophene, and (d) ethyl acetoacetate.

In this work, the thermodynamic properties have been determined for {pyridine (Py) or ethyl acetoacetate (EAA) or thiophene (TS) + [EMIM] [EtSO₄]} binary systems at $T = (298.15, 303.15, 308.15, 313.15, \text{ and } 318.15)$ K over the whole composition range. The study of thermodynamic and transport properties are necessary in order to understanding the intermolecular forces occurring between the components of the binary mixtures. It is important to know the physical properties of ionic liquids together with its binary mixtures, this enable one to design and optimize a chemical process involving the use of ionic liquids (Hasan *et al.* 2010). Physical properties such as density, speed of sound, and refractive are required to study the nature of the binary systems, to

fine tune the properties of the ionic liquid thus increasing their usage on an industrial scale. Physical properties are required to make the process flow easier by calculating pore surfaces, mass, energy transfer, and pressure acceptable in the fluid transport pipes and hydraulic charge pipes. Ionic liquids are normally used for separation purposes, i.e. biomass processing and cellulose dissolution (González *et al.* 2008).

LITERATURE REVIEW

There is a great need for studying the thermodynamic properties of binary mixtures, because the properties of binary mixtures deviate from ideality upon mixing. The study enable one to design a specific chemical process. Excess molar volume dependence on composition is a useful tool to study the molecular interactions between the binary mixtures (Urszula *et al.*2014).

A few authors have done research work and published V_m^E data for the (pyridine or thiophene or ethyl acetoacetate + [EMIM] [EtSO₄]) binary mixtures. The literature qualitative V_m^E data for the IL with a common cation or anion or common organic solute are given in table 2.1. In the discussion below the first component is x_1 and the second component is x_2 .

Table 2.1 Qualitative V_m^E data for IL and organic solute with a common cation or anion or common organic solute obtained from the literature.

| Author | Systems | V_m^E |
|---------------------------------|--|-----------------------|
| Anantharaj and Banerjee (2013) | (Py or TS + [EMIM] [MeSO ₃]) | Negative |
| Anantharaj and Banerjee (2011) | (Py + [EMIM] [EtSO ₄]) | Negative |
| Anantharaj and Banerjee (2011) | (TS + [EMIM] [EtSO ₄]) | Negative and Positive |
| Perez <i>et al.</i> (2012) | (heptane, octane, nonane or decane + TS) | Positive |
| Lehmann <i>et al.</i> (2010) | (organic solvents + [EMIM] [EtSO ₄]) | Negative |
| Sibiya (2008) | (methanol or propanol or 2-propanol + [EMIM] [EtSO ₄]) | Negative |
| Mahendra <i>et al.</i> (2010) | (EAA + dicloromethane or chloroform or acetonitrile) | Positive and Negative |
| Gomez <i>et al.</i> (2006) | (ethanol + [EMIM] [EtSO ₄]) | Negative |
| Domanska and Laskowka (2008) | (1-propanol + [EMIM] [EtSO ₄]) | Negative |
| Yadav <i>et al.</i> (2014) | (chloroform or dimethyl sulfoxide + EAA) | Negative |
| Saini <i>et al.</i> (2011) | (tetrahydropyran + pyridine) | Negative |
| Anantharaj and Barnejee (2011) | ([EMIM] [SCN] + Py or TS) | Negative |
| Domanska and Krolikowska (2013) | ([EMIM] [TCM] + TS) | Negative |
| Alonso <i>et al.</i> (2010) | (2-butanone + pyridine) | Negative |

| | | |
|---|--|----------|
| Rodriguez and Brennecke (2006) | (water + [EMIM] [EtSO ₄]) | Negative |
| Maurya <i>et al.</i> (2015) | (pyridine + ethanol) | Positive |
| Arce <i>et al.</i> (2006) | (2-ethoxy-2-methylpropane or ethanol + [EMIM] [EtSO ₄]) | Negative |
| Gonzalez (2007) | (methanol or 1-propanol or 2-propanol + [EMIM] [EtSO ₄]) | Negative |
| D. Matkowska, A. Goldon, T. Hofman (2010) | (ethanol + [EMIM] [EtSO ₄]) | Negative |
| Rafiee and Frouzesh (2015) | (allyl alcohol or 1,3-dichloro-2-propanol + [EMIM] [EtSO ₄]) | Negative |

Anantharaj and Banerjee (2013) studied the (pyridine or thiophene + [EMIM] [MeSO₃]) binary mixtures and obtained negative V_m^E . However they obtained relatively small absolute values for the negative V_m^E . Anantharaj and Banerjee (2011) studied the (pyridine + [EMIM] [EtSO₄]) binary mixture and obtained negative V_m^E . However they obtained relatively small absolute values for the negative V_m^E . And they also studied the (thiophene + [EMIM] [EtSO₄]) binary mixtures and obtained positive and negative V_m^E .

Lehmann *et al.* (2010) reported V_m^E data for (acetone or acetonitrile or dichloromethane or ethanol or methanol or propylene or water + [EMIM] [EtSO₄]) binary systems over the entire composition of their range at $T = (278.15 \text{ to } 308.15) \text{ K}$. The V_m^E was negative for the binary systems studied.

The data in literature indicate that V_m^E is negative for (pyridine + [EMIM] [EtSO₄]) binary system, the range of the negative V_m^E data at $T = (298.15, 303.15, 308.15, 313.15, \text{ and } 318.15) \text{ K}$ is (-0.0879 to -0.2115, 0.0831 to -0.2082, -0.0791 to -0.2048, -0.0752 to -0.2014, and -0.0673 to -0.1933) $\text{cm}^3 \cdot \text{mol}^{-1}$, respectively (Anantharaj and Banerjee 2011). The data in literature indicate that V_m^E is negative and positive for (thiophene + [EMIM] [EtSO₄]) binary system and ranged from +68.79 - -27.23 $\text{cm}^3 \cdot \text{mol}^{-1}$.

Arce *et al.* (2006) reported experimental density, speed of sound, and refractive index at $T = 298.15 \text{ K}$ for (2-ethoxy-2-methylpropane or ethanol + [EMIM] [EtSO₄]) binary systems over the whole composition range. The V_m^E data is negative for the above systems.

Soriano *et al.* (2010) reported experimental density and refractive index for pure [EMIM] [EtSO₄] system at $T = (293.2 \text{ to } 353.2) \text{ K}$.

Matkowska *et al.* (2010) reported experimental density for (ethanol + [EMIM] [EtSO₄]) binary mixture at $T = (298.15 \text{ to } 343.15) \text{ K}$ and $P = (0.1 \text{ to } 35) \text{ MPa}$ over the whole composition range.

The V_m^E data is negative for the above system.

Gonzalez *et al.* (2008) reported experimental density for pure 1-propanol, 2-propanol, and [EMIM] [EtSO₄] at $T = 298.15 \text{ K}$.

From the data of Anantharaj and Banerjee (2011) $V_{m,\min}^E$ value for (Py + [EMIM] [EtSO₄]) system at $T = 298.15 \text{ K}$ at $x_1 = 0.4$ is $-2.5356 \text{ cm}^3 \cdot \text{mol}^{-1}$, and for (Py + [EMIM] [MeSO₃]) system at $T = 298.15 \text{ K}$ at $x_1 = 0.8$ is $-0.2115 \text{ cm}^3 \cdot \text{mol}^{-1}$. The $V_{m,\min}^E$ for the (Py + [EMIM] [EtSO₄]) system is more negative than for the (Py + [EMIM] [MeSO₃]) system. The larger negative $V_{m,\min}^E$ for (Py + [EMIM] [EtSO₄]) system than for (Py + [EMIM] [MeSO₃]) system imply that in (Py + [EMIM] [EtSO₄]) system there are more strong intermolecular interaction and packing effect than in (PY + [EMIM] [MeSO₃]) system. The $V_{m,\min}^E$ value for (TS + [EMIM] [EtSO₄]) system at $T = 298.15 \text{ K}$ at $x_1 = 0.7$ is $-5.0043 \text{ cm}^3 \cdot \text{mol}^{-1}$, and for (TS + [EMIM] [MeSO₃]) system at $T = 298.15 \text{ K}$ at $x_1 = 0.8$ is $-0.2217 \text{ cm}^3 \cdot \text{mol}^{-1}$. The $V_{m,\min}^E$ for the (TS + [EMIM] [EtSO₄]) system is more negative than for the (TS + [EMIM] [MeSO₃]) system. The larger negative $V_{m,\min}^E$ for (TS + [EMIM] [EtSO₄]) system than for (TS + [EMIM] [MeSO₃]) system imply that in the (TS + [EMIM]

[EtSO₄]) system there are more strong intermolecular interaction and packing effect than in the (TS + [EMIM] [MeSO₃]) system.

Sibiya (2008) reported V_m^E for (methanol or propanol or 2-propanol + [EMIM] [EtSO₄]) binary systems at $T = 298.15$ K over the whole composition range. The $V_{m,\min}^E$ value for (methanol + [EMIM] [EtSO₄]) system at $T = 298.15$ K at $x_1 = 0.3582$ is $-1.171 \text{ cm}^3 \cdot \text{mol}^{-1}$, for (propanol + [EMIM] [EtSO₄]) system at $T = 298.15$ K at $x_1 = 0.4697$ is $-0.599 \text{ cm}^3 \cdot \text{mol}^{-1}$, and for (2-propanol + [EMIM] [EtSO₄]) system at $T = 298.15$ K at $x_1 = 0.3374$ is $-0.452 \text{ cm}^3 \cdot \text{mol}^{-1}$. The $V_{m,\min}^E$ for (methanol + [EMIM] [EtSO₄]) system is more negative than for (propanol or 2-propanol + [EMIM] [EtSO₄]) systems. The larger negative $V_{m,\min}^E$ for (methanol + [EMIM] [EtSO₄]) system than for (propanol or 2-propanol + [EMIM] [EtSO₄]) systems imply that in the (methanol + [EMIM] [EtSO₄]) system there are more strong intermolecular interaction and packing effect than in the (prok2panol or 2-propanol + [EMIM] [EtSO₄]) systems.

Perez *et al.* (2012) reported the density values for alkanes (heptane, octane, nonane or decane + thiophene). The $V_{m,\min}^E$ for (alkane + TS) systems is positive. This indicates that in the (alkane + TS) systems there are repulsive forces existing between the components of the binary mixtures, this effect results in the breaking of hydrogen bonds and an increase in the overall volume of the binary mixtures.

Mahendra *et al.* (2010) reported experimental densities, speed of sound, and refractive index for the (ethyl acetoacetate (EAA) + dichloromethane or chloroform or acetonitrile) binary systems, over the whole composition range at $T = 298.15$ K. The $V_{m,\min}^E$ for (EAA + dichloromethane) system at $T = 298.15$ K at $x_1 = 0.0676$ is $-0.0380 \text{ cm}^3 \cdot \text{mol}^{-1}$. For (EAA + chloroform) system at $T = 298.15$ K at $x_1 = 0.3795$ is $-0.3030 \text{ cm}^3 \cdot \text{mol}^{-1}$ and For (EAA + acetonitrile) system at $T = 298.15$ K at $x_1 = 0.5579$ is $-0.8640 \text{ cm}^3 \cdot \text{mol}^{-1}$. The $V_{m,\min}^E$ for (EAA + acetonitrile) system is more negative than for (ethyl acetoacetate (EAA + dichloromethane or chloroform) systems. The larger negative $V_{m,\min}^E$ for (EAA + acetonitrile) system than for (EAA + dichloromethane or chloroform) systems imply that in the (EAA + acetonitrile) system there are more strong intermolecular interaction and packing effect than in the (EAA + dichloromethane or chloroform) systems.

Gomez *et al.* (2006) reported experimental densities, speed of sound, and refractive indices for (ethanol + [EMIM] [EtSO₄]) binary system over the whole composition of their range at $T = (288.15 \text{ to } 343.15)$ K. The $V_{m,\min}^E$ value for (ethanol+ [EMIM] [EtSO₄]) system at $T = 298.15$ K at $x_1 = 0.9863$ is $-0.081 \text{ cm}^3 \cdot \text{mol}^{-1}$. $V_{m,\min}^E$ for (ethanol + [EMIM] [EtSO₄]) system is negative, this indicate the presence of intermolecular interaction between ethanol and the ionic liquid.

Domanska and Laskowka (2008) determined the experimental densities for (1-propanol + [EMIM] [EtSO₄]) binary system over the whole composition range at $T = 298.15$ K. The $V_{m,\min}^E$ value for (1-propanol + [EMIM] [EtSO₄]) system at $T = 298.15$ K at $x_1 = 0.0036$ is $-0.038 \text{ cm}^3 \cdot \text{mol}^{-1}$. Gomez

et al. (2006) reported the $V_{m,\min}^E$ for (ethanol + [EMIM] [EtSO₄]) system at $T = 298.15$ K at $x_1 = 0.9863$ to be $-0.081 \text{ cm}^3 \cdot \text{mol}^{-1}$. $V_{m,\min}^E$ for the binary mixtures (1-propanol or ethanol + [EMIM] [EtSO₄]) increases in the order ethanol < 1-propanol. $V_{m,\min}^E$ for ethanol is more negative than that for 1-propanol because ethanol can pack into the imidazolium ring resulting in greater intermolecular interaction.

Alonso *et al.* (2010) determined the experimental densities for (2-butanone + pyridine) over the whole range of their composition at $T = 298.15$ K. The $V_{m,\min}^E$ value for (Py + [EMIM] [EtSO₄]) system at $T = 298.15$ K at $x_1 = 0.4$ is $-2.5356 \text{ cm}^3 \cdot \text{mol}^{-1}$, and for (2-butanone + pyridine) system at $T = 298.15$ K at $x_1 = 0.0517$ is $-0.0418 \text{ cm}^3 \cdot \text{mol}^{-1}$. The $V_{m,\min}^E$ for (Py + [EMIM] [EtSO₄]) system is more negative than for the (2-butanone + pyridine) system. The larger negative $V_{m,\min}^E$ for (PY + [EMIM] [EtSO₄]) system than for (2-butanone + pyridine) system imply that in the (Py + [EMIM] [EtSO₄]) system there are more strong intermolecular interaction and packing effect than in the (2-butanone + pyridine) system.

Yadav *et al.* (2014) reported experimental densities for (chloroform or dimethyl sulfoxide + EAA) binary systems over the entire composition range at $T = 298.15$ K. The $V_{m,\min}^E$ value for (chloroform + EAA) system at $T = 298.15$ K at $x_1 = 0.9744$ is $-0.2217 \text{ cm}^3 \cdot \text{mol}^{-1}$. For (dimethyl sulfoxide + EAA) system at $T = 298.15$ K at $x_1 = 0.1663$ is -0.7826 cm^3 . The $V_{m,\min}^E$ for (dimethyl sulfoxide +

EAA) system is more negative than for (chloroform + EAA) system. The larger negative $V_{m,\min}^E$ for (dimethyl sulfoxide + EAA) system than for (chloroform + EAA) system imply that in the (dimethyl sulfoxide + EAA) system there are more strong intermolecular interaction and the packing effect is greater than in the (chloroform + EAA) system.

Saini *et al.* (2011) determined experimental densities for (tetrahydropyran + pyridine) binary system over the whole composition range at $T = (298.15 \text{ to } 308.15) \text{ K}$. The $V_{m,\min}^E$ value for (Py + [EMIM] [EtSO₄]) system at $T = 298.15 \text{ K}$ at $x_1 = 0.4$ is $-2.5356 \text{ cm}^3 \cdot \text{mol}^{-1}$, and for (tetrahydropyran + pyridine) system at $T = 298.15 \text{ K}$ at $x_1 = 0.4642$ is $-0.2190 \text{ cm}^3 \cdot \text{mol}^{-1}$. The $V_{m,\min}^E$ for (Py + [EMIM] [EtSO₄]) system is more negative than for (tetrahydropyran + pyridine) system. The larger negative $V_{m,\min}^E$ for (Py + [EMIM] [EtSO₄]) system than the (tetrahydropyran + pyridine) system imply that in the (Py + [EMIM] [EtSO₄]) system there are more strong intermolecular interaction and packing effect than in the (tetrahydropyran + pyridine) system.

Anantharaj and Banerjee (2011) determined experimental densities for ([EMIM] [SCN] + Py or TS) binary systems over the whole composition range at $T = (298.15 \text{ to } 323.15) \text{ K}$. The $V_{m,\min}^E$ value for ([EMIM] [SCN] + Py) system at $T = 298.15 \text{ K}$ at $x_1 = 0.8$ is $-0.1007 \text{ cm}^3 \cdot \text{mol}^{-1}$, and for ([EMIM] [SCN] + TS) system at $T = 298.15 \text{ K}$ at $x_1 = 0.8$ is $-0.1152 \text{ cm}^3 \cdot \text{mol}^{-1}$. The $V_{m,\min}^E$ for ([EMIM] [SCN] + TS) system is more negative than for ([EMIM] [SCN] + Py) system. $V_{m,\min}^E$ for

thiophene is smaller than that for pyridine because of the similar structure of thiophene and the imidazolium ring (both are 5-membered) resulting in greater intermolecular interaction.

Rodriguez and Brennecke (2006) reported experimental density at $T = (278.15 \text{ to } 348.15) \text{ K}$ for (water + [EMIM] [EtSO₄]) system over the whole composition range. The $V_{m,\min}^E$ value for (Py + [EMIM] [EtSO₄]) system at $T = 298.15 \text{ K}$ at $x_1 = 0.4$ is $-2.5356 \text{ cm}^3 \cdot \text{mol}^{-1}$, and for (water + [EMIM] [EtSO₄]) system at $T = 298.15 \text{ K}$ at $x_1 = 0.5939$ is $-0.415 \text{ cm}^3 \cdot \text{mol}^{-1}$. The $V_{m,\min}^E$ for the (Py + [EMIM] [EtSO₄]) system is more negative than for (water + [EMIM] [EtSO₄]) system. The larger negative $V_{m,\min}^E$ for (Py + [EMIM] [EtSO₄]) system than for (water + [EMIM] [EtSO₄]) system imply that in the (Py + [EMIM] [EtSO₄]) system there are more strong intermolecular interaction and packing effect than in the (water + [EMIM] [EtSO₄]) system.

Maurya *et al.* (2015) reported experimental densities at $T = 303.15 \text{ K}$ for (pyridine + ethanol) binary system over the whole composition range. The $V_{m,\min}^E$ value for (pyridine + ethanol) system at $T = 298.15 \text{ K}$ at $x_1 = 0.0719$ is $0.0587 \text{ cm}^3 \cdot \text{mol}^{-1}$. The $V_{m,\min}^E$ for (pyridine + ethanol) system is positive. This indicates that in the (pyridine + ethanol) system there are repulsive forces existing between the components of the binary mixture, this effect results in the breaking of hydrogen bonds and an increase in the overall volume of the binary mixture.

Gonzalez (2007) reported experimental density, speed of sound, and refractive index for pure [EMIM] [EtSO₄] ionic liquid and for binary mixtures of (methanol or 1-propanol or 2-propanol + [EMIM] [EtSO₄]) at $T = (298.15, 313.15, \text{ and } 328.15) \text{ K}$ over the whole composition range. The

$V_{m,\min}^E$ value for (methanol + [EMIM] [EtSO₄]) system at $T = 298.15$ K at $x_1 = 0.7757$ is -0.912 $\text{cm}^3 \cdot \text{mol}^{-1}$, for (1-propanol + [EMIM] [EtSO₄]) system at $T = 298.15$ K at $x_1 = 0.5159$ is -0.406 $\text{cm}^3 \cdot \text{mol}^{-1}$, and for (2-propanol + [EMIM] [EtSO₄]) system at $T = 298.15$ K at $x_1 = 0.4977$ is -0.558 $\text{cm}^3 \cdot \text{mol}^{-1}$. The $V_{m,\min}^E$ for the (methanol + [EMIM] [EtSO₄]) system is more negative than for (1-propanol or 2-propanol + [EMIM] [EtSO₄]) systems. The larger negative $V_{m,\min}^E$ for (methanol + [EMIM] [EtSO₄]) system than for (1-propanol or 2-propanol + [EMIM] [EtSO₄]) systems imply that in the (methanol + [EMIM] [EtSO₄]) system there are more strong intermolecular interaction and packing effect than in the (propanol or 2-propanol + [EMIM] [EtSO₄]) systems.

Rafiee and Frouzesh (2015) reported experimental density for (allyl alcohol or 1.3-dichloro-2-propanol + [EMIM] [EtSO₄]) binary systems at $T = (298.15$ to $318.15)$ K over the whole composition range. The $V_{m,\min}^E$ value for (allyl alcohol + [EMIM] [EtSO₄]) binary system at $T = 298.15$ K at $x_1 = 0.4939$ is -0.79 $\text{cm}^3 \cdot \text{mol}^{-1}$, and for (1.3-dichloro-2-propanol + [EMIM] [EtSO₄]) binary system at $T = 298.15$ K at $x_1 = 0.9645$ is -0.16 $\text{cm}^3 \cdot \text{mol}^{-1}$. The $V_{m,\min}^E$ for the (allyl alcohol + [EMIM] [EtSO₄]) system is more negative than for the (1.3-dichloro-2-propanol + [EMIM] [EtSO₄]) system. The larger negative $V_{m,\min}^E$ for (allyl alcohol + [EMIM] [EtSO₄]) system than for (1.3-dichloro-2-propanol + [EMIM] [EtSO₄]) system imply that in the (allyl alcohol + [EMIM] [EtSO₄]) system there are more strong intermolecular interaction and packing effect than in the (1.3-dichloro-2-propanol + [EMIM] [EtSO₄]) system.

Table 2.2 below presents Δn data for (ILs + organic solvent) with a common cation or anion or common organic solute obtained from the literature.

Table 2.2 Δn data for (ILs + organic solvent) with a common cation or anion or common organic solute obtained from the literature.

| Author | Systems | Δn |
|--------------------------------|---|-----------------------|
| Anantharaj and Banerjee (2013) | (Py + [EMIM] [MeSO ₃]) | Negative |
| Anantharaj and Banerjee (2013) | (TS + [EMIM] [MeSO ₃]) | Positive and Negative |
| Gomez <i>et al.</i> (2006) | (ethanol + [EMIM] [EtO ₄]) | Negative |
| Shev <i>et al.</i> (2006) | (EAA + ethanol) | Positive |
| Gonzalez <i>et al.</i> (2009) | (1-propanol or ethanol + [EMIM] [EtSO ₄]) | Positive |

Mahendra *et al.* (2010) reported experimental densities, speed of sound, and refractive index for (ethyl acetoacetate (EAA) + dichloromethane or chloroform or acetonitrile) binary systems.

Nath and Pandey (1996) determined experimental refractive index of 1,1,2,2-tetrachloroethane + pyridine, + anisole, + methyl ethyl ketone, and + 1,4-dioxane at 303.15 K.

Anantharaj and Banerjee (2011) determined experimental densities and refractive indices for the binary mixtures of (Py or TS + [EMIM] [EtSO₄]) over the whole composition range. They reported experimental densities at $T = (298.15 \text{ to } 318.15) \text{ K}$, however they reported the experimental refractive index only at 298.15 K. Anantharaj and Banerjee (2013) determined experimental densities and refractive indices for the binary mixtures of (Py or TS + [EMIM] [MeSO₃]) over the whole composition range. They reported experimental densities and refractive index at $T = (298.15 \text{ to } 318.15) \text{ K}$. The Δn_{max} at $T = 298.15 \text{ K}$ at $x_1 = 0.2$ is -0.03254 , for (Py + [EMIM] [MeSO₃]) binary system. And for (TS + [EMIM] [MeSO₃]) binary system, Δn_{max} at $T = 298.15 \text{ K}$ at $x_1 = 0.2$ is 0.08482 .

Gomez *et al.* (2006) determined experimental refractive index for (ethanol + [EMIM] [EtSO₄]) binary system over the whole range of their composition at $T = (288.15 \text{ to } 343.15) \text{ K}$. The Δn_{max} at $T = 298.15 \text{ K}$ at $x_1 = 0.6788$ is -0.037 , for (ethanol + [EMIM] [EtSO₄]) system.

Shev *et al.* (2006), determined the densities and refractive index for (ethyl acetoacetate + ethanol) binary mixture over the whole composition range at $T = (298.15, 308.15 \text{ and } 318.15) \text{ K}$.

The Δn_{max} at $T = 298.15 \text{ K}$ at $x_1 = 0.05$ is 0.00057, for (EAA + ethanol) binary system.

Gonzalez *et al.* (2009) determined the refractive index for (1-propanol or ethanol + [EMIM] [EtSO₄]) binary systems over the whole composition range only at $T = 298.15 \text{ K}$. The Δn_{max} at $T = 298.15 \text{ K}$ at $x_1 = 0.6013$ is 0.0295, for (1-propanol + [EMIM] [EtSO₄]) system, and for (ethanol + [EMIM] [EtSO₄]) binary system, Δn_{max} at $T = 298.15 \text{ K}$ at $x_1 = 0.6033$ is 0.0448.

Table 2.3 below presents k_s data for (ILs + organic solvent) with a common cation or anion or common organic solute obtained from the literature.

Table 2.3 k_s data for (ILs + organic solvent) with a common cation or anion or common organic solute obtained from the literature.

| Author | Systems | k_s |
|-------------------------------|--|----------|
| Gomez <i>et al.</i> (2006) | (ethanol + [EMIM] [EtO ₄]) | Positive |
| Salguero and Fadriqude (2011) | (EAA + water) | Positive |
| Gonzalez (2007) | (methanol or 1-propanol or 2-propanol + [EMIM] [EtSO ₄]) | Positive |
| Gonzalez <i>et al.</i> (2009) | (1-propanol or ethanol + [EMIM] [EtSO ₄]) | Positive |

Gomez *et al.* (2006) reported experimental speed of sound for (ethanol + [EMIM] [EtSO₄]) binary system, as well as for pure components over the whole composition of their range at $T = (288.15$ to $343.15)$ K. The $k_{s, \min}$ at $T = 298.15$ K at $x_1 = 0.10$ is 291.85 T.Pa^{-1} for (ethanol + [EMIM] [EtSO₄]) system. The $k_{s, \min}$ value for the (ethanol + [EMIM] [EtSO₄]) system is positive and this indicates that the components of the binary system are more compressible than the ideal mixture.

Salguero and Fadrique (2011) reported experimental speed of sound for (EAA + water) binary mixture over the whole composition of their range at $T = 298.15$ K. For the (EAA + water) binary mixture, $k_{s, \min}$ at $T = 298.15$ K at $x_1 = 0.0064$ is 432 T.Pa^{-1} . The $k_{s, \min}$ value for the (EAA + water) binary system is positive and this indicates that the components of the binary system are more compressible than the ideal mixture.

Gonzalez (2007) reported experimental density, speed of sound, and refractive index for pure [EMIM] [EtSO₄] ionic liquid and for binary mixtures of (methanol or 1-propanol or 2-propanol + [EMIM] [EtSO₄]) at $T = (298.15, 313.15, \text{ and } 328.15)$ K over the whole composition range.

The $k_{s, \min}$ value for (methanol + [EMIM] [EtSO₄]) system at $T = 298.15$ K at $x_1 = 0.8294$ is $0.03413 \text{ T.Pa}^{-1}$, for (1-propanol + [EMIM] [EtSO₄]) system at $T = 298.15$ K at $x_1 = 0.3360$ is $0.05245 \text{ T.Pa}^{-1}$, and for (2-propanol + [EMIM] [EtSO₄]) system at $T = 298.15$ K at $x_1 = 0.2066$ is $0.05381 \text{ T.Pa}^{-1}$. The results indicate that the components of the three binary systems are more compressible than the ideal mixture, $k_{s, \min}$ follow the order methanol < 1-propanol < 2-propanol.

Gonzalez *et al.* (2009) reported experimental density, speed of sound, and refractive index for the binary mixtures of (1-propanol or ethanol + [EMIM] [EtSO₄]) over the whole composition range at $T = (298.15, 313.15, \text{ and } 328.15)$ K. They reported experimental refractive index only at $T = 298.15$ K over the whole composition range. The $k_{s, \text{ min}}$ value for (1-propanol + [EMIM] [EtSO₄]) binary system at $T = 298.15$ K at $x_1 = 0.0814$ is 283.3 T.Pa^{-1} , and for (ethanol + [EMIM] [EtSO₄]) binary system at $T = 298.15$ K at $x_1 = 0.0476$ is 277.7 T.Pa^{-1} . The results indicate that the components of the two binary systems are more compressible than the ideal mixture, $k_{s, \text{ min}}$ follow the order, ethanol < 1-propanol.

EXPERIMENTAL METHODS AND THEORETICAL FRAMEWORK

A. EXPERIMENTAL METHODS

3.1 Excess molar volumes

3.1.1 Theory

Excess molar volume can be defined as a real liquid mixture either with increase or decrease of volume due to molecular interactions between components of the binary mixture (Patil *et al.* 2011).

$$V_m^E = V_{mixture} - \sum x_i V_i \quad (3.1.1)$$

Where x_i is the mole fraction of component i , $V_{mixture}$ and V_i are the molar volumes of the mixture and components i , respectively.

$$V_m^E = V_{mixture} - (x_1 V_1^\circ + x_2 V_2^\circ) \quad (3.1.2)$$

The change in volume on mixing two liquids, 1 and 2 can be attributed to a number of processes: (a) the breakdown of 1-1 and 2-2 intermolecular interaction which have a positive effect on the volume, (b) the formation of 1-2 intermolecular interaction which results in a decrease of the volume of the mixture, (c) packing effect caused by the difference in the size and shape of the component species and which may have positive or negative effect on the particular species involved and (d) formation of new chemical species (Redhi 2003).

Volume change on mixing of binary mixture, V_m^E at constant pressure and temperature is important in thermodynamics. It serves as an indicator for deviation from ideality of the liquid mixture, the presence of non-ideality in binary liquid mixture can be an indicator of the applicability of the liquid mixture in a specific process, and the volume (V), of a mixture is a function of temperature (T), pressure (P), and number of moles (n).

$$V = V(T, P, n_1, n_2, n_3, \dots, n_f) \quad (3.1.3)$$

At constant pressure and temperature:

$$V = V(n_1, n_2, n_3, \dots, n_f) \quad (3.1.4)$$

The ideal volume of the mixture $V_{m, ideal}$ at atmospheric pressure may be written as:

$$V_{m, ideal} = \sum x_i V_{m, i}^o \quad (3.1.5)$$

Where $V_{m, i}^o$ is the molar volume of the pure species i .

Once the liquids have been mixed together the volume of the mixture $V_{m, mix}$ is not normally, the sum of the volumes of the pure liquids but is given by:

$$V_{m, mix} = (V_{m, mix}) \neq x_1 V_{m, 1} + x_2 V_{m, 2} + \dots + x_i V_{m, i} = \sum x_i V_{m, i}^o \quad (3.1.6)$$

The excess molar volume of mixing, V_m^E is given by:

$$V_m^E = V_{m, mix} - V_{m, pure} = V_{m, real} - V_{m, ideal} = \sum x_i (V_{m, i} - V_{m, i}^o) \quad (3.1.7)$$

Where V_m^E is the excess molar volume at constant temperature and pressure (Patil *et al.* 2011).

$V_{m, i}$ is the partial molar volume of the i^{th} component and $V_{m, i}^o$ is the molar volume of the pure species i .

3.1.2 Experimental methods for measurement of excess molar volumes

The excess molar volume (V_m^E), at a constant concentration of x_1 of component 1 and x_2 of component 2 is given by:

$$V_m^E = V_{m,mix} - (x_1V_1 + x_2V_2) \quad (3.1.8)$$

The excess molar volume (V_m^E), of the binary mixture is measured either directly or indirectly.

The direct method is done by measuring the volume change upon mixing, one typical example is a dilatometric method and indirect method which is done by measuring the density of the pure liquids and the density of the binary mixtures and then calculating the excess molar volume

(V_m^E). The measurements are done using a densimeter and calculating V_m^E , using equation 3.1.7 and 3.1.8 (McLure *et al.* 1967), (Duncan *et al.* 1966), and (Streeti *et al.* 1967). The summary of different kinds of methods used for measurements are stated below.

3.1.2.1 Dilatometer method

This method is used for measuring the excess molar volume (V_m^E), simply by measuring the level of the liquid in the dilatometer capillary before and after the mixing using a cathetometer. The use of this method is advantageous as it requires fewer and less accurate weighing as compared to density methods. Dilatometer method include batch dilatometer and continuous dilution dilatometer. In a batch dilatometer only a single data point per loading of the apparatus is determined and continuous dilution dilatometer allows for the determination of many data points per loading of the apparatus. It is possible to determine excess molar volume values of many liquids since the diameter of dilatometer capillary can be varied on the basis of the magnitude of

V_m^E values. The disadvantage with this method is the change in pressure of the liquids before and after mixing which leads into instrumental error.

(i) Batch method

The batch dilatometer allows the measurement of one data point per loading of the apparatus. It is filled with known masses of pure liquids, which are then separated by mercury. The height of mercury in the calibrated graduated column is measured before and after the mixing of the liquids, the change in the mercury height indicate the volume change. The mixing of the liquids is done by a rotating dilatometer and V_m^E is determined by measuring the change in the height of mercury. The filling of the dilatometer is done using a narrow needle, however it is hard to fill the dilatometer. This is one of the sources of error in the excess molar volume measurement. The results obtained using this method are not accurate because the dilatometer is weighed whilst containing mercury. This leads into an error in mass measurements and in return the V_m^E results become inaccurate (Redhi 2003).

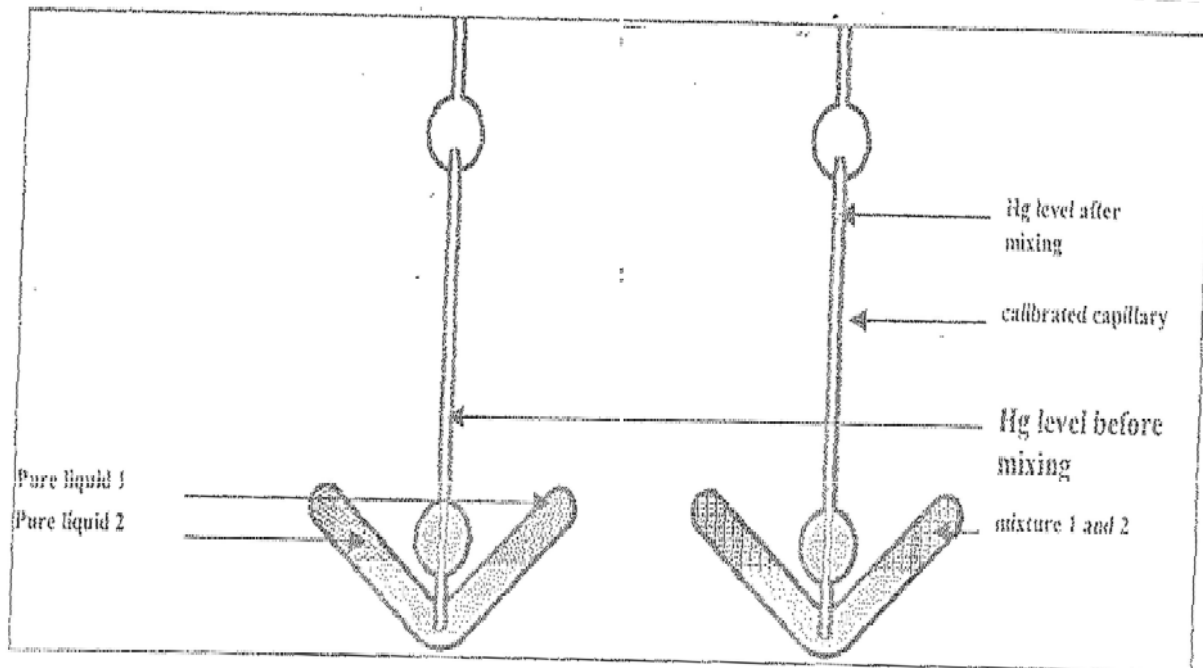


Figure 3.1 Schematic representation of a batch dilatometer (Nevines 1997, Redhi 2003, Sibiya, M. Tech thesis 2008).

(ii) Continuous dilution method

This method is used to measure the excess molar volume (V_m^E), of the binary mixture in a continuous dilution dilatometer. The method allows the determination of many data points per loading of the apparatus. This makes it convenient to use it, because it is not time consuming. The liquid is successively added into the reservoir which contains the other liquid. The liquids are still separated by mercury and height of mercury in the calibrated graduated column is noted before and after the mixing of the liquids. The liquids are progressively mixed in a closed system. After the mixing of the pure liquids, the volume change on mixing is indicated by the change in the height of the mercury in the calibrated graduated column. The excess molar volume is determined from the volume change and the masses of the components. There is a small change in pressure

upon mixing of the liquids, therefore there is a negligible instrumental error when this method is used compare to the batch dilution method.

The volume change measurement is made by filling the burette (e) with one of the pure liquids and the bulb (d) with the other pure liquid. When the dilatometer rotate some of mercury moves into the burette through the capillary (c) to the bottom of the burette. This initiates the mixing of the pure liquids by forcing the pure liquids from the burette into the bulb through the higher capillary (b). The change in the level of the mercury in the calibrated capillary (a) after mixing is noted as the volume change. The change in the height of mercury level is directly proportional to the amount of pure liquid that is displaced. The amount of displacement of pure liquid is used to determine the excess molar volume, (Kumaran and McGlashan. 1977).

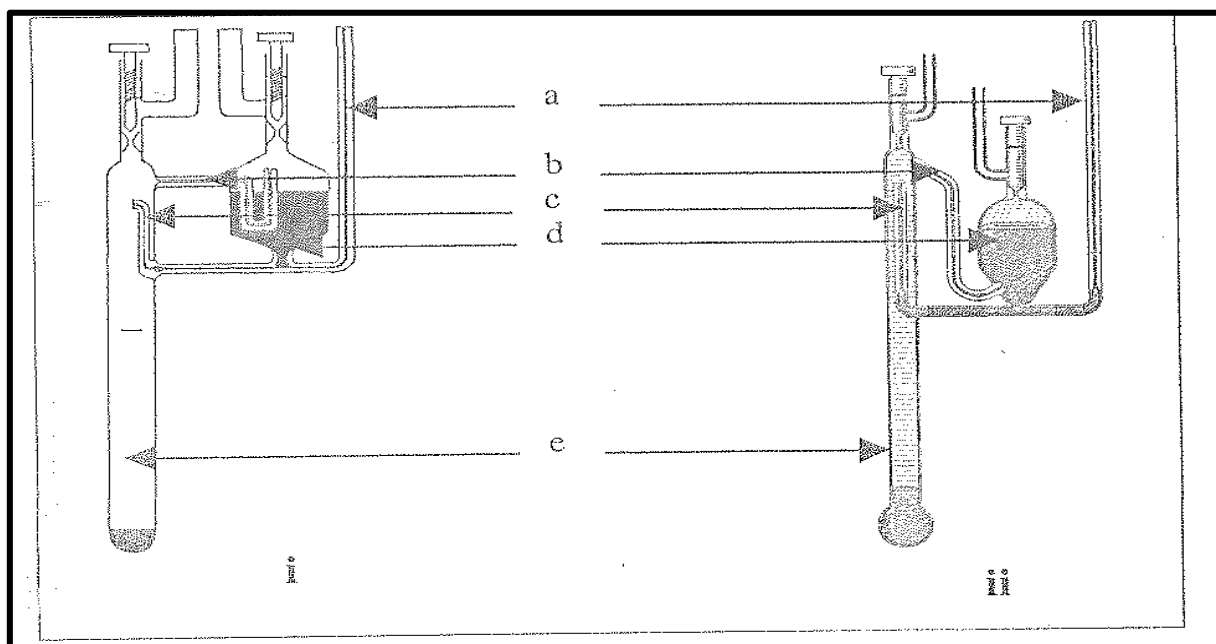


Figure 3.2 Schematic representation of a continuous dilatometer (Bottomly and Scott 1974, Kumaran and McGlashan 1977, Sibiya, M. Tech thesis 2008).

3.1.2.2 Indirect method

This method involves the use of a highly accurate vibrating tube densimeter for V_m^E measurement, it is fully automated which makes the method to be simple. The excess molar volume for binary mixtures are determined using the following equations,

$$V_m^E = \frac{x_1 M_1 + x_2 M_2}{\rho} - \frac{x_1 M_1}{\rho_1} - \frac{x_2 M_2}{\rho_2} \quad (3.1.9)$$

Where x_1 and x_2 are mole fractions, M_1 and M_2 are the molecular masses, and ρ_1 and ρ_2 are densities of the pure components, where 1 and 2 refers to the organic solvent and IL, respectively.

3.1.2.3 Pycnometers

This is a density measurement method which is used to determine V_m^E , the density measurement depends on the composition of the liquid mixture, and therefore it is important to determine the composition of the liquid mixture with high precision. The pycnometer is filled with known masses of the liquid mixture. However, the mixing of the liquid components is not good. This could lead into poor precision, but upon careful measurement of the liquid components and good mixing of liquid components precise results are obtained. A pycnometer capable of a precision of 5×10^{-6} g.cm⁻³ for density measurement translates into a precision of 0.00001 cm³.mol⁻¹ for V_m^E has been reported by (Wood and Brusie 1943). A schematic representation of a pycnometer is shown in figure 3.3.

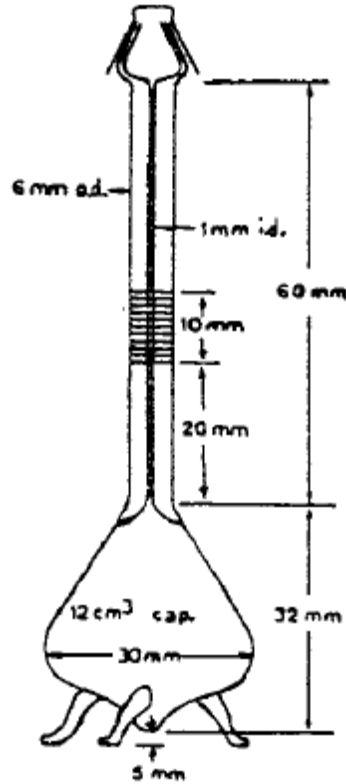


Figure 3.3 Schematic representation of pycnomer (Wood and Brusie 1943).

3.2 Speed of sound and isentropic compressibility

3.2.1 Theory

The speed of sound is a property in the study of binary mixtures. When used along with other properties, allows the derivatization of a wide range of thermophysical properties including isentropic compressibility, isobaric thermal expansion coefficient, heat capacities. These properties are derived directly or indirectly from the speed of sound, the isentropic compressibility in particular, is indirectly derived from the speed of sound. The derived properties are important for an accurate design and optimization of a number of chemical processes (Hasan *et al.* 2010). The speed of sound and density are used to calculate the isentropic compressibility by means of the Newton Laplace equation:-

$$k_s = \left(\frac{1}{\rho u^2} \right) \quad (3.2.1)$$

3.2.2 Mittal ultrasonic interferometer M-81G

There are many instruments used for the measurement of speed of sound, Mittal ultrasonic interferometer M-81G is an example. This instrument is used for the measurement of the speed of sound, the device is complicated to use. The disadvantage of this instrument is that it leads to a high degree of uncertainty. This occurs because the instrument take a series of readings and then calculate the average reading. The instrument consist of two important components namely: (a) high frequency generator, which is used to generate ultrasonic waves in the liquid contained in the measuring cell. The high frequency generator induces ultrasonic waves by exciting the quartz plate located at the bottom of the measuring cell at its peak frequency thus producing ultrasonic waves in the liquid. A macro-ammeter senses the changes in the current and controls for the sensitivity regulation and initial adjustments of the micro-ammeter are provided on the high frequency generator. (b) Measuring cell, is used to maintain the temperature of the liquid and keep it constant during the experiment. The photograph of Mittal Ultrasonic interferometer M-81G instrument is shown in figure 3.4.



**Figure 3.4 Photograph of the Mittal ultrasonic interferometer M-81G instrument.
(Taken from Instruction Manual of Mittal Enterprises Ultrasonic
Interferometer for Liquids)**

The working principle of the Mittal ultrasonic interferometer M-81G instrument is described below.

The principle used in the measurement of velocity (v) is based on the accurate measurement of the wavelength (λ) in the medium. The quartz crystal fixed at the bottom of the cell produce ultrasonic waves of known frequency (f). A movable metallic plate which is parallel to the quartz crystal is responsible for reflecting the waves. If the separation between these two plates is exactly a whole

multiple of the sound wavelength, standing waves are formed in the medium. This acoustic resonance gives rise to an electrical reaction on the generator driving the quartz crystal and the anode current of the generator becomes a maximum. From the knowledge of wavelength, (λ), the velocity or speed of sound, (u), they can be obtained by the relation:

Speed of sound = wavelength \times frequency

$$u = \lambda \times \nu \quad (3.2.2)$$

In this work a DSA 5000 M is used for the determination of speed of sound and isentropic compressibilities. The description of the instrument is given in chapter 4 and in section 4.1.5.

3.3 Refractive indices and molar refraction

3.3.1 Theory

The study and knowledge of the refractive index property at different temperatures of binary mixtures enables one to determine the structure and further characterize the binary mixture. The refractive index measurements are useful to assess the purity of pure components (Shukla *et al.* 2012).

The refractive index, n , is a constant for a pure solvent and can be defined as:

$$n = \frac{\text{speed of light in material 1}}{\text{speed of light in material 2}} \quad (3.3.1)$$

The equation (3.13) can be interpreted as $n_{1,2}$. This means the refractive index in material 2 relative to material 1.

The incident light in a vacuum also called the absolute refractive index of material is 1, however air tend to diffract the incident light to a slight angle and therefore, the practical absolute refractive index in a vacuum is approximately 1.008.

The refractive index is the ratio of the sine of angle of incident (medium 1) θ_1 and the angle of refraction of (medium 2) θ_2 and is given by (Iglesias-Otero *et al.* 2008):

$$n = \frac{\sin\theta_1}{\sin\theta_2} \tag{3.3.2}$$

3.3.2 ATAGO RX 5000 refractometer

The ATAGO RX 5000 refractometer has been developed to a high level of efficiency and effectiveness. Figure 3.5 is the photograph of an ATAGO RX 5000 refractometer.

The instrument is fast, easy to use and gives accurate measurement. The instrument is used to measure the refractive index and gives the results in just four seconds. It report the refractive index results with a very small degree of uncertainty, i.e. ($nD \pm 0.03\%$). The operation of the instrument is simple for most measurements, only two of the five operation keys are needed. This makes the instrument more efficient and easy to use. The performance of the instrument is not compromised in spite of the nature of the sample. The instrument is approximately one-half the size and weight compared to the previous models (ATAGO RX-1000 and RX-3000). It is an excellent choice for measurement used in the structure determination and characterization of liquid mixtures. It is not time consuming as the time required for measurement is cut to four second, three times faster than previous models (ATAGO RX-1000 and RX-3000).

The ease of measurement that characterizes the RX-5000 increases efficiency and makes work easier. Most operations can be carried out with just two of the unit's five keys. All data, including date, time, current temperature, measurement result, measurement temperature, etc., are clearly shown on the large display.



Figure 3.5 Photograph of an ATAGO RX 5000 Refractometer.

(Taken from the ATAGO manual for the refractometer)

B. THEORETICAL FRAMEWORK

3.4 Lorentz-Lorenz equation

The Lorentz-Lorenz was derived by Lorenz only, it is the most widely used theoretical method for predicting the refractive index for binary mixtures of liquids (Herraez and Belda 2006). The refractive index is predicted theoretical using the equation:

$$n = \frac{n_L^2 - 1}{n_L^2 + 2} = \Phi_1 \frac{n_1^2 - 1}{n_1^2 + 2} + \Phi_2 \frac{n_2^2 - 1}{n_2^2 + 2} \quad (3.4.1)$$

where n_L is the refractive index of the mixture according to Lorentz-Lorenz equation; Φ_1 and Φ_2 are the volume fractions of a solvent and ionic liquid which are calculated from volume

determination based on the mass and density measurements, and n_1 and n_2 are the refractive indices of the solvent and ionic liquid, respectively.

Most techniques for determining refractive indices are fast, precise, and accurate. In most cases a small amount of sample is required to do the analysis. In most cases the refractive index is measured together with density and the results tend to be accurate and precise. The techniques used to give proofs of the purity of the designated samples are often inexpensive, (Ziegler *et al.* 1966). In the present time these two quantities have rarely been measured together despite their strong correlation as shown in the Lorentz-Lorenz equation, (Hirschfelder *et al.* 1964) and (Born *et al.* 1983).

$$\left(\frac{n^2 - 1}{n^2 + 2} \right) V_m = \frac{N_A \alpha}{3\epsilon_0} \quad (3.4.2)$$

Where n is the refractive index, V_m is the molar volume, N_A is the Avogadro's number, ϵ_0 is the permittivity of vacuum and A , the mean molecular polarizability. From this equation, the molar refraction, R , can be defined as follows:

$$R = \left(\frac{n^2 - 1}{n^2 + 2} \right) V_m \quad (3.4.3)$$

Simple calculations show that, for a hard-core spherical model, (Wangsness *et al.* 1986), $A = 4\pi\epsilon_0 a^3$, A , being the sphere radius. If one substitutes this expression into equation 3.4.2 yields $R = NA4\pi a^3/3$; therefore, R represents the hard-core molar volume. These equations are only applicable at the zero frequency limit, they have proved to be applicable at optical frequencies in non-highly conductive, non-magnetic materials, (Brocos *et al.* 2003). The molar refraction and molar volume can be used to obtain the molar free volume, V_{mf} which represents the volume not

occupied by molecules or ions, simply as $V_{mf} = V_m - R$. This free volume appears in many liquid-state models, for instance in those based on the famous van der Waals equation-of-state. Therefore, a joint analysis of density and refractive index can provide highly useful information about the volumetric behaviour of a system.

The study of these magnitudes for binary mixtures presents some difficulties, since their values for an ideal solution are not as easily defined as those of typical solutions for thermodynamics quantities such as the volume, heat capacity, or enthalpy. This is a result of the refractive index being by no means an equilibrium property; in fact, it is determined at frequencies in the region of 10^{15} Hz, which is very far from the zero frequency. Many definitions of the “ideal” refractive index and molar refraction are based on analogies with other quantities and on wrong, bold surmises, (Ritzoulis and Fidantsi 2000), (Nath and Mishra 1998), and (Casas *et al.* 2000).

Very simple, reasonable assumptions are used in order to establish meaningful definitions of these “ideal” quantities and obtain results not only consistent with thermodynamic data, but also useful with a view to interpreting microscopic phenomena related to the mixing process (Marchetti *et al.* 1999). The ideal molar refraction is obtained using this equation:

$$R^{id} = xR_1 + (1-x)R_2 \quad (3.4.4)$$

Where x is the mole fraction of component 1 and subscripts 1 and 2 denote pure product properties. The deviation from an ideal mixture, which is equivalent to an excess function for an equilibrium quantity, is given by $\Delta R = R - R^{id}$. If R is assumed to be equivalent to a hard-core volume, then ΔR should be small relative to the excess volume since changes in volume upon mixing are known to result mainly from rearrangement at relative positions of the particles forming the mixture, (Brocos *et al.* 2003) (i.e. changes in free volume).

Therefore, one can anticipate the hard-core volume of the particles to change very little from the pure liquids to a mixture, and hence the molar refraction of the mixture to be very similar to R^{id} . The application of equation 3.4.4 to real mixtures has provided the expected results (i.e. very small ΔR values relative to excess volumes (Brocos *et al.* 2003 and 2002); by contrast, other definitions such as that which establishes R^{id} by weighing pure-product molar refractions with volume fractions, can provide ΔR values that are even higher than excess volumes (Fermeglia and Torriano 1999).

A better definition of the “ideal” refractive index can be obtained from those of the ideal volume and “ideal” molar fraction, using equation 3.4.4, by assuming both quantities obey the volume additivity rule in terms of mole fractions. Building from these assumptions and equation 3.4.4, n^{id} can be calculated using:

$$n^{id} = \left(\frac{n_1^2 n_2^2 + 2\phi n_1^2 + 2(1-\phi)n_2^2}{2 + \phi n_2^2 + (1-\phi)n_1^2} \right)^{1/2} \quad (3.4.5)$$

Where $\phi = \frac{x_1 V_{m,1}}{x_1 \frac{M_1}{\rho_1} + x_2 \frac{M_2}{\rho_2}}$ is the volume fraction and $V_{m,1}$ the molar volume of the first

component. Under the assumption that the difference between the refractive indices of the two components is small, equation 3.4.5 can be substantially simplified, (Missen 1969) to

$$n^{id} = \phi n_1 + (1-\phi)n_2.$$

The deviation of the refractive index is defined as $\Delta n = n - n^{id}$, n^{id} is given by equations 3.4.4 or 3.4.5. This latter definition of n^{id} has mostly been used and provided good, consistent results (Brocos *et al.* 2003), (Marchetti *et al.* 1999), and (Mosteiro *et al.* 2001).

3.4.1 Prediction of density by the Lorentz-Lorentz (L-L) approximation

3.4.1.1 Correlations and predictions

Correlation of excess molar volume by the Lorentz-Lorentz approximation. Iglesias-Otero *et al.*, calculated the V_m^E in an ideal mixture using the equation:

$$V_m^E = (-\Delta n) \frac{3R(n^{id} + n)}{(n^2 - 1)(n^{id})^2 - 1} = (-\Delta n) f(R, n^{id}, n) \quad (3.4.6)$$

For the refractive index in an ideal mixture (Iglesias-Otero *et al.* 2008) and (Brocos *et al.* 2003) proposed:

$$n^{id} = \left(\frac{n_1^2 n_2^2 + 2\phi_1 n_1^2 + 2\phi_2 n_2^2}{2 + \phi_1 n_2^2 + \phi_2 n_1^2} \right)^{1/2} \quad (3.4.7)$$

Where $\phi_1 = x_1 V_m$, $1/V_m^{id}$ is the volume fraction and V_m , V_m^{id} is the molar volume of pyridine or ethyl acetoacetate.

3.4.1.2 Prediction of density or refractive index

The Lorentz-Lorentz equation is used for predicting the density (ρ), which is related to refractive index n , by:

$$\rho = \frac{\left(\frac{n^2 - 1}{n^2 + 2} \right) (x_1 M_1 + x_2 M_2)}{\left(\frac{n_1^2 - 1}{n_1^2 + 2} \right) x_1 \frac{M_2}{\rho_2} + x_2 \left(\frac{n_2^2 - 1}{n_2^2 + 2} \right) \frac{M_2}{\rho_2}} \quad (3.4.8)$$

By using equation 3.4.8, n can be calculated from pure-product density and refractive index data and from experimental density of the mixture. The equation for n is given below:

$$n = \left(\frac{\left[\left(\frac{n_1^2 - 1}{n_1^2 + 2} \right) x_1 \rho \frac{M_1}{\rho_1} + x_2 \left(\frac{n_2^2 - 1}{n_2^2 + 2} \right) \rho \frac{M_2}{\rho_2} \right] + [x_1 M_1 + x_2 M_2]}{\left[x_1 M_1 + x_2 M_2 \right] - \left[\left(\frac{n_1^2 - 1}{n_1^2 + 2} \right) x_1 \rho \frac{M_1}{\rho_1} + x_2 \left(\frac{n_2^2 - 1}{n_2^2 + 2} \right) \rho \frac{M_2}{\rho_2} \right]} \right)^{1/2} \quad (3.4.9)$$

Table 5.8 list the root-mean-square deviation (σ), for excess molar volume, density, and refractive index for the binary mixtures at $T = (298.15, 303.15, 308.15, 313.15, \text{ and } 318.15)$ K.

The Lorentz-Lorenz equation gives a poor correlation for the excess molar volume, but is a good predictor of density or refractive index.

3.5 Redlich-Kister polynomial

The Redlich-Kister polynomial was used to fit the V_m^E , k_s and Δn data (Redlich and Kister 1948) at the temperatures $T = (298.15, 303.15, 308.15, 313.15, \text{ and } 318.15)$ K. The Redlich-Kister equation for the binary mixture is given below.

$$Z = x_1 x_2 \sum_{i=0}^N A_i (2x - 1)^i \quad (3.5.1)$$

Where Z is the deviation property; x_1 is the mole fraction of pyridine or ethyl acetoacetate or thiophene; x_2 is the mole fraction of the ionic liquid; N is the degree of the polynomial expansion; A_i is the Redlich-Kister parameters for the system. The fitting parameters are given in table 5.7, together with the root-mean-square deviations (σ).

$$\sigma = \left(\frac{\sum_i^n (Z_{\text{exp}} - Z_{\text{cal}})^2}{N} \right)^{1/2} \quad (3.5.2)$$

Where Z_{exp} , Z_{cal} , and N are the values of the experimental and calculated property and the number of experimental data points, respectively

INSTRUMENTATION AND EXPERIMENTAL PROCEDURE

A. INSTRUMENTATION FOR EXCESS MOLAR VOLUME, ISENTROPIC COMPRESSIBILITY, AND CHANGE IN REFRACTIVE INDEX

4.1 Apparatus and technique

4.1.1 Density and sound velocity meter (DSA 5000 M)

In this work, the density (ρ) and speed of sound (u) were measured using an Anton Paar DSA 5000 M vibrating U-tube densimeter. The instrument measures these two different kinds of physical properties using one sample. The instrument is equipped with a density cell and a speed of sound cell and is highly accurate and precise for the measurement of the two separate properties. The temperature of the two separate cells is controlled using a built-in Peltier thermostat. It is controlled to ± 0.02 K.

4.1.2 Definition of density

The density (ρ), of a sample is defined as the mass (m), divided by the volume (V):

$$\rho = \frac{m}{V} \tag{4.1}$$

Density values are highly temperature dependent.

4.1.3 Oscillating U-tube method

In this method the sample is introduced into a U-shaped borosilicate glass tube that is excited to vibrate at its peak frequency. This frequency changes depending on the density of the sample. The

determination of the characteristic frequency, followed by mathematical conversion, the density of the sample is determined. Figures 4.1 and 4.2 shows the photographs of the

DSA 5000 M and the DSA 5000 M together with the RXA 156 and Xsample 452. The density (ρ), is calculated from the quotient of the period of oscillation of the U-tube and the reference oscillator:

$$\rho = KA \times Q_2 \times f_1 - KB \times f_2 \quad (4.1.1)$$

KA, KB Apparatus constant

Q_2 Quotient of the period of oscillation of the U-tube divided by the period of oscillation of the reference oscillator.

f_1, f_2 Correction terms for temperature, viscosity and non-linearity.

The value of the density is displayed on the LCD screen. The DSA 5000 M is coupled with a computer which is loaded with software that stores all the measured density values.



Figure 4.1 Photograph of the density and sound velocity meter (DSA 5000 M).

(Taken from Instruction Manual of an Anton Paar DSA 5000 M)



Figure 4.2 Photograph of the DSA 5000 M along with RXA 156 and Xsample 452.

(Taken from Instruction Manual of an Anton Paar DSA 5000 M)

4.1.4 Sound velocity analyser

The sample is placed into the sound velocity measuring cell that is surrounded by an ultrasonic transmitter on the one side, and a receiver on the other side. Then the transmitter sends sound waves of a known period of time through the sample. The speed of sound (u), can be calculated by using the period of the sound waves and the distance between the transmitter and receiver.

$$u \equiv \frac{l \times (1 \div 1.6 \times 10^{-5} \times \Delta T)}{\frac{P_s}{512} - A \times f_3} \quad (4.1.2)$$

Where l is the original path length of the sound waves, ΔT is the deviation in temperature to 278.15 K, P_s is the oscillation period of the received sound waves, A , is an apparatus constant for speed of sound, and f_3 is the correction term for temperature. The density and speed of sound are more temperature dependent, therefore the measuring cells are thermostated precisely using the Peltier elements.

4.1.5 Features of DSA 5000 M

4.1.5.1 Accuracy

DSA 5000 M instrument is equipped with the most developed digital density and speed of sound technology where:

- The instrument is specially adjusted with standards of high viscosity and high density, this lead to an enhanced precision when samples with high viscosity and high density are used.

- DSA 5000 M is equipped with a thermo balance which is an additional reference oscillator that provides long-term stability and allows precise measurements over the whole temperature range of the instrument with only one adjustment at 293.15 K.
- The time of oscillation of the U-tube is measured by optical pickups.
- Two integrated Pt 100 platinum thermometers together with the Peltier elements provide a high precise thermostating of the sample.
- Viscosity-related errors are corrected automatically over the full viscosity range by measuring the damping effect of the viscous sample followed by mathematical correction for the density value.

4.1.5.2 Error detection

- Filling Check: The instrument automatically detects gas bubbles in the density measuring cell by an advanced analysis of its oscillation pattern and generates a warning message.
- A major source of measuring errors when using a density and speed of sound meter are gas bubbles in the measuring cells. To reduce the formation of gas bubbles, an Anton Paar introduces a new feature: U-View using a real-time camera with zoom function, the U-tube can be visually inspected for gas bubbles in the density measuring cell.

Specifications of the DSA 5000 M are given in table 4.1.

Table 4.1 Specifications of the DSA 5000 M.

| | |
|--|----------------------------|
| Measuring range density | 0 to 3 g/cm ³ |
| Measuring range speed of sound | 1000 to 2000 m/s |
| Pressure range | 0 to 3 bar |
| Repeatability density | 0.000001 g/cm ³ |
| Measuring range temperature | 298.15 to 343.15 K |
| Repeatability speed of sound | 0.1 m/s |
| Measuring time per sample | 1 to 4 min |
| Repeatability temperature | 298.15 K |
| Sample volume | approximately 3 ml |
| Automatic bubble detection | Yes |
| Reference oscillator | Yes |
| Visual check of the density measuring cell | Camera |
| Ambient air pressure sensor | Yes |

4.1.5.3 An overview of an Anton Paar refractive index analyzer RXA 156

The RXA 156 module is equipped with a macro flow cell and an integrated Peltier thermostat, to ensure automatic and accurate control of the temperature. A macro flow cell and an integrated Peltier thermostat ensure fast and non-destructive refractive index (RI) measurements.

4.1.5.4 Features of an Anton Paar refractive index analyzer RXA 156

- Simple adjustment of the DSA 5000 M and RXA 156 using air and water in one procedure.
- RXA 156 instruments and DSA 5000 M are used separately.
- Automatic filling and cleaning of the DSA 5000 M and RXA 156 sample.
- It can be combined with a DMA 4100/4500/5000 M, DSA 5000 M or Soft Drink Analyzer.

One measuring cycle, three sample parameters

- It is fast and gives reliable results.
- It saves time by simultaneously determining the density, sound velocity, and refractive index.

Reliable measuring methods

- Highly accurate measurement of the angle of total reflection for measuring the refractive index.
- Established U-tube method for density measurement.

Table 4.2 below lists the specifications of the refractometer RXA 156.

Table 4.2 Specifications of the refractometer RXA 156.

| Refractive Index | |
|----------------------------------|-----------------------|
| Measuring range | 1.32 – 1.56 <i>nD</i> |
| Resolution | 0.000001 |
| Accuracy | 0.00002 |
| Temperature | |
| Measuring temperature | 298.15 to 343.15 K |
| Resolution | 298.15 K |
| Accuracy | 298.15 K |
| Stability | 298.15 K |
| Speed of temperature change from | 20 s |
| Ambient temperature | 298.15 K |

4.2 Chemicals

The IL (CAS No.3425-73-75-5), ethyl acetoacetate (CAS No.141-78-6), thiophene (CAS No. 110-02-1), and pyridine (CAS No. 110-86-1) were purchased from Aldrich and Fluka with mass percent purity > 99.0%. The water content of the IL, pyridine, ethyl acetoacetate, and thiophene were measured using a Metrohm 831 Karl-Fischer coulometer and was found to be 0.007%, 0.01%, 0.2% and 0.02%, respectively. For the test system, the chemicals used were Heptane (CAS No.142-82-5) and ethanol (CAS No.64-17-5). The water content of heptane and ethanol were measured using a Metrohm 831 Karl-Fischer coulometer and was found to be 0.0020% and 0.0009%, respectively. The purity of the IL, ethyl acetoacetate, thiophene, and pyridine was assessed by a comparison of the experimental density, speed of sound, and refractive index with literature values at the experimental temperatures and are given in table 4.4. Densities, speeds of sound, and refractive indices of IL and organic solvents at the experimental temperatures are in good agreement with the corresponding literature values. The IL, ethyl acetoacetate, thiophene, and pyridine were used without further purification. The purity of the ionic liquid is very low (≥ 95), the supplier did not have a highly purified ionic liquid at the time the chemical was bought. The density data is not agreed with reported literature data, because the purity of the chemicals used in this work is relatively low and this was caused by the presence of moisture in the chemicals.

Table 4.3 below lists the chemicals, suppliers, and mass % purity.

Table 4.3 Chemicals, Suppliers, and Mass % Purity.

| Chemicals | Suppliers | Mass % Purity |
|----------------------------|---------------|---------------|
| [EMIM][EtSO ₄] | Sigma Aldrich | ≥95 |
| PY | Sigma Aldrich | ≥99.0 |
| EAA | Sigma Aldrich | ≥99.0 |
| TS | Sigma Aldrich | ≥99.0 |
| Heptane | Sigma Aldrich | ≥99.0 |
| Ethanol | Sigma Aldrich | ≥99.0 |

Table 4.4 below present the comparison of experimental and literature density (ρ), speed of sound (u), and refractive index (n), of pure components at $T = (298.15, 303.15, 308.15, 313.15$ and $318.15)$ K.

Table 4.4 Comparison of experimental and literature density (ρ), speed of sound (u), and refractive index (n), of pure components at $T = (298.15, 303.15, 308.15, 313.15$ and $318.15)$ K.

| Component | T (K) | ρ (g·cm ⁻³) | | u (m·s ⁻¹) | | n | |
|----------------------------|---------|------------------------------|---|--------------------------|---|-----------|--|
| | | This Work | Lit. | This Work | Lit. | This Work | Lit. |
| [EMIM][EtSO ₄] | 298.15 | 1.2338 | 1.24230 (Zafarani and Shekaari 2010) 1.23915 (Khupse and Kumar 2010) 1.23737 (Khupse and Kumar 2010) | 1682.4 | 16830 (Manuel <i>et al.</i> 2008) | 1.4789 | 1.4789 (Anantharaj 2011) 1.4795 (Rabari <i>et al.</i> 2014) |
| | 303.15 | 1.2304 | 1.22920 (Khupse and Kumar 2010) | 1668.8 | 1666.6 (Fortin <i>et al.</i> 2013) | 1.4774 | 1.4776 (Brocos <i>et al.</i> 2003) |
| | 308.15 | 1.2272 | 1.22350 (Rabari <i>et al.</i> 2014) | 1655.4 | 1654.0 (Fortin <i>et al.</i> 2013) | 1.4760 | 1.4763 (Brocos <i>et al.</i> 2003) |
| | 313.15 | 1.2240 | 1.22350 (Rabari <i>et al.</i> 2014) | 1642.0 | 1641.6 (Fortin <i>et al.</i> 2013) | 1.4750 | 1.4753 (Fortin <i>et al.</i> 2013) |
| | 318.15 | 1.2208 | 1.22060 (Rabari <i>et al.</i> 2014) | 1628.0 | 1629.2 (Fortin <i>et al.</i> 2013) | 1.4737 | 1.4739 (Fortin <i>et al.</i> 2013) |
| Py | 298.15 | 0.9783 | 0.97824 (Alvarez <i>et al.</i> 2011) 0.97825 (Vercher <i>et al.</i> 2010) 0.97822 (Manuel <i>et al.</i> 2008) | 1417.9 | 1416.1 (Alvarez <i>et al.</i> 2011) 1417.8 (Manuel <i>et al.</i> 2008) | 1.5067 | 1.5074 (Gonzalez <i>et al.</i> 2007) 1.5074 (Manuel <i>et al.</i> 2008) |
| | 303.15 | 0.9732 | 0.97322 (Vercher <i>et al.</i> 2010) 0.97281 (Sheu and Tu 2006) | 1397.9 | 1398.0 (Vercher <i>et al.</i> 2010) 1398.6 (Gonzalez <i>et al.</i> 2007) | 1.5038 | 1.5025 (Manuel <i>et al.</i> 2008) 1.5047 (Alvarez <i>et al.</i> 2011) |
| | 308.15 | 0.9682 | 0.96817 (Vercher <i>et al.</i> 2010) | 1377.6 | 1377.1 (Sharma <i>et al.</i> 2013) | 1.5009 | 1.5016 (Royal <i>et al.</i> 2010) |
| | 313.15 | 0.9631 | 0.96800 (Vercher <i>et al.</i> 2010) | | | | |
| | 318.15 | 0.9580 | | | | | |
| EAA | 298.15 | 1.0234 | 1.02120 (Royal <i>et al.</i> 2010) | 1333.3 | 1331.0 (Royal <i>et al.</i> 2010) | 1.4187 | 1.4192 (Royal <i>et al.</i> 2010) |
| | 303.15 | 1.0530 | 1.05250 (Royal <i>et al.</i> 2010) | | | 1.4148 | 1.4145 (Royal <i>et al.</i> 2010) |
| | 308.15 | 1.0130 | 1.01020 (Royal <i>et al.</i> 2010) | | | 1.4125 | 1.4120 (Royal <i>et al.</i> 2010) |
| | 313.15 | | | | | | |
| | 318.15 | | | | | | |
| TS | 298.15 | 1.0586 | 1.05840 (Rabari <i>et al.</i> 2014) | | | 1.5251 | 1.5257 (Nayak <i>et al.</i> 2003) |
| | 303.15 | 1.0182 | 1.01490 (Rabari <i>et al.</i> 2014) | | | | |
| | 313.15 | 1.0466 | 1.04650 (Rabari <i>et al.</i> 2014) | | | | |
| | 308.15 | 1.0406 | 1.04050 (Rabari <i>et al.</i> 2014) | | | | |
| | 318.15 | 1.0346 | 1.03440 (Rabari <i>et al.</i> 2014) | | | | |

Standard uncertainties u are $u(T) = \pm 0.03$ K, $u(p) = \pm 0.05$ MPa and the combined expanded uncertainty U_c in density, speed of sound, and refractive index measurements were less than $U_c(\rho) = \pm 4 \cdot 10^{-4}$ g·cm⁻³, $U_c(u) = \pm 1.0$ m·s⁻¹ and $U_c(n) = \pm 4 \cdot 10^{-4}$, respectively (0.95 level of confidence).

4.3 Preparation of binary mixtures

An OHAUS mass balance with a precision of ± 0.0001 g was used to determine the mass of each component of the binary mixture. The estimated uncertainty in the mole fraction was ± 0.0004 . The uncertainty in pressure was ± 0.05 MPa. The binary mixtures were prepared by transferring via a syringe the pure liquids into stoppered vials to prevent evaporation and the mixtures were shaken to ensure homogeneity of the samples. The density and speed of sound were measured using an Anton Paar DSA 5000 M vibrating U-tube densimeter set at the experimental temperatures with an accuracy of ± 0.02 K in temperature. The frequency at which the sound velocity was measured was set at 3 MHz (Vaid *et al.* 2015). The uncertainty in density and speed of sound was ± 0.0004 g·cm⁻³ and ± 1.0 m·s⁻¹, respectively. An Anton Paar RXA 156 refractometer with an accuracy of ± 0.03 K in temperature was used to measure the refractive index. The uncertainty in refractive index was ± 0.0004 . The calibration of the instruments was done as per previously published work. The error in V_m^E , k_s and Δn was ± 0.004 cm³·mol⁻¹, $\pm 0.09 \cdot 10^{10}$ T·Pa⁻¹ and ± 0.0001 , respectively.

B. EXPERIMENTAL PROCEDURE

4.4 Density and speed of sound

The density and the speed of sound were measured using an Anton Paar DSA 5000 M vibrating U-tube densimeter with an accuracy and repeatability of ± 0.001 K for temperature, ($\pm 5 \cdot 10^{-6}$ and $\pm 10^{-6}$) g·cm⁻³ for density, and (± 0.01 and ± 0.1) m·s⁻¹ for speed of sound. The instrument consists of a density and speed of sound cell. An instrument built-in Peltier thermostat controls the cell temperature. The cell was cleaned with ethanol and then dried with acetone in between

measurements. The process was fully automated; an Xsample 452 performs the cleaning and drying process after each run. All the sample residues dissolved in ethanol and washed away from the cell into the waste. Acetone was used to ensure that the measuring cell is free of ethanol; acetone is a highly volatile organic solvent thus is easily evaporated by purging a stream of dry air which removes acetone and dry the measuring cell. After completing the cleaning process, the instrument was then calibrated with ultra-pure water and ambient air. This was done in order to validate the accuracy with which the instrument measures the density and speed of sound. The binary mixture is prepared and placed into a 12 mL vial and the vial is capped to prevent sample loss. Each vial is placed onto the Xsample 452 with a 48 position magazine. The instrument automatically detects the vial in the connected Xsample 452. The sampler automatically fills the binary mixtures from each vial into the measuring cell of the DSA 5000 M. The filling process is efficient with no sample loss or formation of bubbles or evaporation. After each completed measurement, the measuring cell is cleaned with ethanol and washed with acetone followed with subsequent drying with air. The density and speed of sound results are shown simultaneously on the computer software.

4.5 Refractive indices

The refractive indices of the binary mixtures were measured using an Anton Paar RXA 156 refractometer with an accuracy and repeatability of ± 0.03 K for temperature and $\pm 2 \cdot 10^{-5}$ for refractive index. The Anton Paar RXA 156 refractometer is equipped together with DSA 5000 M, this makes it possible to measure the refractive indices with RXA 156 separately. The refractive indices results are measured, displayed, saved and can be easily retrieved by pressing the export or print button. The computer software or LED display show the results for density, speed of sound, and refractive indices. The calibration of the instrument was done by measuring the refractive

index of ultra-pure water and comparing it with the true value prior to each measurement. The calibration was evaluated with the pre liquids of known refractive indices.

4.6 Systems studied in this work

The physical properties: density, speed of sound, and refractive index were measured for the binary mixtures over the complete mole fraction range using an Anton Paar DSA 5000 M vibrating U-tube densimeter and an Anton Paar RXA 156 refractometer, respectively. The measurements were done at $T = (298.15, 303.15, 308.15, 313.15, \text{ and } 318.15)$ K. The experimental data attained was used to calculate the derived properties for the system: excess molar volume (V_m^E), isentropic compressibility (k_s), and deviation in refractive index (Δn).

The Redlich-Kister smoothing equation was used successfully for the correlation of V_m^E and Δn data. The Lorentz-Lorenz equation gave a poor prediction for V_m^E , but a good prediction of density and refractive index.

RESULTS

5.1 Excess molar volume (V_m^E), isentropic compressibility (k_s), change in refractive indices (Δn), and molar refraction (R)

The density (ρ), excess molar volume (V_m^E); speed of sound (u), and isentropic compressibility (k_s) for the binary mixtures {pyridine (x_1) + [EMIM] [EtSO₄] (x_2)} , {ethyl acetoacetate (x_1) + [EMIM] [EtSO₄] (x_2)}, and {thiophene (x_1) + [EMIM] [EtSO₄] (x_2)}, respectively at $T = (298.15, 303.15, 308.15, 313.15, \text{ and } 318.15)$ K over the whole complete composition range are presented in table 5.1-5.3.

$$V_m^E = \frac{x_1 M_1 + x_2 M_2}{\rho} - \frac{x_1 M_1}{\rho_1} - \frac{x_2 M_2}{\rho_2} \quad (5.1)$$

Equation 5.1 was used to calculate the excess molar volume, where x_1 and x_2 are mole fractions, M_1 and M_2 are the molecular masses, and ρ_1 and ρ_2 are densities of the pure components, where 1 and 2 refers to the organic solvent and IL, respectively.

Equation 5.1.1 was used to calculate the isentropic compressibility, (k_s).

$$k_s = \frac{1}{\rho u^2} \quad (5.1.1)$$

Equation 5.1.2 was used to calculate the change in refractive index, (Δn).

$$\Delta n(x_1) = n - \sum_{i=1}^2 x_i n_i \quad (5.1.2)$$

Equation 5.1.3 was used to calculate the molar refraction, (R).

$$R = \left(\frac{n^2 - 1}{n^2 + 2} \right) V_m \quad (5.1.3)$$

k_s , is the isentropic compressibility of the mixture and ρ and u , are the density and speed of sound of the mixtures. n and n_i are the refractive index of the mixture and pure components, V_m is the molar volume.

Tables 5.1-5.3 are the density (ρ), excess molar volume (V_m^E); speed of sound (u), and isentropic compressibility (k_s) for the binary mixtures {pyridine (x_1) + [EMIM] [EtSO₄] (x_2)}, {ethyl acetoacetate (x_1) + [EMIM] [EtSO₄] (x_2)}, and {thiophene (x_1) + [EMIM] [EtSO₄] (x_2)}, respectively at $T = (298.15, 303.15, 308.15, 313.15, \text{ and } 318.15)$ K over the complete mole fraction range. The refractive index (n), change in refractive index (Δn), and molar fraction (R) is given in tables 5.4-5.6.

Table 5.1 Density (ρ), excess molar volume (V_m^E), speed of sound (u), and isentropic compressibility (k_s), for the binary mixture {pyridine (x_1) + [EMIM] [EtSO₄]

(x_2)} at $T = (298.15, 303.15, 308.15, 313.15, \text{ and } 318.15) \text{ K}$.

| x_1 | $\rho/$ (g·cm ⁻³) | $V_m^E /$ (cm ³ ·mol ⁻¹) | $u/$ (m·s ⁻¹) | $k_s/$ (10 ¹⁰ T· Pa ⁻¹) | x_1 | $\rho/$ (g·cm ⁻³) | $V_m^E /$ (cm ³ ·mol ⁻¹) | $u/$ (m·s ⁻¹) | $k_s/$ (10 ¹⁰ T· Pa ⁻¹) |
|------------------------|----------------------------------|--|------------------------------|---|--------|----------------------------------|--|------------------------------|---|
| $T = 298.15 \text{ K}$ | | | | | | | | | |
| 0.0000 | 1.2338 | 0.000 | 1582.41 | 2.86 | 0.6609 | 1.1306 | -1.276 | 1459.89 | 3.43 |
| 0.0729 | 1.2295 | -0.584 | 1582.41 | 2.87 | 0.7323 | 1.1097 | -1.284 | 1436.85 | 3.63 |
| 0.1502 | 1.2214 | -0.774 | 1562.87 | 2.96 | 0.8517 | 1.0640 | -1.016 | 1389.81 | 3.81 |
| 0.2235 | 1.2122 | -0.848 | 1528.73 | 3.02 | 0.8903 | 1.0449 | -0.800 | 1346.63 | 4.23 |
| 0.3639 | 1.1925 | -1.052 | 1523.62 | 3.16 | 0.9438 | 1.0158 | -0.516 | 1338.30 | 4.70 |
| 0.4086 | 1.1850 | -1.104 | 1520.71 | 3.19 | 0.9604 | 1.0058 | -0.409 | 1317.90 | 4.81 |
| 0.5065 | 1.1670 | -1.217 | 1501.00 | 3.21 | 1.0000 | 0.9783 | -0.000 | 1371.53 | 5.08 |
| 0.5596 | 1.1556 | -1.233 | 1487.64 | 3.34 | | | | | |
| $T = 303.15 \text{ K}$ | | | | | | | | | |
| 0.0000 | 1.2304 | 0.000 | 1563.47 | 2.94 | 0.6609 | 1.1267 | -1.321 | 1473.17 | 3.51 |
| 0.0729 | 1.2260 | -0.582 | 1561.28 | 2.96 | 0.7323 | 1.1055 | -1.308 | 1444.67 | 3.72 |
| 0.1502 | 1.2179 | -0.781 | 1550.45 | 3.01 | 0.8517 | 1.0596 | -1.053 | 1420.82 | 3.91 |
| 0.2235 | 1.2088 | -0.864 | 1539.61 | 3.08 | 0.8903 | 1.0404 | -0.830 | 1372.32 | 4.35 |
| 0.3639 | 1.1888 | -1.081 | 1515.57 | 3.22 | 0.9438 | 1.0111 | -0.535 | 1327.62 | 4.85 |
| 0.4086 | 1.1814 | -1.137 | 1510.48 | 3.26 | 0.9604 | 1.0010 | -0.424 | 1319.09 | 4.96 |
| 0.5065 | 1.1633 | -1.258 | 1507.31 | 3.28 | 1.0000 | 0.9732 | 0.000 | 1297.88 | 5.26 |
| 0.5596 | 1.1518 | -1.275 | 1487.14 | 3.41 | | | | | |
| $T = 308.15 \text{ K}$ | | | | | | | | | |
| 0.0000 | 1.2271 | 0.000 | 1549.93 | 2.99 | 0.6609 | 1.2279 | -1.366 | 1458.71 | 3.59 |
| 0.0729 | 1.2226 | -0.575 | 1548.59 | 3.01 | 0.7323 | 1.1014 | -1.354 | 1429.33 | 3.81 |
| 0.1502 | 1.2145 | -0.784 | 1537.96 | 3.07 | 0.8517 | 1.0553 | -1.091 | 1404.78 | 4.01 |
| 0.2235 | 1.2053 | -0.877 | 1526.90 | 3.13 | 0.8903 | 1.0359 | -0.859 | 1354.82 | 4.48 |
| 0.3639 | 1.1852 | -1.108 | 1502.25 | 3.29 | 0.9438 | 1.0064 | -0.554 | 1308.48 | 5.01 |
| 0.4086 | 1.1778 | -1.168 | 1496.93 | 3.32 | 0.9604 | 0.9962 | -0.440 | 1299.65 | 5.12 |
| 0.5065 | 1.1596 | -1.297 | 1493.80 | 3.34 | 1.0000 | 0.9682 | 0.000 | 1177.61 | 5.44 |
| 0.5596 | 1.1480 | -1.316 | 1473.14 | 3.48 | | | | | |

| $T = 313.15 \text{ K}$ | | | | | | | | | | |
|------------------------|--------|--------|---------|------|--------|--------|--------|---------|------|--|
| 0.0000 | 1.2239 | 0.000 | 1529.81 | 3.08 | 0.6609 | 1.1189 | -1.410 | 1444.18 | 3.67 | |
| 0.0729 | 1.2192 | -0.558 | 1533.90 | 3.07 | 0.7323 | 1.0973 | -1.399 | 1414.02 | 3.81 | |
| 0.1502 | 1.2111 | -0.779 | 1525.61 | 3.12 | 0.8517 | 1.0509 | -1.128 | 1388.72 | 4.11 | |
| 0.2235 | 1.2018 | -0.881 | 1514.30 | 3.19 | 0.8903 | 1.0314 | -0.890 | 1337.12 | 4.61 | |
| 0.3639 | 1.1816 | -1.129 | 1488.90 | 3.35 | 0.9438 | 1.0016 | -0.574 | 1289.43 | 5.17 | |
| 0.4086 | 1.1742 | -1.195 | 1483.59 | 3.89 | 0.9604 | 0.9914 | -0.455 | 1280.26 | 5.29 | |
| 0.5065 | 1.1559 | -1.332 | 1480.38 | 3.41 | 1.0000 | 0.9631 | 0.000 | 1257.39 | 5.64 | |
| 0.5596 | 1.1443 | -1.355 | 1459.26 | 3.56 | | | | | | |

| $T = 318.15 \text{ K}$ | | | | | | | | | | |
|------------------------|--------|--------|---------|------|--------|--------|--------|---------|------|--|
| 0.0000 | 1.2207 | 0.000 | 1502.99 | 3.19 | 0.6609 | 1.1150 | -1.456 | 1429.51 | 3.75 | |
| 0.0729 | 1.2158 | -0.544 | 1514.03 | 3.16 | 0.7323 | 1.0933 | -1.446 | 1398.59 | 3.99 | |
| 0.1502 | 1.2076 | -0.777 | 1513.20 | 3.18 | 0.8517 | 1.0465 | -1.168 | 1372.76 | 4.22 | |
| 0.2235 | 1.1983 | -0.889 | 1505.08 | 3.24 | 0.8903 | 1.0269 | -0.921 | 1319.71 | 4.74 | |
| 0.3639 | 1.1780 | -1.153 | 1474.42 | 3.42 | 0.9438 | 0.9969 | -0.595 | 1270.50 | 5.34 | |
| 0.4086 | 1.1706 | -1.224 | 1470.29 | 3.46 | 0.9604 | 0.9865 | -0.472 | 1260.95 | 5.47 | |
| 0.5065 | 1.1522 | -1.371 | 1467.06 | 3.48 | 1.0000 | 0.9580 | 0.000 | 1237.41 | 5.83 | |
| 0.5596 | 1.1405 | -1.396 | 1445.48 | 3.63 | | | | | | |

Standard uncertainties u are $u(x_1) = \pm 0.0004$, $u(T) = \pm 0.03 \text{ K}$, $u(p) = \pm 0.05 \text{ MPa}$ and the combined expanded uncertainty U_c in density and speed of sound were less than $U_c(\rho) = \pm 4 \cdot 10^{-4} \text{ g} \cdot \text{cm}^{-3}$ and $U_c(u) = \pm 1.0 \text{ m} \cdot \text{s}^{-1}$, respectively (0.95 level of confidence).

Table 5.2 Density (ρ), excess molar volume (V_m^E), speed of sound (u), and isentropic compressibility (k_s), for the binary mixtures {ethyl acetoacetate (x_1) + [EMIM [EtSO₄] (x_2)] at $T = (298.15, 303.15, 308.15, 313.15, \text{ and } 318.15) \text{ K}$.

| x_1 | $\rho/$ (g·cm ⁻³) | $V_m^E /$ (cm ³ ·mol ⁻¹) | $u/$ (m·s ⁻¹) | $k_s/$ (10 ¹⁰ T· Pa ⁻¹) | x_1 | $\rho/$ (g·cm ⁻³) | $V_m^E /$ (cm ³ ·mol ⁻¹) | $u/$ (m·s ⁻¹) | $k_s/$ (10 ¹⁰ T· Pa ⁻¹) |
|------------------------|----------------------------------|--|------------------------------|---|--------|----------------------------------|--|------------------------------|---|
| $T = 298.15 \text{ K}$ | | | | | | | | | |
| 0.0000 | 1.2369 | 0.000 | 1581.0 | 2.94 | 0.5424 | 1.1519 | -1.246 | 1420.6 | 3.51 |
| 0.0451 | 1.2314 | -0.154 | 1571.5 | 2.96 | 0.6227 | 1.1344 | -1.236 | 1391.4 | 3.72 |
| 0.1097 | 1.2235 | -0.409 | 1553.7 | 3.01 | 0.7608 | 1.1005 | -1.113 | 1336.6 | 3.91 |
| 0.1489 | 1.2181 | -0.512 | 1542.9 | 3.08 | 0.8314 | 1.0808 | -0.956 | 1307.8 | 4.35 |
| 0.2112 | 1.2093 | -0.680 | 1526.1 | 3.22 | 0.9041 | 1.0582 | -0.690 | 1277.6 | 4.85 |
| 0.3103 | 1.1943 | -0.942 | 1497.3 | 3.26 | 0.9638 | 1.0374 | -0.347 | 1251.5 | 4.96 |
| 0.3808 | 1.1822 | -1.032 | 1474.9 | 3.28 | 1.0000 | 1.0234 | 0.000 | 1233.2 | 5.26 |
| 0.4366 | 1.1725 | -1.149 | 1457.2 | 3.41 | | | | | |
| $T = 303.15 \text{ K}$ | | | | | | | | | |
| 0.0000 | 1.2335 | 0.000 | 1568.75 | 2.91 | 0.5424 | 1.1479 | -1.295 | 1405.62 | 3.84 |
| 0.0451 | 1.2279 | -0.161 | 1558.08 | 2.96 | 0.6227 | 1.1302 | -1.285 | 1375.83 | 4.06 |
| 0.1097 | 1.2199 | -0.424 | 1541.58 | 3.04 | 0.7608 | 1.0960 | -1.156 | 1319.71 | 4.52 |
| 0.1489 | 1.2146 | -0.531 | 1530.28 | 3.09 | 0.8314 | 1.0761 | -0.994 | 1290.43 | 4.81 |
| 0.2112 | 1.2057 | -0.706 | 1513.39 | 3.19 | 0.9041 | 1.0534 | -0.717 | 1259.61 | 5.14 |
| 0.3103 | 1.1906 | -0.978 | 1483.81 | 3.35 | 0.9638 | 1.0325 | -0.361 | 1233.12 | 5.44 |
| 0.3808 | 1.1784 | -1.072 | 1460.99 | 3.48 | 1.0000 | 1.0182 | 0.000 | 1214.57 | 5.68 |
| 0.4366 | 1.1687 | -1.193 | 1442.95 | 3.59 | | | | | |
| $T = 308.15 \text{ K}$ | | | | | | | | | |
| 0.0000 | 1.2301 | 0.000 | 1555.39 | 2.97 | 0.5424 | 1.1439 | -1.345 | 1390.49 | 3.94 |
| 0.0451 | 1.2246 | -0.167 | 1542.92 | 3.02 | 0.6227 | 1.1261 | -1.335 | 1360.05 | 4.17 |
| 0.1097 | 1.2165 | -0.439 | 1528.79 | 3.01 | 0.7608 | 1.0915 | -1.202 | 1303.07 | 4.65 |
| 0.1489 | 1.2110 | -0.552 | 1517.54 | 3.16 | 0.8314 | 1.0715 | -1.033 | 1273.30 | 4.95 |
| 0.2112 | 1.2021 | -0.733 | 1500.38 | 3.25 | 0.9041 | 1.0485 | -0.746 | 1241.94 | 5.21 |
| 0.3103 | 1.1939 | -1.011 | 1470.20 | 3.31 | 0.9638 | 1.0275 | -0.375 | 1215.01 | 5.63 |
| 0.3808 | 1.1746 | -1.114 | 1446.94 | 3.56 | 1.0000 | 1.0129 | 0.000 | 1196.15 | 5.87 |
| 0.4366 | 1.1648 | -1.239 | 1428.54 | 3.68 | | | | | |
| $T = 313.15 \text{ K}$ | | | | | | | | | |
| 0.0000 | 1.2267 | 0.000 | 1514.97 | 3.00 | 0.5424 | 1.1398 | -1.397 | 1375.46 | 4.03 |
| 0.0451 | 1.2211 | -0.172 | 1529.47 | 3.08 | 0.6227 | 1.1219 | -1.388 | 1344.37 | 4.27 |
| 0.1097 | 1.2129 | -0.454 | 1516.26 | 3.16 | 0.7608 | 1.0871 | -1.250 | 1286.42 | 4.79 |
| 0.1489 | 1.2075 | -0.571 | 1504.92 | 3.22 | 0.8314 | 1.0668 | -1.075 | 1256.15 | 5.01 |
| 0.2112 | 1.1985 | -0.760 | 1487.46 | 3.31 | 0.9041 | 1.0436 | -0.776 | 1224.20 | 5.46 |

| | | | | | | | | | |
|------------------------|--------|--------|---------|------|--------|--------|--------|---------|------|
| 0.3103 | 1.1832 | -1.052 | 1456.73 | 3.49 | 0.9638 | 1.0224 | -0.391 | 1196.84 | 5.82 |
| 0.3808 | 1.1708 | -1.157 | 1433.03 | 3.63 | 1.0000 | 1.0078 | -0.000 | 1177.70 | 6.08 |
| 0.4366 | 1.1609 | -1.287 | 1414.27 | 3.76 | | | | | |
| $T = 318.15 \text{ K}$ | | | | | | | | | |
| 0.0000 | 1.2234 | 0.000 | 1528.04 | 3.08 | 0.5424 | 1.1358 | -1.453 | 1360.55 | 4.13 |
| 0.0451 | 1.2176 | -0.178 | 1510.98 | 3.16 | 0.6227 | 1.1177 | -1.444 | 1328.83 | 4.38 |
| 0.1097 | 1.2095 | -0.471 | 1503.56 | 3.22 | 0.7608 | 1.0826 | -1.302 | 1269.19 | 4.92 |
| 0.1489 | 1.2040 | -0.593 | 1492.45 | 3.28 | 0.8314 | 1.0622 | -1.119 | 1239.19 | 5.24 |
| 0.2112 | 1.1949 | -0.789 | 1474.35 | 3.38 | 0.9041 | 1.0388 | -0.808 | 1206.64 | 5.64 |
| 0.3103 | 1.1794 | -1.093 | 1443.29 | 3.55 | 0.9638 | 1.0173 | -0.409 | 1178.84 | 6.01 |
| 0.3808 | 1.1671 | -1.203 | 1419.24 | 3.71 | 1.0000 | 1.0025 | 0.000 | 1159.45 | 6.29 |
| 0.4366 | 1.1571 | -1.337 | 1400.09 | 3.84 | | | | | |

Standard uncertainties u are $u(x_1) = \pm 0.0004$, $u(T) = \pm 0.03 \text{ K}$, $u(p) = \pm 0.05 \text{ MPa}$ and the

combined expanded uncertainty U_c in density and speed of sound were less than $U_c(\rho) = \pm 4 \cdot 10^{-4}$

$\text{g} \cdot \text{cm}^{-3}$ and $U_c(u) = \pm 1.0 \text{ m} \cdot \text{s}^{-1}$, respectively (0.95 level of confidence).

Table 5.3 Density (ρ), excess molar volume (V_m^E), speed of sound (u), and isentropic compressibility (k_s), for the binary mixtures {thiophene (x_1) + [EMIM] [EtSO₄] (x_2)} at $T = (298.15, 303.15, 308.15, 313.15, \text{ and } 318.15) \text{ K}$.

| x_1 | $\rho/$ (g·cm ⁻³) | $V_m^E /$ (cm ³ ·mol ⁻¹) | $u/$ (m·s ⁻¹) | $k_s/$ (10 ¹⁰ T·Pa ⁻¹) | x_1 | $\rho/$ (g·cm ⁻³) | $V_m^E /$ (cm ³ ·mol ⁻¹) | $u/$ (m·s ⁻¹) | $k_s/$ (10 ¹⁰ T·Pa ⁻¹) |
|------------------------|----------------------------------|--|------------------------------|--|--------|----------------------------------|--|------------------------------|--|
| $T = 298.15 \text{ K}$ | | | | | | | | | |
| 0.0000 | 1.2345 | 0.000 | 1579.24 | 2.95 | 0.5358 | 1.1937 | -1.797 | 1445.85 | 3.51 |
| 0.0717 | 1.2332 | -0.638 | 1566.50 | 3.01 | 0.6277 | 1.1802 | -1.870 | 1406.39 | 3.74 |
| 0.1317 | 1.2290 | -0.727 | 1556.48 | 3.14 | 0.8164 | 1.1291 | -0.781 | 1182.70 | 5.34 |
| 0.2132 | 1.2245 | -1.074 | 1542.58 | 3.24 | 0.9147 | 1.0755 | 1.264 | 1185.74 | 5.62 |
| 0.3289 | 1.2155 | -1.384 | 1510.72 | 3.34 | 0.9672 | 1.0589 | 1.017 | 1185.74 | 5.71 |
| 0.4086 | 1.2083 | -1.582 | 1488.82 | 3.28 | 1.0000 | 0.9783 | 0.000 | 1179.59 | 5.77 |
| 0.4709 | 1.2016 | -1.698 | 1469.01 | 3.38 | | | | | |
| $T = 303.15 \text{ K}$ | | | | | | | | | |
| 0.0000 | 1.2311 | 0.000 | 1563.89 | 2.93 | 0.5358 | 1.1898 | -1.847 | 1431.43 | 3.58 |
| 0.0717 | 1.2298 | -6.330 | 1553.93 | 2.97 | 0.6277 | 1.1760 | -1.922 | 1391.06 | 3.82 |
| 0.1317 | 1.2255 | -0.729 | 1540.70 | 3.03 | 0.8164 | 1.1244 | -0.828 | 1162.09 | 5.58 |
| 0.2132 | 1.2209 | -1.090 | 1524.52 | 3.10 | 0.9147 | 1.0697 | 1.300 | 1162.74 | 5.86 |
| 0.3289 | 1.2119 | -1.415 | 1497.73 | 3.23 | 0.9672 | 1.0529 | 1.041 | 1162.94 | 5.74 |
| 0.4086 | 1.2046 | -1.622 | 1475.43 | 3.34 | 1.0000 | 1.0526 | 0.000 | 1163.53 | 5.95 |
| 0.4709 | 1.1978 | -1.743 | 1455.20 | 3.45 | | | | | |
| $T = 308.15 \text{ K}$ | | | | | | | | | |
| 0.0000 | 1.2278 | 0.000 | 1551.48 | 2.94 | 0.5358 | 1.1859 | -1.895 | 1417.09 | 3.66 |
| 0.0717 | 1.2263 | -6.332 | 1540.62 | 3.03 | 0.6277 | 1.1719 | -1.974 | 1375.82 | 3.92 |
| 0.1317 | 1.2220 | -0.725 | 1524.03 | 3.10 | 0.8164 | 1.1191 | -0.822 | 1142.35 | 5.74 |
| 0.2132 | 1.2173 | -1.101 | 1503.06 | 3.11 | 0.9147 | 1.0639 | 1.334 | 1143.22 | 6.08 |
| 0.3289 | 1.2082 | -1.443 | 1483.69 | 3.21 | 0.9672 | 1.0469 | 1.066 | 1143.44 | 6.18 |
| 0.4086 | 1.2008 | -1.659 | 1461.40 | 3.42 | 1.0000 | 1.0466 | 0.000 | 1142.40 | 6.19 |
| 0.4709 | 1.1940 | -1.787 | 1441.16 | 3.53 | | | | | |
| $T = 313.15 \text{ K}$ | | | | | | | | | |
| 0.0000 | 1.2246 | 0.000 | 1538.61 | 3.04 | 0.5358 | 1.1819 | -1.946 | 1403.23 | 3.74 |
| 0.0717 | 1.2229 | -0.611 | 1527.53 | 3.09 | 0.6277 | 1.1677 | -2.029 | 1360.83 | 4.01 |
| 0.1317 | 1.2185 | -0.722 | 1475.76 | 3.31 | 0.8164 | 1.1136 | -0.794 | 1124.26 | 5.99 |
| 0.2132 | 1.2138 | -1.113 | 1474.50 | 3.32 | 0.9147 | 1.0579 | 1.380 | 1123.05 | 6.32 |
| 0.3289 | 1.2046 | -1.472 | 1466.92 | 3.38 | 0.9672 | 1.0409 | 1.091 | 1123.05 | 6.42 |
| 0.4086 | 1.1971 | -1.699 | 1446.88 | 3.49 | 1.0000 | 1.0406 | 0.000 | 1123.01 | 6.42 |
| 0.4709 | 1.1902 | -1.833 | 1427.45 | 3.60 | | | | | |

$T = 318.15 \text{ K}$

| | | | | | | | | | |
|--------|--------|--------|---------|------|--------|--------|--------|---------|------|
| 0.0000 | 1.2214 | 0.000 | 1514.03 | 3.16 | 0.5358 | 1.1780 | -1.999 | 1398.59 | 3.82 |
| 0.0717 | 1.2195 | -0.601 | 1513.20 | 3.14 | 0.6277 | 1.1637 | -2.085 | 1372.76 | 4.11 |
| 0.1317 | 1.2151 | -0.719 | 1505.08 | 3.60 | 0.8164 | 1.1084 | -0.806 | 1319.71 | 6.22 |
| 0.2132 | 1.2104 | -1.127 | 1474.42 | 3.45 | 0.9147 | 1.0517 | 1.447 | 1270.50 | 6.57 |
| 0.3289 | 1.2010 | -1.503 | 1470.29 | 3.47 | 0.9672 | 1.0349 | 1.117 | 1260.95 | 6.67 |
| 0.4086 | 1.1934 | -1.740 | 1467.06 | 3.56 | 1.0000 | 1.0346 | 0.000 | 1237.41 | 6.69 |
| 0.4709 | 1.1864 | -1.880 | 1445.48 | 3.67 | | | | | |

Standard uncertainties u are $u(x_1) = \pm 0.0004$, $u(T) = \pm 0.03 \text{ K}$, $u(p) = \pm 0.05 \text{ MPa}$ and the

combined expanded uncertainty U_c in density and speed of sound were less than $U_c(\rho) = \pm 4 \cdot 10^{-4}$

$\text{g} \cdot \text{cm}^{-3}$ and $U_c(u) = \pm 1.0 \text{ m} \cdot \text{s}^{-1}$, respectively (0.95 level of confidence).

Table 5.4 Refractive index (n), molar refraction (R), and deviation in refractive index (Δn) for the binary mixture {pyridine (x_1) + [EMIM] [EtSO₄] (x_2)} at $T =$ (298.15, 303.15, 308.15, 313.15, and 318.15) K.

| x_1 | n | Δn | $R/(\text{cm}^3 \cdot \text{mol}^{-1})$ | x_1 | n | Δn | $R/(\text{cm}^3 \cdot \text{mol}^{-1})$ |
|------------------------|--------|------------|---|--------|--------|------------|---|
| $T = 298.15 \text{ K}$ | | | | | | | |
| 0.0000 | 1.4784 | 0.0000 | 54.19 | 0.6609 | 1.4955 | -0.0013 | 42.13 |
| 0.0729 | 1.4799 | -0.0006 | 53.19 | 0.7323 | 1.4845 | -0.0008 | 40.33 |
| 0.1502 | 1.4813 | -0.0013 | 51.74 | 0.8517 | 1.5027 | -0.0006 | 37.29 |
| 0.2235 | 1.4828 | -0.0019 | 50.88 | 0.8903 | 1.5060 | 0.0010 | 35.72 |
| 0.3639 | 1.4864 | -0.0022 | 49.49 | 0.9438 | 1.5064 | 0.0013 | 34.10 |
| 0.4086 | 1.4872 | -0.0024 | 47.29 | 0.9604 | 1.5063 | 0.0012 | 32.78 |
| 0.5065 | 1.4875 | -0.0021 | 45.72 | 1.0000 | 1.5043 | 0.0000 | 31.99 |
| 0.5596 | 1.4904 | -0.0021 | 44.48 | | | | |
| $T = 303.15 \text{ K}$ | | | | | | | |
| 0.0000 | 1.4770 | 0.0000 | 54.21 | 0.6609 | 1.4903 | -0.0006 | 37.28 |
| 0.0729 | 1.4785 | -0.0004 | 51.91 | 0.7323 | 1.4938 | -0.0002 | 34.23 |
| 0.1502 | 1.4799 | -0.0011 | 49.63 | 0.8517 | 1.4961 | 0.0011 | 32.23 |
| 0.2235 | 1.4814 | -0.0015 | 47.43 | 0.8903 | 1.5005 | 0.0015 | 28.47 |
| 0.3639 | 1.4848 | -0.0018 | 43.19 | 0.9438 | 1.5034 | 0.0016 | 27.34 |
| 0.4086 | 1.4857 | -0.0018 | 42.29 | 0.9604 | 1.5034 | 0.0011 | 25.74 |
| 0.5065 | 1.4860 | -0.0013 | 41.84 | 1.0000 | 1.5019 | 0.0000 | 25.23 |
| 0.5596 | 1.4892 | -0.0014 | 38.89 | | | | |
| $T = 308.15 \text{ K}$ | | | | | | | |
| 0.0000 | 1.4754 | 0.0000 | 54.31 | 0.6609 | 1.4866 | -0.0001 | 37.29 |
| 0.0729 | 1.4772 | -0.0002 | 52.02 | 0.7323 | 1.4919 | 0.0004 | 34.23 |
| 0.1502 | 1.4784 | -0.0008 | 49.65 | 0.8517 | 1.4942 | 0.0016 | 32.06 |
| 0.2235 | 1.4803 | -0.0012 | 47.44 | 0.8903 | 1.4984 | 0.0018 | 28.49 |
| 0.3639 | 1.4833 | -0.0014 | 43.21 | 0.9438 | 1.5009 | 0.0018 | 27.35 |
| 0.4086 | 1.4837 | -0.0013 | 42.31 | 0.9604 | 1.5012 | 0.0017 | 25.75 |
| 0.5065 | 1.4845 | -0.0011 | 41.86 | 1.0000 | 1.5005 | 0.0000 | 25.26 |
| 0.5596 | 1.4872 | -0.0009 | 38.81 | | | | |
| $T = 313.15 \text{ K}$ | | | | | | | |
| 0.0000 | 1.4742 | 0.0000 | 54.31 | 0.6609 | 1.4901 | 0.0004 | 37.31 |
| 0.0729 | 1.4762 | -0.0001 | 52.03 | 0.7323 | 1.4923 | 0.0009 | 34.24 |
| 0.1502 | 1.4767 | -0.0005 | 49.67 | 0.8517 | 1.4962 | 0.0020 | 32.08 |
| 0.2235 | 1.4785 | -0.0009 | 47.46 | 0.8903 | 1.4984 | 0.0021 | 28.41 |
| 0.3639 | 1.4818 | -0.0008 | 43.23 | 0.9438 | 1.4986 | 0.0020 | 27.36 |
| 0.4086 | 1.4828 | -0.0009 | 42.32 | 0.9604 | 1.4977 | 0.0018 | 25.77 |

| | | | | | | | | |
|------------------------|--------|----------|-------|--|--------|--------|---------|-------|
| 0.5065 | 1.4855 | -0.0005 | 41.87 | | 1.0000 | 1.4972 | 0.0000 | 25.27 |
| 0.5596 | 1.4870 | -0.00031 | 38.91 | | | | | |
| $T = 318.15 \text{ K}$ | | | | | | | | |
| 0.0000 | 1.4727 | 0.00000 | 54.31 | | 0.6609 | 1.4858 | 0.00090 | 37.32 |
| 0.0729 | 1.4744 | 0.00010 | 52.05 | | 0.7323 | 1.4886 | 0.00144 | 34.25 |
| 0.1502 | 1.4761 | -0.00033 | 49.68 | | 0.8517 | 1.4907 | 0.00243 | 32.09 |
| 0.2235 | 1.4767 | -0.00054 | 47.48 | | 0.8903 | 1.4944 | 0.00213 | 28.51 |
| 0.3639 | 1.4804 | -0.00038 | 43.24 | | 0.9438 | 1.4963 | 0.00193 | 27.37 |
| 0.4086 | 1.4806 | -0.00047 | 42.32 | | 0.9604 | 1.4964 | 0.00204 | 25.78 |
| 0.5065 | 1.4813 | 5.6E-07 | 41.88 | | 1.0000 | 1.4952 | 0.00000 | 25.28 |
| 0.5596 | 1.4843 | 0.00030 | 38.92 | | | | | |

Standard uncertainties u are $u(x_1) = \pm 0.0004$, $u(T) = \pm 0.03 \text{ K}$, $u(p) = \pm 0.05 \text{ MPa}$ and the

combined expanded uncertainty U_c in refractive index measurements was less than $U_c(n) =$

$\pm 4 \cdot 10^{-4}$, respectively (0.95 level of confidence).

Table 5.5 Refractive index (n), molar refraction (R), and deviation in refractive index (Δn) for the binary mixture {ethyl acetoacetate (x_1) + [EMIM] [EtSO₄] (x_2)} at $T = (298.15, 303.15, 308.15, 313.15, \text{ and } 318.15) \text{ K}$.

| x_1 | n | Δn | $R/(\text{cm}^3 \cdot \text{mol}^{-1})$ | x_1 | n | Δn | $R/(\text{cm}^3 \cdot \text{mol}^{-1})$ |
|------------------------|--------|------------|---|--------|--------|------------|---|
| $T = 298.15 \text{ K}$ | | | | | | | |
| 0.0000 | 1.4786 | 0.00000 | 54.17 | 0.5424 | 1.4549 | 0.00993 | 42.11 |
| 0.0451 | 1.4771 | 0.00129 | 53.17 | 0.6227 | 1.4497 | 0.00973 | 40.32 |
| 0.1097 | 1.4744 | 0.00308 | 51.72 | 0.7608 | 1.4400 | 0.00868 | 37.28 |
| 0.1489 | 1.4733 | 0.00407 | 50.86 | 0.8314 | 1.4341 | 0.00709 | 35.70 |
| 0.2112 | 1.4784 | 0.00552 | 49.47 | 0.9041 | 1.4273 | 0.00481 | 34.09 |
| 0.3103 | 1.4669 | 0.00751 | 47.27 | 0.9638 | 1.4213 | 0.00216 | 32.77 |
| 0.3808 | 1.4635 | 0.00853 | 45.71 | 1.0000 | 1.4161 | 0.00000 | 31.97 |
| 0.4366 | 1.4608 | 0.00925 | 44.46 | | | | |
| $T = 303.15 \text{ K}$ | | | | | | | |
| 0.0000 | 1.4773 | 0.00000 | 54.19 | 0.5424 | 1.4532 | 0.01002 | 42.13 |
| 0.0451 | 1.4758 | 0.00131 | 53.19 | 0.6227 | 1.4479 | 0.00978 | 40.33 |
| 0.1097 | 1.4735 | 0.00311 | 51.74 | 0.7608 | 1.4381 | 0.00872 | 37.29 |
| 0.1489 | 1.4720 | 0.00416 | 50.88 | 0.8314 | 1.4321 | 0.00710 | 35.72 |
| 0.2112 | 1.4695 | 0.00556 | 49.49 | 0.9041 | 1.4252 | 0.00482 | 34.10 |
| 0.3103 | 1.4654 | 0.00764 | 47.29 | 0.9638 | 1.4188 | 0.00218 | 32.78 |
| 0.3808 | 1.4620 | 0.00862 | 45.72 | 1.0000 | 1.4144 | 0.00000 | 31.99 |
| 0.4366 | 1.4592 | 0.00935 | 44.48 | | | | |
| $T = 308.15 \text{ K}$ | | | | | | | |
| 0.0000 | 1.4760 | 0.00000 | 54.22 | 0.5424 | 1.4515 | 0.01017 | 42.14 |
| 0.0451 | 1.4741 | 0.00129 | 53.20 | 0.6227 | 1.4461 | 0.00992 | 40.35 |
| 0.1097 | 1.4722 | 0.00319 | 51.76 | 0.7608 | 1.4364 | 0.00906 | 37.32 |
| 0.1489 | 1.4710 | 0.00423 | 50.81 | 0.8314 | 1.4302 | 0.00726 | 35.73 |
| 0.2112 | 1.4682 | 0.00566 | 49.51 | 0.9041 | 1.4232 | 0.00494 | 34.12 |
| 0.3103 | 1.4643 | 0.00776 | 47.02 | 0.9638 | 1.4171 | 0.00223 | 32.79 |
| 0.3808 | 1.4604 | 0.00875 | 45.74 | 1.0000 | 1.4121 | 0.00000 | 32.00 |
| 0.4366 | 1.4571 | 0.00947 | 44.49 | | | | |
| $T = 313.15 \text{ K}$ | | | | | | | |
| 0.0000 | 1.4750 | 0.00000 | 54.23 | 0.5424 | 1.4502 | 0.01032 | 42.15 |
| 0.0451 | 1.4734 | 0.00133 | 53.23 | 0.6227 | 1.4448 | 0.01007 | 40.36 |
| 0.1097 | 1.4712 | 0.00326 | 51.78 | 0.7608 | 1.4341 | 0.00918 | 37.33 |
| 0.1489 | 1.4696 | 0.00426 | 50.91 | 0.8314 | 1.4286 | 0.00737 | 35.75 |
| 0.2112 | 1.4671 | 0.00573 | 49.52 | 0.9041 | 1.4215 | 0.00499 | 34.13 |
| 0.3103 | 1.4628 | 0.00787 | 47.32 | 0.9638 | 1.4149 | 0.00228 | 32.81 |

| | | | | | | | |
|------------------------|--------|----------|-------|--------|--------|---------|-------|
| 0.3808 | 1.4592 | 0.00887 | 45.75 | 1.0000 | 1.4103 | 0.00000 | 32.02 |
| 0.4366 | 1.4564 | 0.00962 | 44.51 | | | | |
| $T = 318.15 \text{ K}$ | | | | | | | |
| 0.0000 | 1.4733 | 0.000000 | 54.25 | 0.5424 | 1.4482 | 0.01049 | 42.17 |
| 0.0451 | 1.4717 | 0.001379 | 53.25 | 0.6227 | 1.4427 | 0.01025 | 40.38 |
| 0.1097 | 1.4693 | 0.003242 | 51.79 | 0.7608 | 1.4328 | 0.00938 | 37.35 |
| 0.1489 | 1.4678 | 0.004302 | 50.92 | 0.8314 | 1.4263 | 0.00756 | 35.76 |
| 0.2112 | 1.4653 | 0.005835 | 49.54 | 0.9041 | 1.4124 | 0.00510 | 33.67 |
| 0.3103 | 1.4609 | 0.007999 | 47.34 | 0.9638 | 1.4112 | 0.00237 | 32.41 |
| 0.3808 | 1.4573 | 0.009023 | 45.77 | 1.0000 | 1.4081 | 0.00000 | 32.06 |
| 0.4366 | 1.4544 | 0.009766 | 44.51 | | | | |

Standard uncertainties u are $u(x_1) = \pm 0.0004$, $u(T) = \pm 0.03 \text{ K}$, $u(p) = \pm 0.05 \text{ MPa}$ and the

combined expanded uncertainty U_c in refractive index measurements was less than $U_c(n) = \pm 4$

$\cdot 10^{-4}$, respectively (0.95 level of confidence).

Table 5.6 Refractive index (n), molar refraction (R), and deviation in refractive index (Δn) for the binary mixture {thiophene (x_1) + [EMIM] [EtSO₄] (x_2)} at $T =$ (298.15, 303.15, 308.15, 313.15, and 318.15) K.

| x_1 | n | Δn | $R/(\text{cm}^3 \cdot \text{mol}^{-1})$ | x_1 | n | Δn | $R/(\text{cm}^3 \cdot \text{mol}^{-1})$ |
|------------------------|--------|------------|---|--------|--------|------------|---|
| $T = 298.15 \text{ K}$ | | | | | | | |
| 0.0000 | 1.4780 | 0.00000 | 22.52 | 0.5358 | 1.4996 | -0.00170 | 23.36 |
| 0.0717 | 1.4810 | -0.00074 | 22.62 | 0.6277 | 1.5045 | -0.00088 | 23.56 |
| 0.1317 | 1.4823 | -0.00222 | 22.67 | 0.8164 | 1.5251 | 0.00731 | 24.36 |
| 0.2132 | 1.4856 | -0.00274 | 22.81 | 0.9147 | 1.5249 | 0.00329 | 24.35 |
| 0.3289 | 1.4900 | -0.00373 | 22.98 | 0.9672 | 1.5248 | 0.00131 | 24.35 |
| 0.4086 | 1.4934 | -0.00410 | 23.12 | 1.0000 | 1.5251 | 0.00000 | 24.36 |
| 0.4709 | 1.4963 | -0.00409 | 23.23 | | | | |
| $T = 303.15 \text{ K}$ | | | | | | | |
| 0.0000 | 1.4773 | 0.00000 | 22.60 | 0.5358 | 1.4978 | -0.00341 | 23.42 |
| 0.0717 | 1.4796 | -0.00091 | 22.69 | 0.6277 | 1.5026 | -0.00267 | 23.61 |
| 0.1317 | 1.4812 | -0.00202 | 22.75 | 0.8164 | 1.5219 | 0.00821 | 24.37 |
| 0.2132 | 1.4842 | -0.00267 | 22.87 | 0.9147 | 1.5217 | 0.00360 | 24.37 |
| 0.3289 | 1.4885 | -0.00349 | 23.05 | 0.9672 | 1.5217 | 0.00130 | 24.37 |
| 0.4086 | 1.4918 | -0.00379 | 23.18 | 1.0000 | 1.5219 | 0.00000 | 24.38 |
| 0.4709 | 1.4946 | -0.00372 | 23.29 | | | | |
| $T = 308.15 \text{ K}$ | | | | | | | |
| 0.0000 | 1.4759 | 0.00000 | 22.67 | 0.5358 | 1.4961 | -0.00273 | 23.49 |
| 0.0717 | 1.4783 | -0.00070 | 22.77 | 0.6277 | 1.5007 | -0.00209 | 23.67 |
| 0.1317 | 1.4799 | -0.00167 | 22.83 | 0.8164 | 1.5188 | 0.00796 | 24.39 |
| 0.2132 | 1.4828 | -0.00228 | 22.95 | 0.9147 | 1.5186 | 0.00357 | 24.38 |
| 0.3289 | 1.4861 | -0.00299 | 23.12 | 0.9672 | 1.5187 | 0.00143 | 24.39 |
| 0.4086 | 1.4902 | -0.00316 | 23.25 | 1.0000 | 1.5186 | 0.00000 | 24.39 |
| 0.4709 | 1.4931 | -0.00299 | 23.37 | | | | |
| $T = 313.15 \text{ K}$ | | | | | | | |
| 0.0000 | 1.4744 | 0.00000 | 22.74 | 0.5358 | 1.4941 | -0.00227 | 23.54 |
| 0.0717 | 1.4769 | -0.00039 | 22.84 | 0.6277 | 1.4986 | -0.00151 | 23.73 |
| 0.1317 | 1.4785 | -0.00128 | 22.91 | 0.8164 | 1.5155 | 0.00765 | 24.40 |
| 0.2132 | 1.4813 | -0.00182 | 23.02 | 0.9147 | 1.5153 | 0.00341 | 24.32 |
| 0.3289 | 1.4854 | -0.00244 | 23.19 | 0.9672 | 1.5154 | 0.00138 | 24.39 |
| 0.4086 | 1.4886 | -0.00253 | 23.19 | 1.0000 | 1.5154 | 0.00000 | 24.31 |
| 0.4709 | 1.4913 | -0.00241 | 23.32 | | | | |
| $T = 318.15 \text{ K}$ | | | | | | | |
| 0.0000 | 1.4721 | 0.00000 | 22.81 | 0.5358 | 1.4923 | -0.0017 | 23.61 |

| | | | | | | | |
|--------|--------|----------|-------|--------|--------|---------|-------|
| 0.0717 | 1.4756 | -0.00019 | 22.92 | 0.6277 | 1.4967 | -0.0009 | 23.79 |
| 0.1317 | 1.4770 | -0.00110 | 22.98 | 0.8164 | 1.5123 | 0.0073 | 24.42 |
| 0.2132 | 1.4798 | -0.00149 | 23.09 | 0.9147 | 1.5121 | 0.0032 | 24.40 |
| 0.3289 | 1.4838 | -0.00209 | 23.26 | 0.9672 | 1.5122 | 0.0013 | 24.41 |
| 0.4086 | 1.4867 | -0.00223 | 23.38 | 1.0000 | 1.5122 | 0.0000 | 24.41 |
| 0.4709 | 1.4893 | -0.00210 | 23.49 | | | | |

Standard uncertainties u are $u(x_1) = \pm 0.0004$, $u(T) = \pm 0.03$ K, $u(p) = \pm 0.05$ MPa and the

combined expanded uncertainty U_c in refractive index measurements was less than $U_c(n) = \pm 4$

$\cdot 10^{-4}$, respectively (0.95 level of confidence).

The plot of excess molar volumes (V_m^E), for the binary systems {pyridine (Py) or ethyl acetoacetate (EAA) or thiophene (TS) + [EMIM] [EtSO₄]} at $T = (298.15 \text{ K } (\diamond), 303.15 \text{ K } (\square), 308.15 \text{ K } (\triangle), 313.15 \text{ K } (x) \text{ and } 318.15 \text{ K } (*))$ over the complete composition range are given in figures 5.1-5.3. The excess molar volumes are negative, and decrease as the temperature increases for each binary system.

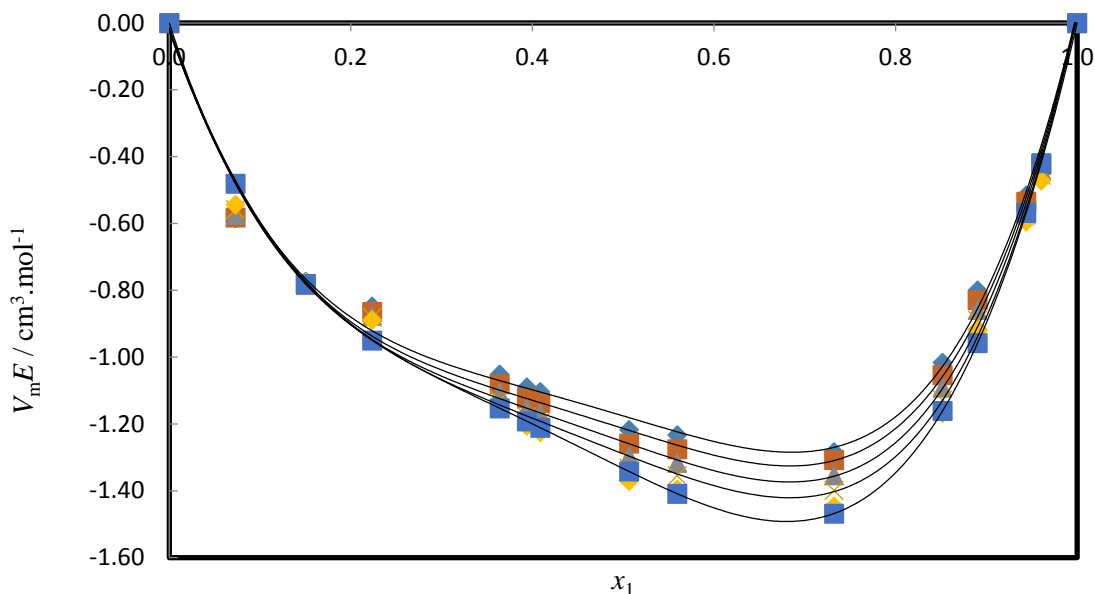


Figure 5.1 Plot of excess molar volume (V_m^E), for the binary system {pyridine (x_1) + [EMIM] [EtSO₄] (x_2)} against mole fraction of pyridine; at $T = (298.15, 303.15, 308.15, 313.15, \text{ and } 318.15) \text{ K}$. The solid lines represents the Redlich-Kister correlation equation 3.5.1.

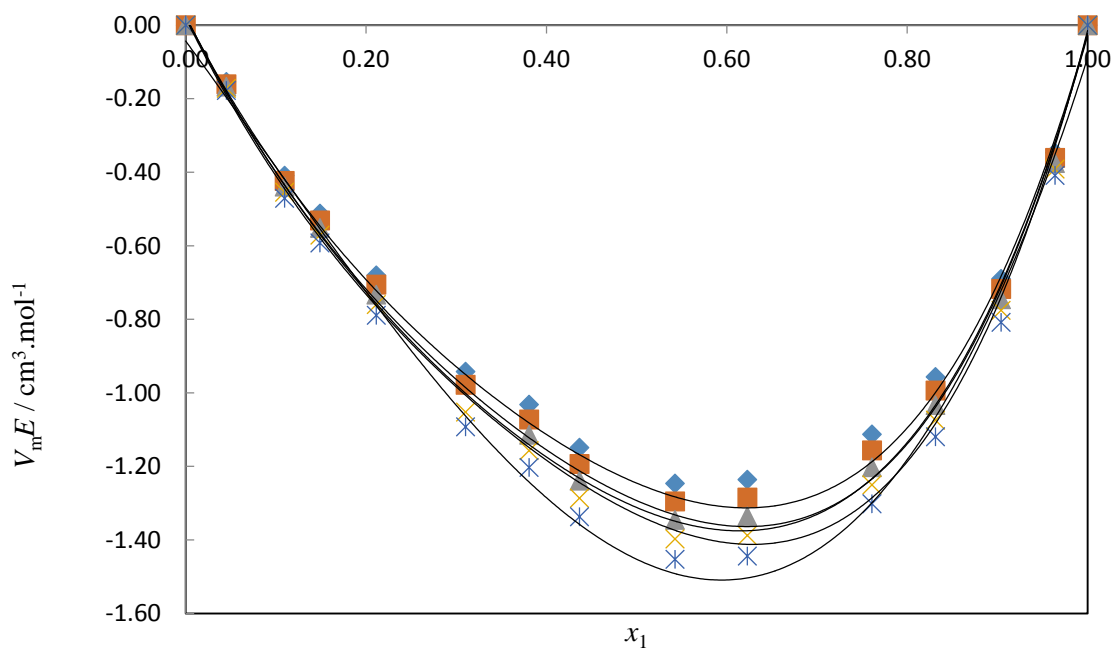
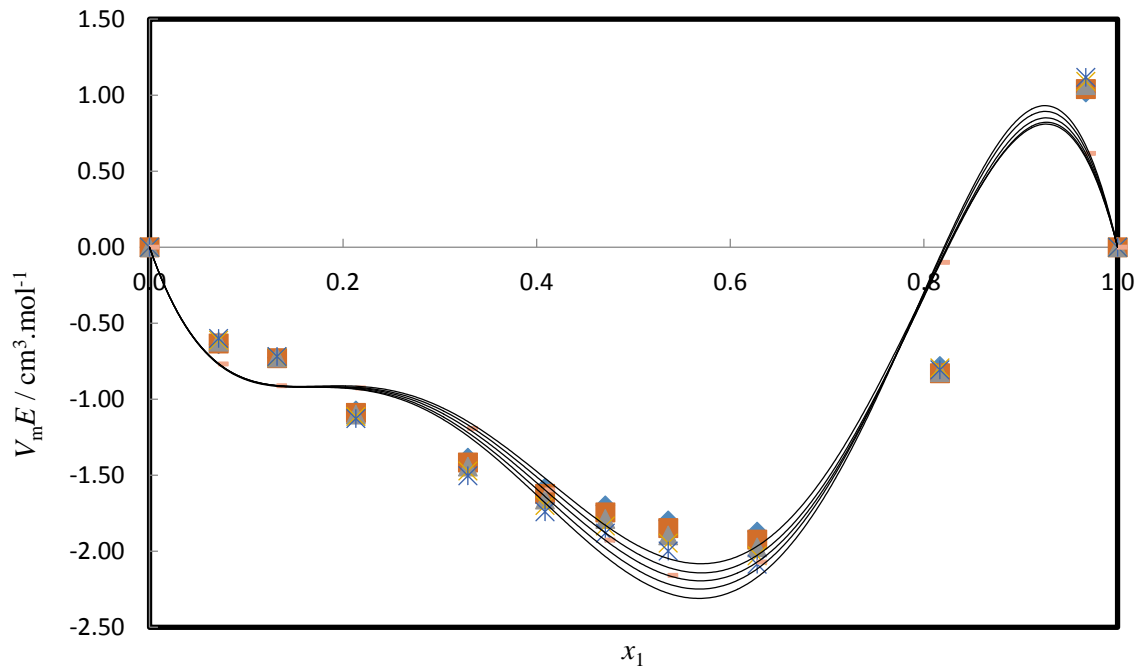
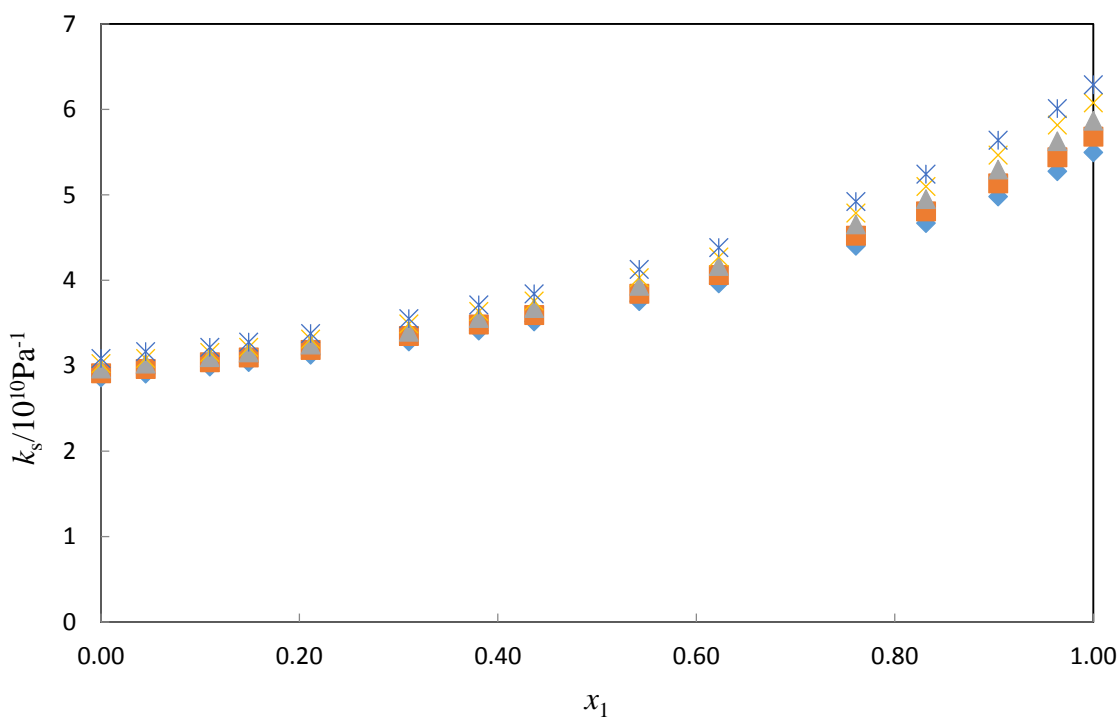


Figure 5.2 Plot of excess molar volume (V_m^E), for the binary system {ethyl acetoacetate (x_1) + [EMIM] [EtSO₄] (x_2)} against mole fraction of ethyl acetoacetate; at $T = (298.15, 303.15, 308.15, 313.15, \text{ and } 318.15) \text{ K}$. The solid lines represents the Redlich-Kister correlation equation 3.5.1.

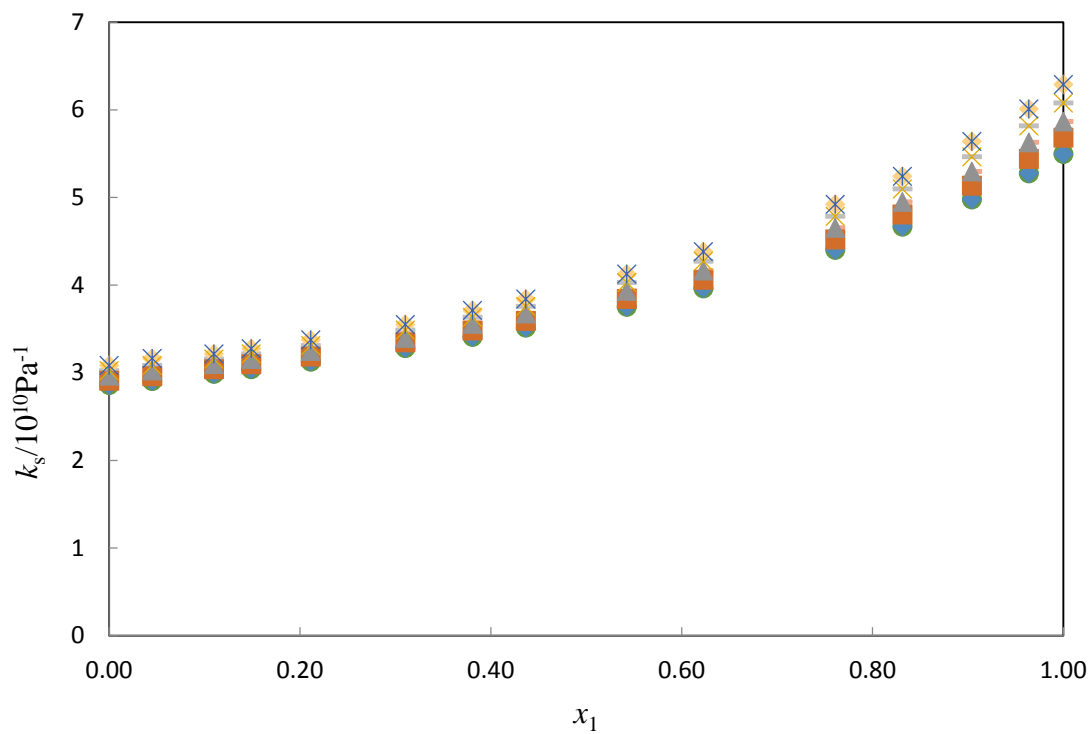


5.3 Plot of excess molar volume (V_m^E), for the binary system {thiophene (x_1) + [EMIM] [EtSO₄] (x_2)} against mole fraction of thiophene; at $T = (298.15, 303.15, 308.15, 313.15, \text{ and } 318.15)$ K. The solid lines represents the Redlich-Kister correlation equation 3.5.1.

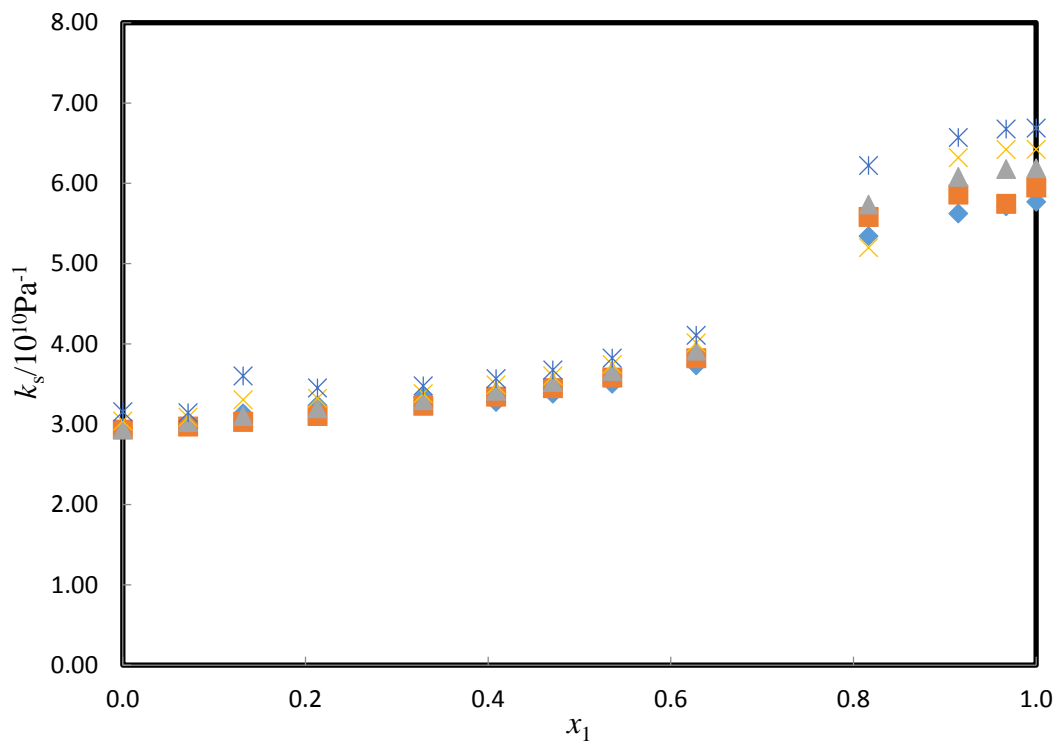
The plot of isentropic compressibility (k_s), for the binary systems {pyridine (Py) or ethyl acetoacetate (EAA) or thiophene (TS) + [EMIM] [EtSO₄]} at $T = (298.15 \text{ K } (\diamond), 303.15 \text{ K } (\square), 308.15 \text{ K } (\triangle), 313.15 \text{ K } (x) \text{ and } 318.15 \text{ K } (*))$ over the complete composition range are given in figures 5.4-5.6. The isentropic compressibility values are positive, and increases as the temperature increases for each binary system.



5.4 Plot of isentropic compressibility (k_s), for the binary system {pyridine (x_1) + [EMIM] [EtSO₄] (x_2)} against mole fraction of pyridine; at $T = (298.15, 303.15, 308.15, 313.15, \text{ and } 318.15) \text{ K}$.

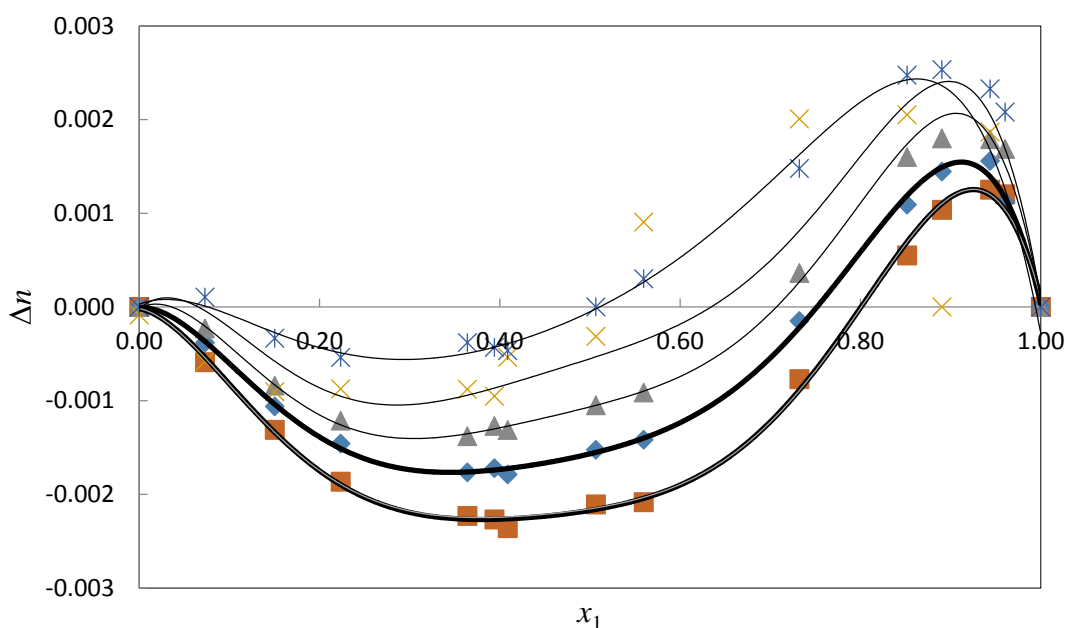


5.5 Plot of isentropic compressibility (k_s), for the binary system {ethyl acetoacetate (x_1) + [EMIM] [EtSO₄] (x_2)} against mole fraction of ethyl acetoacetate; at $T = (298.15, 303.15, 308.15, 313.15, \text{ and } 318.15) \text{ K}$.

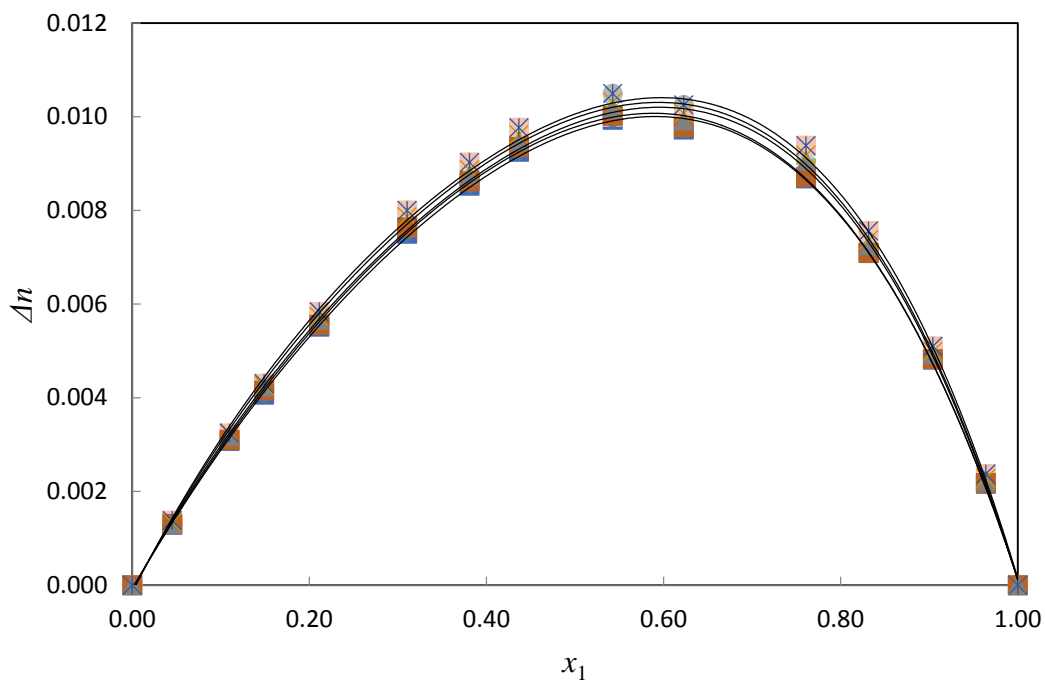


5.6 Plot of isentropic compressibility (k_s), for the binary system {thiophene (x_1) + [EMIM] [EtSO₄] (x_2)} against mole fraction of thiophene; at $T = (298.15, 303.15, 308.15, 313.15, \text{ and } 318.15) \text{ K}$.

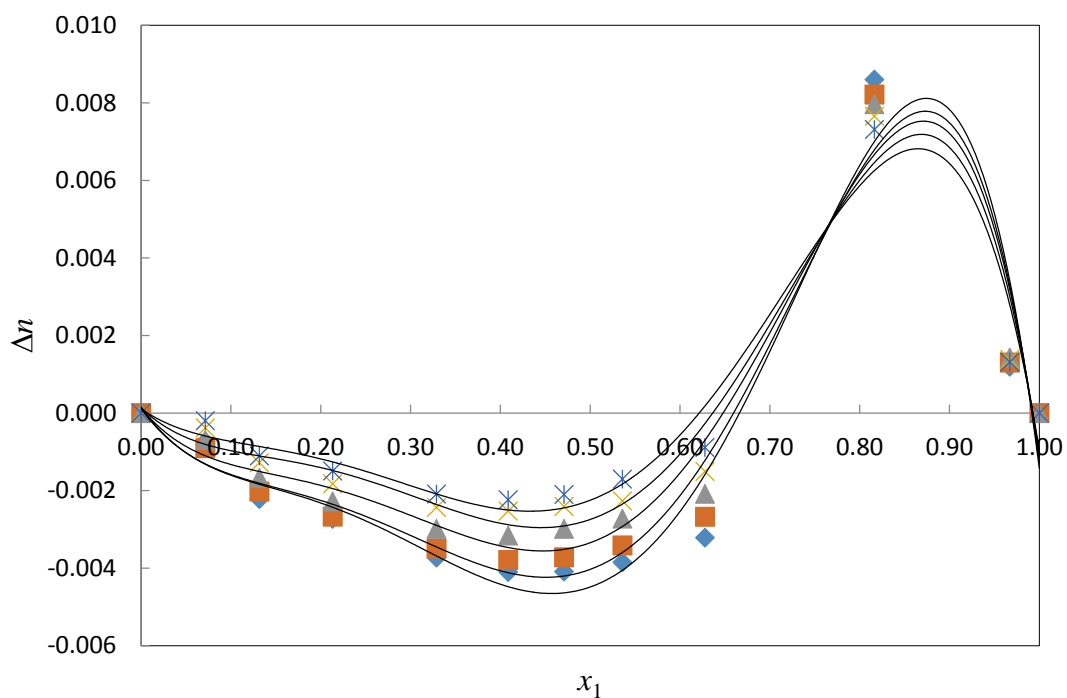
The plot of change in refractive index (Δn), for the binary systems {pyridine (Py) or ethyl acetoacetate (EAA) or thiophene (TS) + [EMIM] [EtSO₄]} at $T = (298.15 \text{ K } (\diamond), 303.15 \text{ K } (\square), 308.15 \text{ K } (\triangle), 313.15 \text{ K } (\times) \text{ and } 318.15 \text{ K } (*))$ over the complete composition range are given in figures 5.7-5.9. The change in refractive index is negative for the binary systems {pyridine (PY) + [EMIM] [EtSO₄]}, and {thiophene (TS) + [EMIM] [EtSO₄]}, but is positive for the binary system {ethyl acetoacetate (EAA) + [EMIM] [EtSO₄]}.



5.7 Plot of change in refractive index (Δn), for the binary system {pyridine (x_1) + [EMIM] [EtSO₄] (x_2)} against mole fraction of pyridine; at $T = (298.15, 303.15, 308.15, 313.15, \text{ and } 318.15) \text{ K}$. The solid lines represents the Redlich-Kister correlation equation 3.5.1.



5.8 Plot of change in refractive index (Δn), for the binary system {ethyl acetoacetate (x_1) + [EMIM] [EtSO₄] (x_2)} against mole fraction of ethyl acetoacetate; at $T = (298.15, 303.15, 308.15, 313.15, \text{ and } 318.15) \text{ K}$. The solid lines represents the Redlich-Kister correlation equation 3.5.1



5.9 Plot of change in refractive index (Δn), for the binary system {thiophene (x_1) + [EMIM] [EtSO₄] (x_2)} against mole fraction of thiophene; at $T = (298.15, 303.15, 308.15, 313.15, \text{ and } 318.15)$ K. The solid lines represents the Redlich-Kister correlation equation 3.5.1.

Table 5.7 below list the Redlich-Kister fitting parameter and root-mean-square deviation (σ), for the binary mixtures at $T = (298.15, 303.15, 308.15, 313.15, \text{ and } 318.15)$ K.

Table 5.7 Redlich-Kister fitting parameter and root-mean-square deviation (σ), for the binary mixtures at $T = (298.15, 303.15, 308.15, 313.15, \text{ and } 318.15)$ K.

| | T/K | A_0 | A_1 | A_2 | A_3 | σ |
|---|--------|---------|---------|--------|---------|----------|
| {Py (x_1) + [EMIM] [EtSO ₄]} (x_2) | | | | | | |
| $V_m^E / (\text{cm}^3 \cdot \text{mol}^{-1})$ | 298.15 | -4.698 | 2.141 | -4.851 | -1.703 | 0.041 |
| | 303.15 | -4.850 | 2.172 | -4.847 | -1.452 | 0.041 |
| | 308.15 | -5.006 | 2.292 | -4.843 | -1.292 | 0.040 |
| | 313.15 | -5.149 | 2.435 | -4.785 | -1.062 | 0.038 |
| | 318.15 | -5.303 | 2.573 | -4.750 | -0.842 | 0.037 |
| Δn | 298.15 | -0.0092 | -0.0026 | 0.0120 | -0.0160 | 0.0004 |
| | 303.15 | -0.0066 | -0.0048 | 0.0160 | -0.0170 | 0.0002 |
| | 308.15 | -0.0050 | -0.0048 | 0.0180 | -0.0200 | 0.0003 |
| | 313.15 | -0.0031 | -0.0057 | 0.0200 | -0.0210 | 0.0003 |
| | 318.15 | -0.0096 | -0.0065 | 0.0210 | -0.0210 | 0.0003 |
| {EAA (x_1) + [EMIM] [EtSO ₄]} (x_2) | | | | | | |
| $V_m^E / (\text{cm}^3 \cdot \text{mol}^{-1})$ | 298.15 | -4.777 | 1.478 | -1.675 | -1.506 | 0.021 |
| | 303.15 | -4.963 | 1.544 | -1.738 | -1.738 | 0.022 |
| | 308.15 | -5.154 | 1.622 | -1.809 | -1.602 | 0.023 |
| | 313.15 | -5.356 | 1.682 | -1.874 | -1.710 | 0.024 |
| | 318.15 | -5.569 | 1.760 | -1.956 | -1.791 | 0.025 |
| Δn | 298.15 | 0.0390 | -0.0110 | 0.0070 | 0.0064 | 0.0001 |
| | 303.15 | 0.0390 | -0.0110 | 0.0069 | 0.0068 | 0.0001 |
| | 308.15 | 0.0400 | -0.0110 | 0.0078 | 0.0067 | 0.0001 |

| | | | | | | |
|---|--|---------|---------|--------|---------|--------|
| | 313.15 | 0.0400 | -0.0120 | 0.0078 | 0.0066 | 0.0001 |
| | 318.15 | 0.0410 | -0.0120 | 0.0082 | 0.0075 | 0.0001 |
| | {TS (x_1) + [EMIM] [EtSO ₄]} (x_2) | | | | | |
| $V_m^E / (\text{cm}^3 \cdot \text{mol}^{-1})$ | 298.15 | -7.787 | 7.144 | 11.043 | -28.577 | 0.349 |
| | 303.15 | -8.004 | 7.417 | 11.406 | -29.154 | 0.365 |
| | 308.15 | -8.211 | 7.559 | 12.014 | -29.657 | 0.369 |
| | 313.15 | -8.43 | 7.674 | 12.766 | -30.290 | 0.361 |
| | 318.15 | -8.665 | 7.918 | 13.455 | -31.103 | 0.383 |
| Δn | 298.15 | -0.017 | -0.024 | 0.066 | -0.041 | 0.0016 |
| | 303.15 | -0.015 | -0.024 | 0.062 | -0.038 | 0.0014 |
| | 308.15 | -0.012 | -0.023 | 0.058 | -0.035 | 0.0013 |
| | 313.15 | -0.0098 | -0.022 | 0.0055 | -0.030 | 0.0012 |
| | 318.15 | -0.0080 | -0.023 | 0.052 | -0.023 | 0.0011 |

Standard uncertainties u are $u(x_1) = \pm 0.0004$, $u(T) = \pm 0.03$ K, $u(p) = \pm 0.05$ MPa and the combined expanded uncertainty U_c in density and refractive index measurements was less than $U_c(\rho) = \pm 4 \cdot 10^{-4}$ g · cm⁻³ and $U_c(n) = \pm 4 \cdot 10^{-4}$, respectively (0.95 level of confidence).

5.2 Prediction of density or refractive index

The Lorentz-Lorenz equation is used for predicting the density (ρ), which is related to refractive index (n), by:

$$\rho = \frac{\left(\frac{n^2 - 1}{n^2 + 2}\right)(x_1 M_1 + x_2 M_2)}{\left(\frac{n_1^2 - 1}{n_1^2 + 2}\right)x_1 \frac{M_1}{\rho_1} + x_2 \left(\frac{n_2^2 - 1}{n_2^2 + 2}\right) \frac{M_2}{\rho_2}} \quad (5.3.1)$$

By using equation 5.3.1, n can be calculated from pure-product density and refractive index data and from experimental density of the mixture. The equation for n is given below:

$$n = \left(\frac{\left[\left(\frac{n_1^2 - 1}{n_1^2 + 2}\right)x_1 \rho \frac{M_1}{\rho_1} + x_2 \left(\frac{n_2^2 - 1}{n_2^2 + 2}\right) \rho \frac{M_2}{\rho_2} \right] + [x_1 M_1 + x_2 M_2]}{\left[x_1 M_1 + x_2 M_2 \right] - \left[\left(\frac{n_1^2 - 1}{n_1^2 + 2}\right)x_1 \rho \frac{M_1}{\rho_1} + x_2 \left(\frac{n_2^2 - 1}{n_2^2 + 2}\right) \rho \frac{M_2}{\rho_2} \right]} \right)^{1/2} \quad (5.3.2)$$

Table 5.8 below list the root-mean-square deviation (σ), for excess molar volume, density, and refractive index for the binary mixtures at $T = (298.15, 303.15, 308.15, 313.15, \text{ and } 318.15)$ K.

The Lorentz-Lorenz equation gives a poor correlation for the excess molar volume, but is a good predictor of density or refractive index.

Table 5.8 Root mean square deviation (σ), obtained from the Lorentz-Lorenz equation, for V_m^E , ρ and n for the binary mixtures at $T = (298.15, 303.15, 308.15, 313.15$ and $318.15)$ K.

| Properties | σ | | | | |
|--|--|---------|---------|---------|---------|
| | T/K | | | | |
| | 298.15 | 303.15 | 308.15 | 313.15 | 318.15 |
| | {Py (x_1) + [EMIM] [EtSO ₄] (x_2)} | | | | |
| $V_m^E / (\text{cm}^{-3} \cdot \text{mol}^{-1})$ | 0.33140 | 0.29867 | 0.28583 | 0.26215 | 0.23401 |
| $\rho / (\text{g} \cdot \text{cm}^{-3})$ | 0.00269 | 0.00240 | 0.00192 | 0.00048 | 0.00048 |
| n | 0.00134 | 0.00120 | 0.00114 | 0.00105 | 0.00095 |
| | {EAA (x_1) + [EMIM][EtSO ₄] (x_2)} | | | | |
| $V_m^E / (\text{cm}^{-3} \cdot \text{mol}^{-1})$ | 0.11124 | 0.12915 | 0.12595 | 0.13952 | 0.14314 |
| $\rho / (\text{g} \cdot \text{cm}^{-3})$ | 0.00034 | 0.00045 | 0.00048 | 0.00049 | 0.00050 |
| n | 0.00020 | 0.00020 | 0.00091 | 0.00023 | 0.00227 |
| | {TS (x_1) + [EMIM][EtSO ₄] (x_2)} | | | | |
| $V_m^E / (\text{cm}^{-3} \cdot \text{mol}^{-1})$ | 1.00718 | 1.00168 | 0.99078 | 0.98003 | 0.97827 |
| $\rho / (\text{g} \cdot \text{cm}^{-3})$ | 0.01181 | 0.01065 | 0.01027 | 0.01011 | 0.00999 |
| n | 0.19659 | 0.19527 | 0.19400 | 0.19276 | 0.17945 |

Standard uncertainties u are $u(x_1) = \pm 0.0004$, $u(T) = \pm 0.03$ K, $u(p) = \pm 0.05$ MPa and the combined expanded uncertainty U_c in density and refractive index measurements was less than $U_c(\rho) = \pm 4 \cdot 10^{-4} \text{ g} \cdot \text{cm}^{-3}$ and $U_c(n) = \pm 4 \cdot 10^{-4}$, respectively (0.95 level of confidence).

DISCUSSION

6.1 Density**6.1.1 Effect of temperature and composition on density**

The experimental density data (ρ), of (pyridine or ethyl acetoacetate or thiophene + [EMIM] [EtSO₄]) binary systems over the complete composition and at all different experimental temperatures are listed in tables 5.1-5.3. The density decreases with T and an increase in the composition of the IL for the binary mixtures (pyridine or ethyl acetoacetate or thiophene + [EMIM] [EtSO₄]). The smaller size of the cation and anion of the IL results in stronger interactions with the aromatic pyridine or thiophene molecules (Anantharaj and Banerjee. 2011). The electron-rich N and S atoms of the pyridine or thiophene molecules, respectively, form hydrogen bonds with the H atom located on the alkyl group of the imidazolium cation (Anantharaj and Banerjee. 2011). Also, the electrostatic interaction between the ions of the IL (ion-ion interactions) are weaker than that between the pyridine or thiophene and IL molecules, the former is due to the larger alkyl substituent on the N atom of the imidazolium cation (Anantharaj and Banerjee. 2011).

6.2 Excess molar volume**6.2.1 Effect of temperature and composition on the excess molar volume**

The results for the excess molar volume of the binary systems (pyridine or ethyl acetoacetate or thiophene + [EMIM] [EtSO₄]) are given in tables 5.1-5.3 and plotted in figures 5.1-5.3. V_m^E is negative for all the systems at experimental temperatures and decreases when the temperature is increased, however for the binary mixture (thiophene + [EMIM] [EtSO₄]), V_m^E is negative at low

mole fractions of thiophene and becomes positive at high mole fractions (> 0.9) of thiophene. This behavior occurs because hydrogen bonding increases as the temperature is increased. This results is similar with the work of (Anantharaj and Banerjee 2013). The kinetic energy of molecules is directly proportional to the temperature thus more kinetically favored interactions occurs as the temperature is increased. The hydrogen bonding is also directly proportional to the composition of the binary mixture. When the concentration of the components increases more molecules are present to cause effective interaction through hydrogen bonding. Figure 5.3 does not follow a definite trend and this is because thiophene is an unstable and a volatile compound, hence it does not mix well with the ionic liquid. This affect the densities of the binary mixtures, causing the plot to be indefinite. $V_{m,min}^E$ for the binary mixtures increases in the order $TS < Py < EAA$. $V_{m,min}^E$ for thiophene is smaller than that for pyridine because of the similar structure of thiophene and the imidazolium ring (both are 5-membered) resulting in greater intermolecular interaction (Anantharaj and Banerjee 2011). The $V_{m,min}^E$ values at $T = 298.15$ K at $x_1 = 0.7323$ is -1.284 , $x_1 = 0.5424$ is -1.246 , $x_1 = 0.6277$ is -1.870 , for (pyridine + [EMIM] [EtSO₄]), (ethyl acetoacetate + [EMIM] [EtSO₄]), and (thiophene + [EMIM] [EtSO₄]), respectively.

The negative contributions may be due to the strong attractive intermolecular interactions such as hydrogen bonding between (pyridine + [EMIM] [EtSO₄]), (ethyl acetoacetate + [EMIM] [EtSO₄]), and (thiophene + [EMIM] [EtSO₄]) components of the binary mixtures. The electron-rich N and S atoms of the pyridine or thiophene molecules, respectively, form hydrogen bonds with the H atom located on the alkyl group of the imidazolium cation (Anantharaj and Banerjee. 2011). For the binary mixture (ethyl acetoacetate + [EMIM] [EtSO₄]) hydrogen bonding occurs between the H atom located on the alkyl group of the imidazolium cation and a CH₃ group located next to the carbon-oxygen double bond group of the EAA molecules. For the (thiophene + [EMIM][EtSO₄])

binary mixture the positive V_m^E at high mole fractions of the thiophene molecule can possibly be due to the larger S atom present in the thiophene molecule leading to the disruption of the intramolecular bonding in the IL.

6.3 Isentropic compressibility

6.3.1 Effect of temperature and composition on speed of sound

The speed of sound (u), and isentropic compressibility (k_s), data of (pyridine or ethyl acetoacetate or thiophene + [EMIM] [EtSO₄]) binary systems over the entire composition range at different temperatures are listed in tables 5.1-5.3. For each binary mixture, isentropic compressibility (k_s) of the binary mixtures is plotted against the mole fraction of pyridine or ethyl acetoacetate or thiophene, at all temperatures and are given in figures 5.1-5.3. The speed of sound of binary mixtures increase with an increase in temperature and with an increase in the composition of the binary mixtures.

For the binary mixtures (pyridine or ethyl acetoacetate or thiophene + [EMIM] [EtSO₄]) the isentropic compressibility is positive at the five experimental temperatures and over the entire composition range, therefore the binary mixtures are more compressible than the ideal mixture.

The $k_{s, \min}$ at $T = 298.15$ K at $x_1 = 0.0729$ is 287 T. Pa⁻¹ for (Py + [EMIM] [EtSO₄]) system, $x_1 = 0.0451$ is 296 T. Pa⁻¹ for (EAA + [EMIM] [EtSO₄]), $x_1 = 0.0717$ is 301 T. Pa⁻¹ for (TS + [EMIM] [EtSO₄]). The $k_{s, \min}$ for the binary mixtures increases in the order Py < EAA < TS.

6.4 Change in refractive index

6.4.1 Effect of temperature and composition on refractive index

The refractive index data is given in tables 5.4-5.6. Refractive index decrease with an increase in the temperature but increases in the order ethyl acetoacetate < pyridine < thiophene.

The refractive index for the binary mixtures (pyridine or thiophene + [EMIM] [EtSO₄]) decreases with increasing IL composition possibly due to a more efficient packing and increases for the binary mixture (ethyl acetoacetate + [EMIM] [EtSO₄]) with an increase in the IL composition , (Anantharaj and Banerjee 2011).

The change in refractive index (Δn), of the binary mixture is plotted against mole fraction of pyridine or ethyl acetoacetate or thiophene at all temperatures. For the binary mixture (pyridine + [EMIM] [EtSO₄]), Δn is negative at mole fractions < 0.75 of pyridine and positive at mole fractions > 0.75 at all temperatures and decreases with an increase in temperature. For the binary system (ethyl acetoacetate + [EMIM] [EtSO₄]), Δn values are positive over the entire composition range and at all temperatures and increases with an increase in temperature. Δn values for the (thiophene + IL) binary system are negative for mole fractions of thiophene < 0.62 and becomes positive for mole fractions of thiophene > 0.62 and Δn also increases with an increase in temperature.

$\Delta n_{, \max}$ at $T = 298.15$ K at $x_1 = 0.9438$ is 0.00013, for (pyridine + [EMIM] [EtSO₄]) binary system and for the for (EAA + [EMIM] [EtSO₄]) binary system; $\Delta n_{, \max}$ at $T = 298.15$ K at $x_1 = 0.5424$ is 0.00993.

For (thiophene + [EMIM] [EtSO₄]) binary system; $\Delta n_{, \max}$ at $T = 298.15$ K at $x_1 = 0.8164$ is 0.00731. $\Delta n_{, \max}$ for the binary mixtures increases in the order EAA $>$ TS $>$ Py.

The plot of comparison between experimental and literature, V_m^E , for the binary systems {pyridine (Py) or thiophene (TS) + [EMIM] [EtSO₄]} at $T = 298.15$ K over the complete composition range are given in figures 6.1- 6.2. V_m^E results reported in this work are similar to those obtained from literature but are quantitatively different.

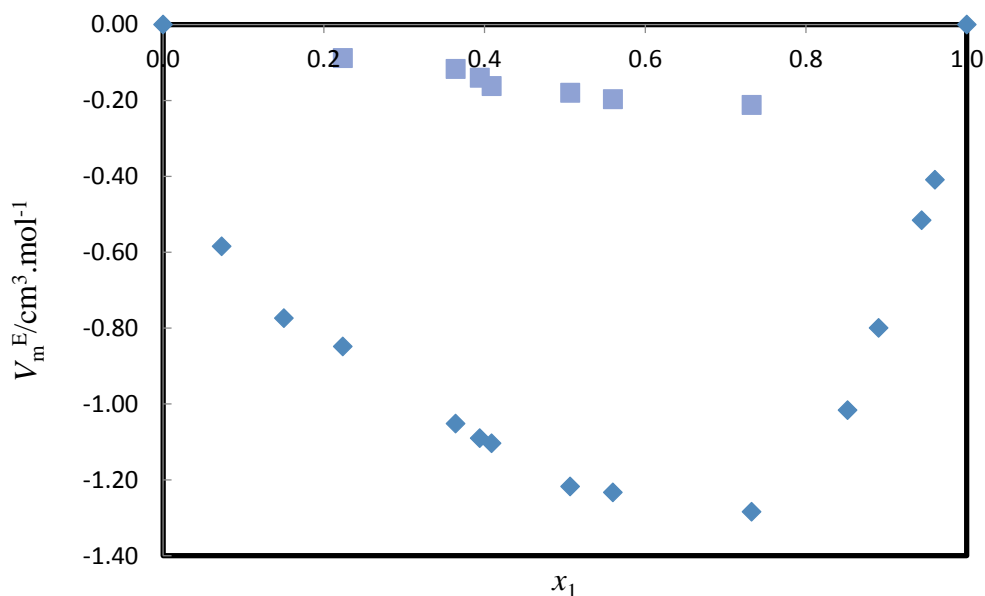
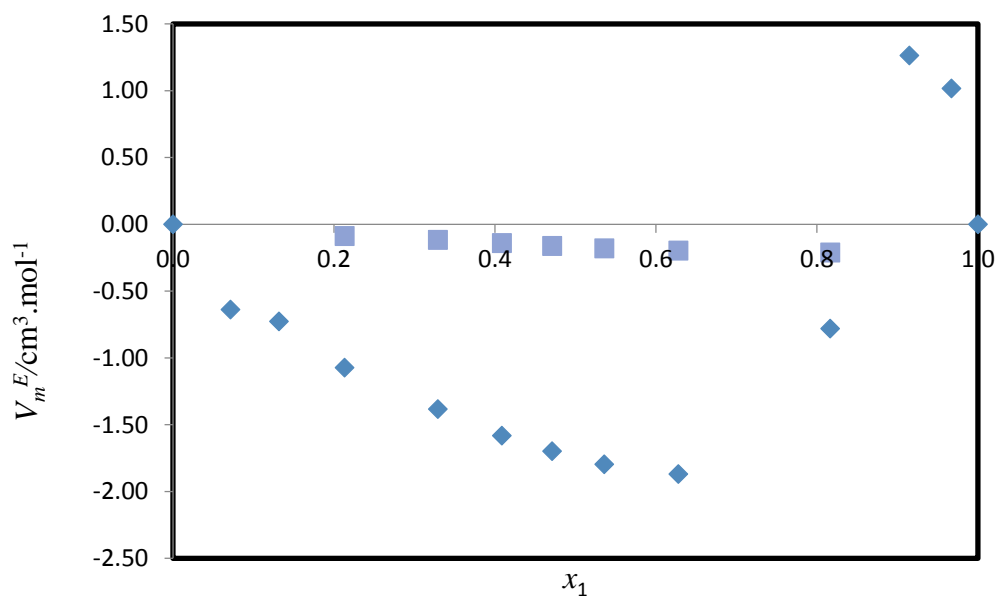


Figure 6.1 Excess molar volume (V_m^E), of the binary mixture plotted against mole fraction x_1 of pyridine at $T = 298.15$ K {pyridine (x_1) + [EMIM] [MeSO₄] (x_2)}, \diamond , this work and \blacksquare , (Anantharaj and Banerjee 2013).



6.2 Excess molar volume (V_m^E), of the binary mixture plotted against mole fraction x_1 of thiophene at $T = 298.15 \text{ K}$ {thiophene (x_1) + [EMIM] [MeSO₄] (x_2)}, \diamond , this work and \square , (Anantharaj and Banerjee 2013).

6.5 Prediction of density by Lorentz-Lorenz (L-L) approximation

The molar refraction for the binary mixture is assumed to behave as an ideal mixture, the following predictive expression for the density (ρ), can be obtained from equations 3.4.8 and 3.4.9 within the frame-work of the Lorentz–Lorenz approximation.

$$\rho = \frac{\left(\frac{n^2 - 1}{n^2 + 2}\right)(x_1 M_1 + x_2 M_2)}{\left(\frac{n_1^2 - 1}{n_1^2 + 2}\right)x_1 \frac{M_2}{\rho_2} + x_2 \left(\frac{n_2^2 - 1}{n_2^2 + 2}\right) \frac{M_2}{\rho_2}} \quad (3.4.8)$$

The plot of experimental density (ρ), for the binary systems {pyridine (Py) or ethyl acetoacetate (EAA) or thiophene (TS) + [EMIM] [EtSO₄]} at $T = (298.15 \text{ K } (\diamond), 303.15 \text{ K } (\square), 308.15 \text{ K } (\triangle), 313.15 \text{ K } (x) \text{ and } 318.15 \text{ K } (*))$ over the complete composition range are given in figures 6.3-6.5. The density is positive, and decrease as the organic solute composition increases for each binary system.

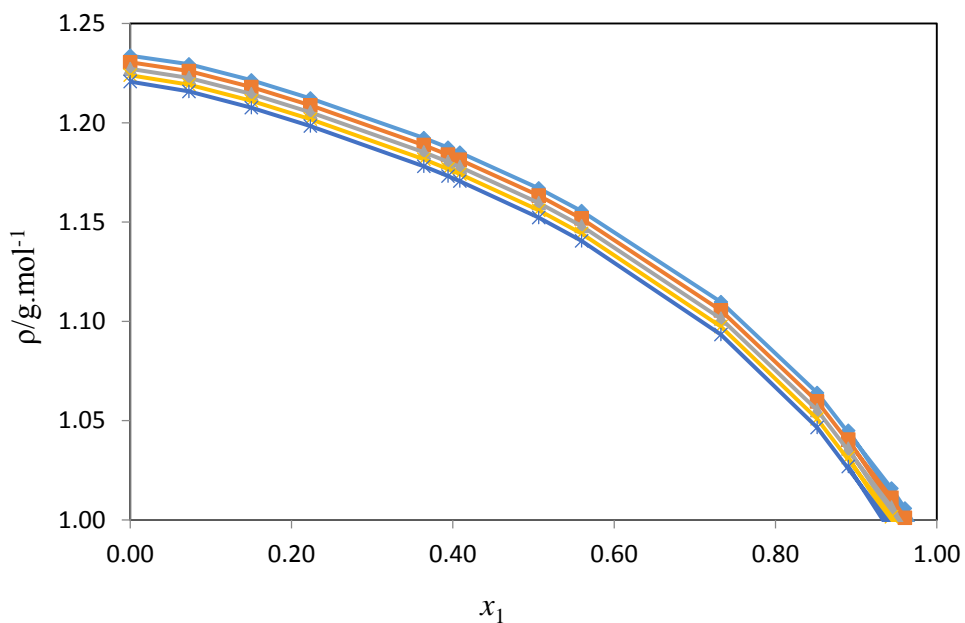


Figure 6.3 Experimental density (ρ), of the binary mixture plotted against mole fraction x_1 of pyridine at $T = (298.15 \text{ to } 318.15) \text{ K}$. $T = 298.15 \text{ K}$; \diamond , $T = 303.15 \text{ K}$; \square , $T = 308.15 \text{ K}$; \triangle , $T = 313.15 \text{ K}$; x , and 318.15 ; x . For the binary mixture {pyridine (x_1) + [EMIM] [EtSO₄] (x_2)}. The solid lines represent the corresponding prediction by the L-L approximation equation 3.4.8.

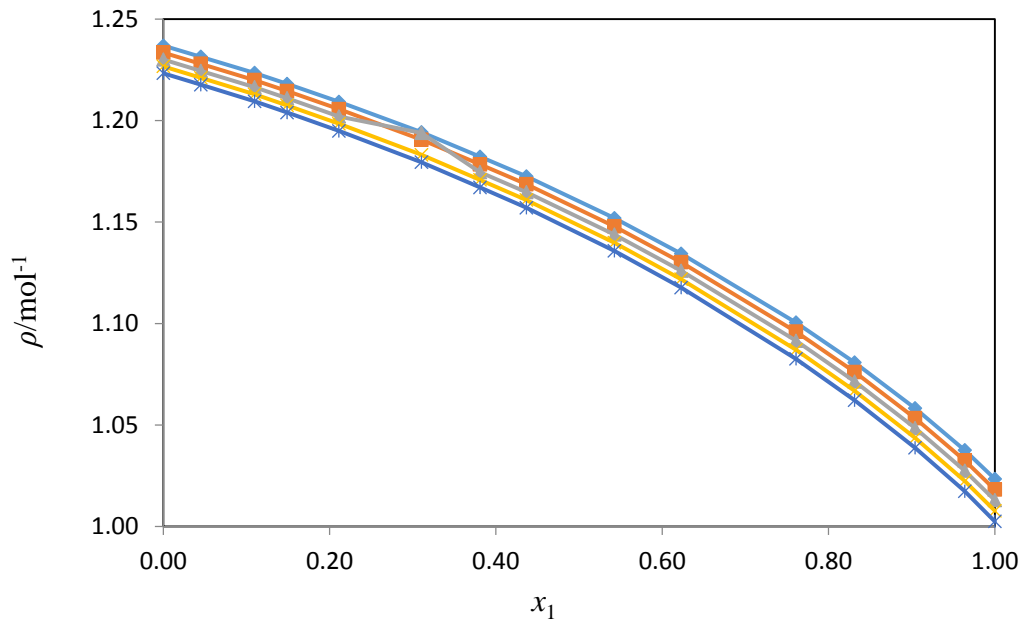


Figure 6.4 Experimental density (ρ), of the binary mixture plotted against mole fraction x_1 of ethyl acetoacetate at $T = (298.15 \text{ to } 318.15) \text{ K}$. $T = 298.15 \text{ K}$; \diamond , $T = 303.15 \text{ K}$; \square , $T = 308.15 \text{ K}$; \triangle , $T = 313.15 \text{ K}$; \times , and 318.15 ; \times . For the binary mixture {EAA (x_1) + [EMIM] [EtSO₄] (x_2)}. The solid lines represent the corresponding prediction by the L-L approximation equation 3.4.8.

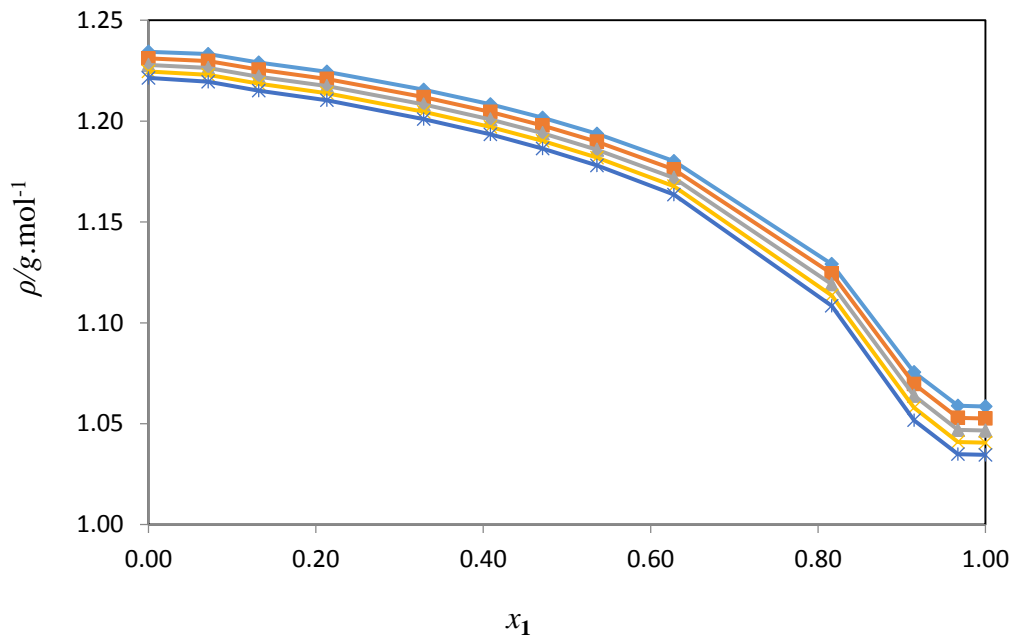


Figure 6.5 Experimental density (ρ), of the binary mixture plotted against mole fraction x_1 of thiophene at $T = (298.15 \text{ to } 318.15) \text{ K}$. $T = 298.15 \text{ K}$; \diamond , $T = 303.15 \text{ K}$; \square , $T = 308.15 \text{ K}$; Δ , $T = 313.15 \text{ K}$; \times , and 318.15 ; \times . For the binary mixture $\{\text{TS} (x_1) + [\text{EMIM}] [\text{EtSO}_4] (x_2)\}$. The solid lines represent the corresponding prediction by the L-L approximation equation 3.4.8.

Table 6.1 below lists the root mean square deviation (RMSD) (σ), between the experimental and the predicted density using the Lorentz-Lorenz equation for the binary mixtures at $T = (298.15, 303.15, 308.15, 313.15, \text{ and } 318.15)$ K.

Table 6.1 Root mean square deviation (σ), between the experimental and the predicted density using the Lorentz-Lorenz equation for the binary mixtures at $T = (298.15, 303.15, 308.15, 313.15, \text{ and } 318.15)$ K.

| | T/K | | | | |
|----------------------|------------------------------------|---------|---------|---------|---------|
| | 298.15 | 303.15 | 308.15 | 313.15 | 318.15 |
| | {Py + [EMIM][EtSO ₄]} | | | | |
| RMSD (σ) | 0.00264 | 0.02532 | 0.02439 | 0.02429 | 0.02416 |
| | {EAA + [EMIM][EtSO ₄]} | | | | |
| RMSD (σ) | 0.00034 | 0.00045 | 0.00199 | 0.00048 | 0.00732 |
| | {TS + [EMIM][EtSO ₄]} | | | | |
| RMSD (σ) | 0.01229 | 0.01204 | 0.01054 | 0.01168 | 0.01153 |

6.6 Correlation of excess molar volume by Lorentz-Lorenz (L-L) approximation

The correlation of the excess molar volume can be obtained using the refractive index obtained for the binary mixture by the Lorentz-Lorenz approximation. The experimental V_m^E and Δn data are given in tables 5.1-5.3 and 5.4-5.7, respectively. Equation 3.4.6 was used to correlate the experimental V_m^E data.

$$V_m^E = (-\Delta n) \frac{3R(n^{id} + n)}{(n^2 - 1)(n^{id})^2 - 1} = (-\Delta n) f(R, n^{id}, n) \quad (3.4.6)$$

The greatest increase in RMSD occurred for (Py + [EMIM] [EtSO₄]) system because pyridine is the most volatile solvent among three solvents used in this work. The root mean square deviation (σ), between the experimental and correlated V_m^E for the binary systems at $T = (298.15, 303.15, 308.15, 313.15, \text{ and } 318.15) \text{ K}$ are shown in table 6.2. The maximum RMSD is $\pm 1.00718 \text{ cm}^3 \cdot \text{mol}^{-1}$ which was obtained for the (thiophene + [EMIM] [EtSO₄]) binary system. The isentropic compressibility for the (thiophene + [EMIM] [EtSO₄]) binary system is relatively higher, because the components of the mixture are not mixed easily. This is due to thiophene being an unstable and a volatile compound, thus the deviation is very high for the TS system.

Table 6.2 below lists the root mean square deviation (σ), obtained from the Lorentz-Lorenz equation for V_m^E , of the binary mixtures at $T = (298.15, 303.15, 308.15, 313.15$ and $318.15)$ K.

Table 6.2 Root mean square deviation (σ), obtained from the Lorentz-Lorenz equation for V_m^E , of the binary mixtures at $T = (298.15, 303.15, 308.15, 313.15$ and $318.15)$ K.

| | | RMSD (σ) | | | | |
|---|---------|--|---------|--------|---------|---------|
| | | T/K | | | | |
| | | 298.15 | 303.15 | 308.15 | 313.15 | 318.15 |
| | | {Py (x_1) + [EMIM] [EtSO ₄] (x_2)} | | | | |
| $V_m^E / (\text{cm}^3 \cdot \text{mol}^{-1})$ | 0.33142 | 0.29868 | 0.28583 | | 0.26215 | 0.23401 |
| | | {EAA (x_1) + [EMIM][EtSO ₄] (x_2)} | | | | |
| $V_m^E / (\text{cm}^3 \cdot \text{mol}^{-1})$ | 0.11124 | 0.12915 | 0.12595 | | 0.13952 | 0.14314 |
| | | {TS (x_1) + [EMIM][EtSO ₄] (x_2)} | | | | |
| $V_m^E / (\text{cm}^3 \cdot \text{mol}^{-1})$ | 1.00718 | 1.00168 | 0.99078 | | 0.98003 | 0.97827 |

6.7 Prediction of refractive index by the Lorentz-Lorenz (L-L) approximation

Equation 3.4.9 was used in a modelling to obtain the inverse prediction of n from pure solvent density and refractive index data and from the experimental density of the binary mixture. The Lorentz-Lorenz equation for the prediction of the refractive index (n), is given below:

$$n = \left(\frac{\left[\left(\frac{n_1^2 - 1}{n_1^2 + 2} \right) x_1 \rho \frac{M_1}{\rho_1} + x_2 \left(\frac{n_2^2 - 1}{n_2^2 + 2} \right) \rho \frac{M_2}{\rho_2} \right] + [x_1 M_1 + x_2 M_2]}{[x_1 M_1 + x_2 M_2] - \left[\left(\frac{n_1^2 - 1}{n_1^2 + 2} \right) x_1 \rho \frac{M_1}{\rho_1} + x_2 \left(\frac{n_2^2 - 1}{n_2^2 + 2} \right) \rho \frac{M_2}{\rho_2} \right]} \right)^{1/2} \quad (3.4.9)$$

The plot of the refractive index (n), for the binary systems {pyridine (Py) or ethyl acetoacetate (EAA) or thiophene (TS) + [EMIM] [EtSO₄]} at $T = 298.15$ K (\diamond), 303.15 K (\square), 308.15 K (\triangle), 313.15 K (\times) and 318.15 K ($*$) over the complete composition range are given in figures 6.6 – 6.8. The refractive index is positive for the binary systems {pyridine (Py) + [EMIM] [EtSO₄]}, {ethyl acetoacetate + [EMIM] [EtSO₄]}, and {thiophene (TS) + [EMIM] [EtSO₄]}.

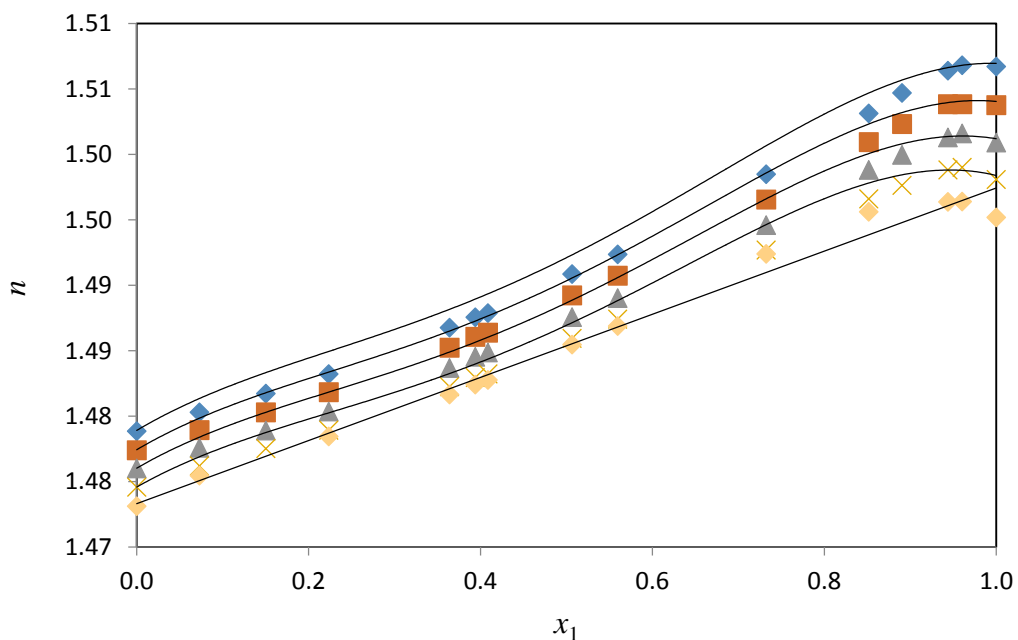


Figure 6.6 Refractive index (n), of the binary mixture plotted against mole fraction x_1 of pyridine at $T = (289.15$ K to $318.15)$ K. \diamond , $T = 298.15$ K; \square , $T = 303.15$ K; \triangle , $T = 308.15$ K; \times , $T = 313.15$ K; and \square , $T = 318.15$ K. The solid lines represents the Lorentz – Lorenz (L-L) approximation equation 3.4.9.

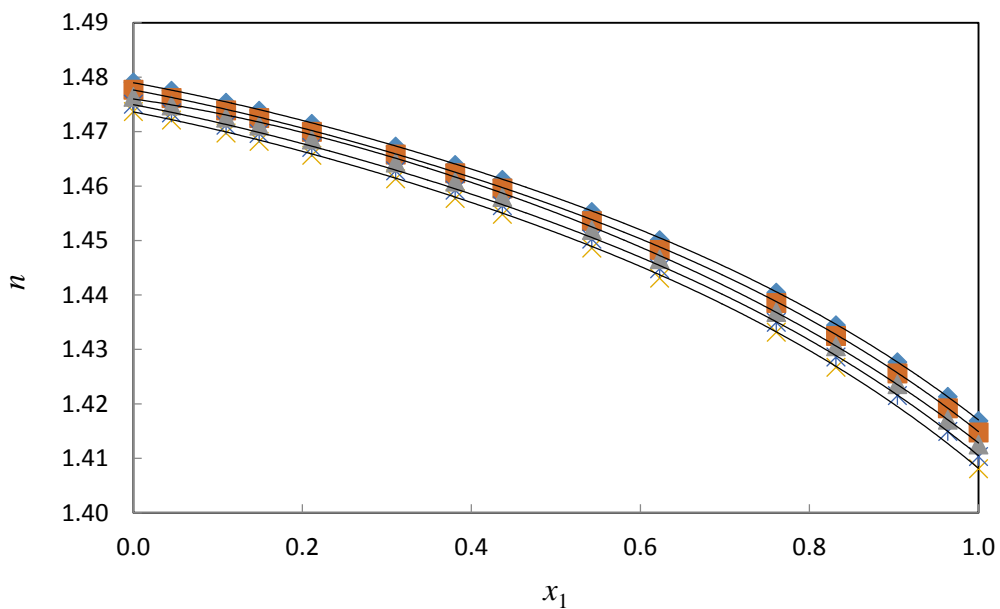


Figure 6.7 Refractive index (n), of the binary mixture plotted against mole fraction x_1 of ethyl acetoacetate at $T = (289.15 \text{ K to } 318.15 \text{ K})$. \diamond , $T = 298.15 \text{ K}$; \square , $T = 303.15 \text{ K}$; Δ , $T = 308.15 \text{ K}$; \times , $T = 313.15 \text{ K}$; and \square , $T = 318.15 \text{ K}$. The solid lines represents the Lorentz – Lorenz (L-L) approximation equation 3.4.9.

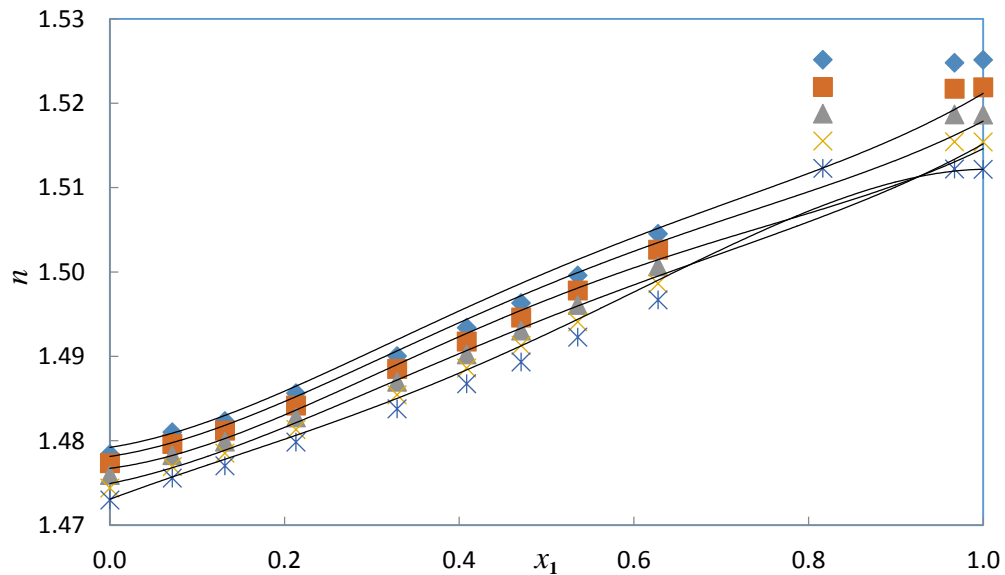


Figure 6.8 Refractive index (n), of the binary mixture plotted against mole fraction x_1 of thiophene at $T = (289.15 \text{ K to } 318.15 \text{ K})$. \diamond , $T = 298.15 \text{ K}$; \square , $T = 303.15 \text{ K}$; \triangle , $T = 308.15 \text{ K}$; \times , $T = 313.15 \text{ K}$; and \square , $T = 318.15 \text{ K}$. The solid lines represents the Lorentz – Lorenz (L-L) approximation equation 3.4.9.

Table 6.3 below lists the root mean square deviation (σ), obtained from the Lorentz-Lorenz equation for n , of the binary mixtures at $T = (298.15, 303.15, 308.15, 313.15 \text{ and } 318.15) \text{ K}$.

Table 6.3 Root mean square deviation (σ), obtained from the Lorentz-Lorenz equation for n , of the binary mixtures at $T = (298.15, 303.15, 308.15, 313.15 \text{ and } 318.15) \text{ K}$.

| | | RMSD (σ) | | | | |
|-----|--|--|--------|--------|----------|----------|
| | | T/K | | | | |
| | | 298.15 | 303.15 | 308.15 | 313.15 | 318.15 |
| | | {Py (x_1) + [EMIM] [EtSO ₄] (x_2)} | | | | |
| n | | 0.0013 | 0.0012 | 0.0011 | 0.0011 | 0.0010 |
| | | {EAA (x_1) + [EMIM][EtSO ₄] (x_2)} | | | | |
| n | | 0.0002 | 0.0002 | 0.0009 | 0.0002 | 0.0023 |
| | | {TS (x_1) + [EMIM][EtSO ₄] (x_1)} | | | | |
| n | | 0.0014 | 0.0046 | 0.0045 | 0.004419 | 0.004487 |

CONCLUSION

The excess molar volume, isentropic compressibility, and deviation in refractive index for the binary systems (pyridine or ethyl acetoacetate or thiophene + [EMIM] [EtSO₄]) were calculated from the density, speed of sound, and refractive index data, respectively, at $T = (298.15, 303.15, 308.15, 313.15, \text{ and } 318.15)$ K over the whole composition range. For the binary mixtures (pyridine or ethyl acetoacetate + [EMIM] [EtSO₄]) V_m^E is negative over the entire composition range and at all temperatures and decreases as the temperature increases. For the binary mixture (thiophene + [EMIM] [EtSO₄]) V_m^E is negative at low mole fractions of thiophene and becomes positive at high mole fractions (> 0.9) of thiophene. For each system, k_s was positive over the entire composition range and at all temperatures indicating that the binary mixtures are more compressible than the ideal mixture.

For the binary mixture (pyridine + [EMIM] [EtSO₄]), Δn is negative at mole fractions < 0.75 of pyridine and positive at mole fractions > 0.75 at all temperatures and decreases with an increase in temperature. For the binary system (ethyl acetoacetate + [EMIM] [EtSO₄]), Δn values are positive over the entire composition range and at all temperatures and increases with an increase in temperature. Δn values for the (thiophene + IL) system are positive for mole fractions of thiophene < 0.62 and becomes positive for mole fractions of thiophene > 0.62 and Δn increases with an increase in temperature.

The Redlich-Kister smoothing equation was used successfully for the correlation of V_m^E and Δn data. The Lorentz-Lorenz equation was used to correlate the excess molar volume and predict the

density or refractive index for the binary mixtures (pyridine or ethyl acetoacetate or thiophene + [EMIM] [EtSO₄]). The Lorentz-Lorenz equation gives a poor correlation for the excess molar volume, but a good prediction of density or refractive index.

REFERENCES

- Anantharaj, R. and Banerjee, T., *J. Thermodyn.* (2011) 978324.
- Armand, M., Endres, F., MacFarlane, D., Ohno, H. and Scrosati, B., *Nat. Mater.* 8 (2009) 621-629.
- Abbott, A. and Ryder, K., *Annu. Rev. Mater. Res.*, 43 (2013) 335-358.
- Andreani, L. and Rocha, J., *Brazilian J. Chem. Eng.* 29 (2012) 1-13.
- Ansary, A. and Omar, H., *Bull Faculty Pharm.*, (2001) 39:17.
- Anantharaj, R., Banerjee, T., *Can. J. Chem. Eng.* 91 (2013) 245–256.
- Alonso, I., Mozo, I., Fuente, I., Antonio, J. and Cobos, J., *J. Chem. Eng. Data*, 55 (2010) 5400-5405.
- Anantharaj, R. and Banerjee, T., *Int. J. Chem. Eng.* (2011) 209435.
- Arce, A., Rodil, E. and Soto, A., *J. Chem. Eng. Data*, 51 (2006) 1453-1457.
- Alvarez, H., Mattedi, S., Martin-Pastor, M., Aznar, M. and Iglesias, M., *J. Chem. Thermodyn.* 43 (2011) 997-1010.
- Binnemans, K., *Chem. Rev.* 105 (2005) 4148.
- Bottomly, G. and Scott, R., *J. Chem. Thermodyn.* 6 (10), (1974) 973-981.
- Born, M. and Wolf, E., *Principles of Optics*, Pergamon, Oxford, (1983).
- Brocos, P., Pineiro, A., Bravo, R. and Amigo, A., *Phys. Chem. Chem. Phys.* 5 (2003) 550–557.
- Brocos, P., Pineiro, A., Bravo, R. and Amigo, A., *Phys. Chem.* 5 (2003) 550-557.

Brocos, P., Pineiro, A., Bravo, R. and Amigo, A., *J. Chem. Eng. Data*, 47 (2002) 351–358.

Brocos, P., Pineiro, A., Bravo, R. and Amigo, A., *Phys. Chem.* 5 (2003) 550-557.

Chaudhary, A., *J Adv Sci Res.* 3 (3), (2012) 03-10.

Dyson, P. and Geldbach, T., *Metal-Catalyzed Reactions in Ionic Liquids*, Springer (2007).

Domanska, U. and Laskowka, M., *J. Soln. Chem.* 37 (2008) 1271-1287.

Domanska, U., Krolikowska, M. and Walczak, K., *Physicochem. Eng. Aspects*, 436 (2013) 504-511.

Duncan, W., Sheridan, J., Swinton, F., *Trans. Faraday. Soc.* 62 (1966) 1090.

EUROPEAN COMMISSION, JOINT RESEARCH CENTRE, Special Publication I.02. 75 (2002).

Fuller, J., Carlin, R., De Long, H. and Haworth, D., *J. Chem. Soc. Chem. Commun.* (1994).

Faridbod, F., Ganjali, M., Larijani, B. and Norouzi, P., *Electrochem. Acta*, 55, 1 (2011) 234-239.

Freemantle, M., *Chem. Eng. News*, 76 (1998) 32-37.

Fermeglia, M. and Torriano, G., *J. Chem. Eng. Data*, 44 (1999) 965–969.

Fortin, J., Laesecke, A., Freund, M. and Outcalt, S., *J. Chem. Thermodyn.* 57 (2013) 276-285.

Gonzalez, E., Alonso, L. and Dominguez, A., *J. Chem. Eng. Data*, 51 (2006) 1446-1452.

Gonzalez, E., Gonzalez, B., Calvar, N., Gomez, E. and Dominguez, A., *J. Chem. Thermodyn.* 40 (2008) 1274-1281.

Gomez, E., Gonzalez, B., Calvar, N., Tojo, E. and Dominguez, A., *J. Chem. Eng. Data*, 51 (2006) 2096-2102.

Gonzalez, E., Gonzalez, B., Calvar, N. and Dominguez, A., *J. Chem. Eng. Data*, 52 (2007) 1641-6148.

Gonzalez, B., Calvar, N., Gomez, E., Dominguez, I. and Dominguez, A., *J. Chem. Eng. Data*, 54 (2009) 1353-1358.

Gonzalez, B., Calvar, N., Gonzalez, E. and Dominguez, A., *J. Chem. Eng. Data*, 53 (2008) 881-887.

Hermanutz, F., Gaehr, F., Uerdingen, E., Meister, F. and Kosan, B., *Macromolecular Symposia* 262 (2008) 23-27.

Hasan, M., Hiray, A., Kadam, U., Shirude, D., Kurhe, K. and Sawant, A., *J. Chem. Eng. Data*, 55 (2010) 535-538.

Herraez, J. and Belda, R., *J. Soln. Chem.* 35 (2006) 1315-1328.

Hwa, S., Ziegler, W., *J. Phys. Chem.* 70 (1966) 2572-2593.

Hirschfelder, J., Curtiss, C. and Bird, R., *Molecular Theory of Gases and Liquids*, Wiley, London, (1964).

Iglesias-Otero, M., Troncoso, J., Carballo, E. and Romani, L., *J. Chem. Thermodyn.* 40 (2008) 949-956.

Jung, H., Hassoun, J., Park, J., Sun, Y. and Scrosati, B., *Nature Chem.* 4 (2012) 579-585.

Jiang, H. and Kong, J., *Polymers*, 5 (2013) 1203-1214.

Jimenez, E., Casas, H., Segade, L. and Franjo, C., *J. Chem. Eng. Data*, 45 (2000) 862-866.

Khupse, N. and Kumar, A., *Indian J. Chem.* 47 (2010) 495-503.

Kumaran, M. and McGlashan, M., *J. Chem. Thermodyn.* 9 (3), (1977), 259-267.

Lehmann, J., Rausch, M., Leipertz, A. and Froba, A., *J. Chem. Eng. Data*, 55 (2010) 4068-4074.

MacFarlane, D., Meakin, P., Sun, J., Amini, N. and Forsyth, M., *J. Phys. Chem. B* 103, (1999) 4164.

Manuel, I., Tronsoco, J., Carballo, E. and Romani, L., *J. Chem. Thermodyn.* 40 (2008) 949-956.

Mahendra, R., Sarkar, L. and Dewan, R., *Bull. Chem. Soc. Ethiop.* 24 (1), (2010) 103-114.

Maurya, A., Gautam, S. and Gautam, M., *IJRANSS*, 2 (3), (2015) 111-116.

Matkowska, D., Goldon, A. and Hofman, T., *J. Chem. Data*, 55 (2010) 685-693.

Mclure, I., Benette, J., Watson, A. and Benson, G., *J. Phys. Chem.* 69 (1965) 2759.

Marchetti, A., Tassi, L., Ulrici, A., Vaccari, G. and Sanna, G., *J. Chem. Thermodyn.* 31 (1999) 647-660.

Missen, R., *Ind. Eng. Chem. Fundam.* 8 (1969) 81-84.

Mosteiro, L., Mascato, E., Cominges, B., Iglesias, T. and J. Legido, *J. Chem. Thermodyn.* 33 (2001) 787-801.

Nath, J. and Pandey, J., *J. Chem. Eng. Data*, 41 (1996) 844-847.

Nevines, J., Thermodynamics of nonelectrolytes liquid mixtures, PhD thesis, UKZN, Durban, (1997) 78-80.

Nath, J. and Mishra, S., *Fluid Phase Equilibria*, 145 (1998) 89-97.

Nayak, J., Aralaguppi, M. and Aminabhavi, T., *J. Chem. Eng. Data*, 48 (2003) 1489-1494.

Plechkova, N. and Seddon, K., *Chem. Soc. Rev.* 37 (2008) 123-150.

Perez, E., Carmen, M., German, R., Maria, E., Ramirez, M. and Moreno, A., *J. Soln. Chem.* 41 (2012) 1054-1066.

Patil, P., Patil, S., Borse, A. and Hundiware, D., *Rasayan J. Chem.* 4 (2011) 599-604.

Reddy, R., Zhang, Z., Arenas, M. and Blake, D., *High Temperature Materials and Processes* 22 (2), (2003) 87-94.

Rogers, D. and Seddon, R., *Ionic Liquids-Solvent of the future? Science*, 302 (2003) 792-793.

Rodriguez, H. and Brennecke, J., *J. Chem. Eng. Data*, 51 (2006) 2145-2155.

Rafiee, H. and Frouzesh, F., *Thermochimica Acta*, 611 (2015) 36-46.

Redhi, G., Thermodynamics of liquid mixtures containing carboxylic acids, PhD thesis, UKZN, Durban, (2003), 6-16.

Ritzoulis, G. and Fidantsi, A., *J. Chem. Eng. Data*, 45 (2000) 207-209.

Rabari, D., Patel, N., Joshipura, M. and Banerjee, T., *J. Chem. Eng. Data*, 59 (2014) 571-578.

Royal, M., Sarkar, L. and Dewan, R., *Bull. Chem. Soc. Ethiop.* 24 (2010) 103-114.

Redlich, O. and Kister, A., *Ind. Eng. Chem.* 40 (1948) 345-348.

Singh, G. and Kumar, A., *Indian J. Chem.* 47A (2008) 495-503.

Sadoway, D.: The missing link to renewable energy. *Presented at Ted conferences LLC*, (2012).

Santodonato, J., Bosch, S., Meylan, W., Becker, J. and Neal, M., *Pyridine* (1985), (Report No. SRC-TR-84-1119).

Sibiya, N., excess molar volumes, partial molar volumes and isentropic compressibilities of binary systems (ionic liquid + alkanol), M. Tech thesis, DUT, Durban, (2008).

Saini, N., Jangra, R., Yadav, J., Sharma, D. and Sharma, V., *Thermochimica Acta*, 518 (2011) 13-26.

Shev, Y. and Tu, C., *J. Chem. Eng. Data*, 51 (2006) 1690-1697.

Salguero, C. and Fadrique, J., *J. Chem. Eng. Data*, 56 (2011) 3823-3829.

Soriano, A., Doma, B. and Li, M., *J. Taiwan. Inst. Chem. Eng.* 41(2010) 115-121.

Streeti, W. and Stawely, L., *J. Chem. Phys.* 47 (1967) 2449.

Shukla, R., Kumar, A., Srivastava, U., Srivastava, K. and Gangwar, V., *Arabian J. Chem.* (2012).

Sheu, L. and Tu, C., *J. Chem. Eng. Data*, 51 (2006) 545-553.

Sharma, V., Bhagour, S., Solanki, S. and Rohilla, A., *J. Chem. Eng. Data*, 58 (2013) 1939-1954.

Urszula, M., Matteoli, E., Leonelli, F., Mocci, F., Marincola, F., Gontrani, L. and Porcedda, S., *Fluid Phase Equilibria*, 383 (2014) 49-54.

Vercher, E., Liopis, L., Gonzalez-Alfaro, M. and Martinez-Andreu, A., *J. Chem. Eng. Data*, 55 (2010) 1377-1388.

Vaid, Z., More, U., Ijardar, S. and Malek, N., *J. Chem. Thermodyn.* 86 (2015) 143-153.

Walden, P. *Bull. Acad. Imper. Sci. St. Petersburg*, 8 (1914) 405-422.

Wasserscheid, P. and Welton, T., *Ionic Liquid in Synthesis*, Wiley-VCH: Weinheim (2007).

Wilkes, J. and Zaworotko, M., *J. Chem. Soc. Chem. Commun.* (1992) 965-967.

Wood, E. and Brusie, J., *J. Am. Chem. Soc.* 65 (1943) 1891.

Wangsness, R., *Electromagnetic Fields*, Wiley, New York, (1986).

Yadav, P., Kumar, M., Yadav, R., *Physics and Chemistry of Liquids*, 52 (2014) 331-341.

Zafarani, M. and Shekaari, H., *J. Chem. Eng. Data*, 50 (2005) 1694-1699.

Appendix

Thermodynamic properties of 1-ethyl-3-methylimidazolium ethyl sulphate with nitrogen and sulphur compounds at $T = (298.15 - 318.15)$ K and $p = 1$ bar

Siyanda Brian Chule and Nirmala Deenadayalu